Declassified and Approved For Release 2013/03/01 : CIA-RDP10-02196R000300100005-6

Russian Original Vol. 32, No. 6, June, 1972
Translation published December, 1972

SATEAZ 32(6) 533-630 (1972)

[redacted]

SOVIET ATOMIC ENERGY

АТОМНАЯ ЭНЕРГИЯ
(ATOMNAYA ÉNERGIYA)

TRANSLATED FROM RUSSIAN

CONSULTANTS BUREAU, NEW YORK

Declassified and Approved For Release 2013/03/01 : CIA-RDP10-02196R000300100005-6

Declassified and Approved For Release 2013/03/01 : CIA-RDP10-02196R000300100005-6

SOVIET ATOMIC ENERGY

Soviet Atomic Energy is a cover-to-cover translation of *Atomnaya Énergiya*, a publication of the Academy of Sciences of the USSR.

An arrangement with Mezhdunarodnaya Kniga, the Soviet book export agency, makes available both advance copies of the Russian journal and original glossy photographs and artwork. This serves to decrease the necessary time lag between publication of the original and publication of the translation and helps to improve the quality of the latter. The translation began with the first issue of the Russian journal.

Editorial Board of *Atomnaya Énergiya:*

Editor: M. D. Millionshchikov

Deputy Director
I. V. Kurchatov Institute of Atomic Energy
Academy of Sciences of the USSR
Moscow, USSR

Associate Editors: N. A. Kolokol'tsov
N. A. Vlasov

A. A. Bochvar
N. A. Dollezhal'
V. S. Fursov
I. N. Golovin
V. F. Kalinin
A. K. Krasin
A. I. Leipunskii
V. V. Matveev
M. G. Meshcheryakov
P. N. Palei
V. B. Shevchenko
D. L. Simonenko
V. I. Smirnov
A. P. Vinogradov
A. P. Zefirov

Copyright © 1972 Consultants Bureau, New York, a division of Plenum Publishing Corporation, 227 West 17th Street, New York, N. Y. 10011. All rights reserved. No article contained herein may be reproduced for any purpose whatsoever without permission of the publishers.

Consultants Bureau journals appear about six months after the publication of the original Russian issue. For bibliographic accuracy, the English issue published by Consultants Bureau carries the same number and date as the original Russian from which it was translated. For example, a Russian issue published in December will appear in a Consultants Bureau English translation about the following June, but the translation issue will carry the December date. When ordering any volume or particular issue of a Consultants Bureau journal, please specify the date and, where applicable, the volume and issue numbers of the original Russian. The material you will receive will be a translation of that Russian volume or issue.

Subscription
$75.00 per volume (6 issues)
2 volumes per year
(Add $5 for orders outside the United States and Canada.)

Single Issue: $30
Single Article: $15

CONSULTANTS BUREAU, NEW YORK AND LONDON

227 West 17th Street
New York, New York 10011

Davis House
8 Scrubs Lane
Harlesden, NW10 6SE
England

Published monthly. Second-class postage paid at Jamaica, New York 11431.

Declassified and Approved For Release 2013/03/01 : CIA-RDP10-02196R000300100005-6

Declassified and Approved For Release 2013/03/01 : CIA-RDP10-02196R000300100005-6

SOVIET ATOMIC ENERGY

A translation of *Atomnaya Énergiya*
Translation published December, 1972

Volume 32, Number 6 June, 1972

CONTENTS

	Engl.	Russ.
Thermonuclear Wave of Combustion in a Limited Plasma – A.F.Nastoyashchii and L.P.Shevchenko	533	451
Elementary Solution of the Neutron Transport Equation with Anisotropic Scattering – N.V.Sultanov	539	457
On Estimating the Cost of Processing Liquid Radioactive Waste – B.S.Pavlov-Verevkin and M.F.Krasnaya	547	463
Tissue Doses from High-Energy Nucleons – I.M.Dmitrievskii, Ya.I.Kabakov, E.L.Potemkin, and V.V.Frolov	549	465
ABSTRACTS		
Computation of Thermal Constriction Resistance in the Presence of Contact of Laminas Washed by Heat Transfer Agent – V.V.Kharitonov, L.S.Kokorev, and V.K.Yurenko	554	471
Contact Conductivity of Cylindrical Bodies in Dense and Rarefied Gaseous Media – N.N.Del'vin, L.S.Kokorev, Ya.A.Bychko, and E.K.Shmachkov	555	471
A Method for Optimizing Certain Characteristics of Metal–Water Shields – Yu.N.Borisov, A.A.Gordeev, and O.Ya.Shakh	556	472
Multigroup Heterogeneous Description of a Rod of Finite Radius – S.S.Gorodkov	557	473
Gasthermal Disintegration of Fuel Elements of a Water-Cooled Water-Moderated Power Reactor with Separation of Fuel – A.T.Ageenkov and V.F.Savel'ev	558	474
Experimental Investigation of Contact Heat Exchange between Coaxial Cylindrical Casings in Vacuum – I.I.Novikov, L.S.Kokorev, and N.N.Del'vin	559	474
LETTERS TO THE EDITOR		
Possibility of Neglecting Elastic Scattering in Calculating the Velocities of Nuclear Reactions in a Uniform Sphere – V.K.Kapyshev and V.I.Sakharov	560	477
Fusibility Diagrams of Systems Involving Lithium Chloride, Uranium Trichloride, and Uranium Tetrachloride – V.N.Desyatnik, N.N.Kurbatov, S.P.Raspopin, and I.I.Trifonov	563	479
Optimization of a Reactor for Physical Investigations by Means of Fuel Profiling – T.S.Zaritskaya, Yu.V.Petrov, A.P.Rudik, and E.G.Sakhnovskii	565	480
Use of Solid Track Detectors in Reactor Experiments – V.A.Kuznetsov, A.I.Mogil'ner, V.P.Koroleva, V.S.Samovarov, and L.A.Chernov	567	481
A New Intermetallic Compound in a Zirconium–Iron System – Yu.F.Babikova, V.I.Filippov, and I.I.Shtan'	570	484
Measurement of the Neutron Spectrum at the Outlet of the Horizontal Channels in a Heavy Water Reactor and the SM-2 Reactor by the Time of Flight Method – S.M.Kalebin, M.Adib, G.V.Rukolaine, O.M.Gudkov, T.S.Belanova, N.G.Kocherygin, and S.N.Nikol'skii	573	485

Declassified and Approved For Release 2013/03/01 : CIA-RDP10-02196R000300100005-6

Declassified and Approved For Release 2013/03/01 : CIA-RDP10-02196R000300100005-6

CONTENTS

(continued)

	Engl./Russ.
Study of the Dispersion (Particle-Size) Composition of Radioactive Aerosols in the Layer of Air Close to the Earth – B. I. Ogorodnikov, O. G. Skotnikova, V. I. Skitovich, L. S. Soldaeva, and I. E. Konstantinov	576 488
Interaction and Wettability in Uranium Dioxide and Zirconium-Based Melts – A. T. Ageenkov, S. E. Bibikov, G. P. Novoselov, and V. F. Savel'ev	579 490
X-Ray Fluorescence Analysis of Heavy Elements by αX-Coincidence – B. M. Aleksandrov, S. M. Solov'ev, L. I. Tyvin, and V. P. Éismont	581 491
Effective Neutron Absorption Cross Sections for Cf^{252} and Cf^{253} in the Central Channel of an SM-2 Reactor – V. A. Anufriev, V. D. Gavrilov, Yu. S. Zamyatnin, V. V. Ivanenko, and G. N. Yakovlev	584 493
Unfolding Fast-Neutron Spectra from Threshold Detector Activities – A. M. Aglitskii, S. S. Lomakin, A. G. Morozov, V. I. Petrov, and S. G. Popov	585 494
Angular Distributions of Photoneutrons from Al, Ti, Cu, Mo, W, and Pb – V. P. Kovalev, V. P. Kharin, V. V. Gordeev, and V. I. Isaev	588 496
Calculation of the Boundary Effect in Particle-Transport Problems – S. I. Durinov, V. V. Uchaikin, and A. M. Kol'chuzhkin	590 497
Methods for Calculating Nonstationary Processes Involving Separation of Multicomponent Isotopic Mixtures in Packed Columns – I. A. Vereninov and Yu. V. Rakitskii	593 499
Asymptotic Stability of a Reactor with Thermionic Converter – V. P. Gorbunov, N. V. Isaev, O. V. Komarov, A. V. Kryanev, N. N. Petrov, A. F. Piskunkov, and S. B. Shikhov	596 501
Calculation of Buildup Factors at Deep Penetrations – Sh. S. Nikolaishvili, A. I. Gabrashvili, N. N. Dzhgarkava, and E. A. Iordanishvili	600 504
Production and Acceleration of Multiply-Charged Phosphorus and Zinc Ions – A. S. Pasyuk, Yu. P. Tret'yakov, and B. A. Zager	602 505
CHRONICLES	
Meeting on Prognosis of Development of Nuclear Energetics – Yu. I. Koryakin	606 509
Exchange of Experience in the Field of Development and Utilization of Equipment of a Water-Cooled Water-Moderated Reactor – A. P. Barchenkov	608 510
Diary of Collaboration	609 511
INFORMATION	
The Thirty-First Session of the Scientific Council of the Joint Institute for Nuclear Research (USSR) – V. A. Biryukov	611 513
Third All-Union Conference on Dissociating Gases – V. B. Nesterenko	616 516
Fourth International Conference on High Energy Physics and Structure of the Nucleus – R. A. Éramzhyan	618 517
International Conference on the Statistical Properties of Nuclei – U. G. Abov and S. I. Drozdov	621 518
Portable Pulsed X-Ray Equipment "Kvant," IRA-3, RINA-1D – I. I. Komyak and E. A. Peliks	623 520
On the Plan of Collaboration with the Atomic Energy Commission of the Iraqian Republic – B. Yu. Golovanov	626 521
BOOK REVIEWS	
N. M. Beskorovainyi, Yu. S. Belomyttsev, M. D. Abramovich, and V. K. Ivanov – Nuclear and Thermophysical Properties, Fundamentals of Corrosion and Fire Resistance [Vol. 1. Construction Materials of Nuclear Reactors] – Reviewed by I. S. Lupakov	627 523

Declassified and Approved For Release 2013/03/01 : CIA-RDP10-02196R000300100005-6

Declassified and Approved For Release 2013/03/01 : CIA-RDP10-02196R000300100005-6

CONTENTS

(continued)

Engl./Russ.

N. I. Chesnokov and A. A. Petrosov – Systems of Exploitation of Uranium Ore Deposits – Reviewed by I. F. Medvedev, N. S. Zontov, and L. Ch. Pukhal'skii. 629 523

The Russian press date (podpisano k pechati) of this issue was 5/25/1972. Publication therefore did not occur prior to this date, but must be assumed to have taken place reasonably soon thereafter.

Declassified and Approved For Release 2013/03/01 : CIA-RDP10-02196R000300100005-6

Declassified and Approved For Release 2013/03/01 : CIA-RDP10-02196R000300100005-6

THERMONUCLEAR WAVE OF COMBUSTION IN A LIMITED PLASMA

A. F. Nastoyashchii and L. P. Shevchenko

UDC 621.039.616

Let us consider a thermonuclear plasma with a density close to that of solid matter. Such a plasma may be created, for example, by heating a solid target with a laser pulse or electron beam. Let us suppose that the plasma is surrounded by a material shell which prevents the escape of the plasma, and that energy is released in it by virtue of a fusion reaction. At the same time, as a result of the contact between the plasma and the walls restricting it, heat leaks away by thermal conduction. The radiation from the plasma also causes a loss of heat.

Since the heat losses may be compensated by the thermal effect of the fusion reaction, it is reasonable to consider the possibility of a self-sustaining reaction in which the "combustion" of the thermonuclear substance occurs in an almost steady-state manner. A problem of this kind was considered in [1] in relation to three very simple plasma configurations: an infinite plane layer, an infinitely long cylinder, and a sphere. It was shown that steady states could only occur in the presence of a specific relationship between the temperature T_0 in the center of the volume occupied by the plasma and the product of the density by the characteristic dimension $(n_0 d)$.

There is furthermore a minimum possible value of the parameter $(n_0 d)_{cr}$ for which thermal equilibrium may occur. For $(n_0 d) < (n_0 d)_{cr}$ a steady state of thermal equilibrium is impossible: the plasma initially heated to thermonuclear temperatures will quickly cool. For $(n_0 d) > (n_0 d)_{cr}$ two states with different temperature T_0 may exist; however, only the state with the higher temperature is stable.

Presentation of the Problem

Let us consider a system similar to that just described. We shall assume, however, that only some of the plasma is heated to the thermonuclear temperature, so that at the initial instant of time there is a certain boundary between the hot and cold material (Fig. 1). The question arises: under what conditions (if any) can this boundary move in the direction of the cold material, i.e., can a thermonuclear combustion wave occur?

The heat-balance condition (heat-conduction equation) is [2]

$$\rho C_p \frac{\partial T}{\partial t} = -\operatorname{div} \mathbf{q} + Q_s(\rho, T), \tag{1}$$

where $\mathbf{q}$ is that heat-flow vector, related to the temperature gradient and the hydrodynamical velocity of the material $\mathbf{v}$ by

$$\mathbf{q} = -\varkappa \Delta T + \rho \mathbf{v} \left(C_p T + \frac{v^2}{2} \right); \tag{2}$$

Q_S is the amount of heat evolved by the heat source in unit volume in 1 sec; ρ is the mass of unit volume; C_p is the specific heat at constant pressure.

Since a considerable part is played by the radiation loss Q_R in the plasma, the plasma being almost transparent to this radiation for $n \approx 10^{22}$ cm^{-3} and $T \approx 10^8$°K, we must include these losses in $Q_S(\rho, T)$:

$$Q_s(\rho, T) = Q_F - Q_R. \tag{3}$$

In writing down the expression for the thermal effect of the reaction Q_F we must remember that, if the dimensions of the plasma are small compared with the range of the charged particles constituting the

Translated from Atomnaya Énergiya, Vol. 32, No. 6, pp. 451-455, June, 1972. Original article submitted July 5, 1971.

© 1972 Consultants Bureau, a division of Plenum Publishing Corporation, 227 West 17th Street, New York, N. Y. 10011. All rights reserved. This article cannot be reproduced for any purpose whatsoever without permission of the publisher. A copy of this article is available from the publisher for $15.00.

Declassified and Approved For Release 2013/03/01 : CIA-RDP10-02196R000300100005-6

Declassified and Approved For Release 2013/03/01 : CIA-RDP10-02196R000300100005-6

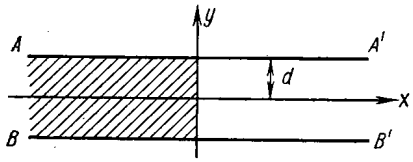

Fig. 1

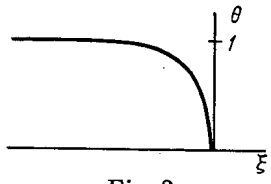

Fig. 2

Fig. 1. Layer of plasma contained by the walls AA' and BB'. The region occupied by the hot plasma is shown shaded.

Fig. 2. Temperature θ at the leading edge of the wave as a function of the coordinate ξ.

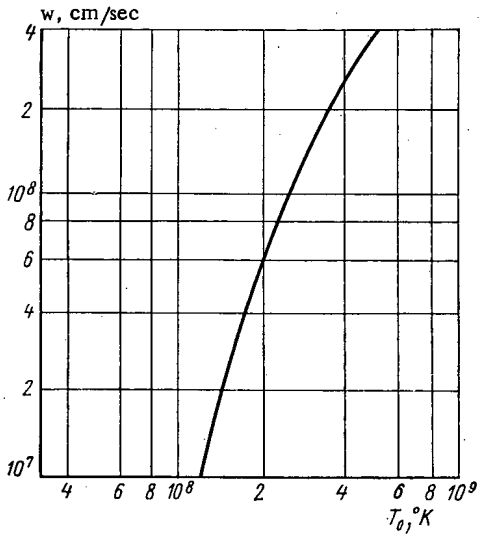

Fig. 3. Dependence of the velocity of the thermonuclear wave of combustion on T_0.

reaction products, then only a part of the energy evolved will be used in heating the plasma [1].

The expressions for Q_F and Q_R may be found in the monograph [3]. We shall assume that the thermal conductivity is a power function of temperature

$$\varkappa = \beta T^k. \tag{4}$$

For a Coulomb plasma in the absence of an external magnetic field the power index in (4) equals k = 5/2, $\beta = 2.1 \cdot 10^{-6}$ erg $\cdot cm^{-1} \cdot sec^{-1} \cdot deg^{-7/2}$.

The divergence term in (2) describes the flow of heat along the system and to the walls. The problem may be greatly simplified if in order to describe the flow of heat to the walls we make use of the expression derived in [1], which described the flow of heat to the walls in an equilibrium state

$$Q_\chi = \frac{2s\beta}{k+1} \frac{T^{k+1}}{d^2}, \tag{5}$$

where s = 1 for a plane layer and s = 2 for an infinitely long cylinder. After introducing this simplifying assumption the problem will essentially be one-dimensional. We shall seek a solution to the heat conduction equation in the form of a plane wave moving at a constant velocity w' along the x axis, i.e., in the form

$$T = T(x - w't), \tag{6}$$

or in a system of coordinates moving with the wave in the form $T = T(x')$. As earlier, we denote the temperature in the center of the plasma volume (this is obviously the maximum temperature in the system, and thermal equilibrium exists at this point) by T_0 and introduce the dimensionless temperature $\theta = TT_0^{-1}$ and the dimensionless coordinate $\xi = x'd^{-1} \equiv (x - w't)d^{-1}$. We thus obtain a dimensionless heat-conduction equation (here and subsequently $k_\parallel$ are the power indices relating to the thermal conductivity along the system; in general we may have $k \neq k_\parallel$):

$$(\theta^{k_\parallel}\theta_\xi)_\xi + \nu\theta_\xi = \phi(\theta; n_0 d, T_0). \tag{7}$$

Here

$$\nu = \frac{mC_p}{\beta T_0^{k_\parallel}} \cdot n_0' d \cdot w'; \quad \phi = d^2 \frac{Q_F - Q_R - Q_\chi}{\beta T_0^{k_\parallel}};$$

n_0' is the density of the plasma immediately in front of the leading edge of the wave. In Eq. (7) we must remember that the density of the plasma is not constant, but temperature-dependent; it will later be shown that the velocity of the wave is lower than the velocity of sound over a fairly wide temperature range, so that the pressure may be regarded as constant, and then $n \approx 1/T$.

Let us formulate the boundary conditions. We take the origin of coordinates in a system of reference connected to the wave directly in front of the latter. Then according to Fig. 2 the region with $\theta > 0$ occurs in $\xi < 0$. In the region $\xi \geq 0$ we put $\theta = 0$. The second boundary condition for $\theta = 0$ corresponds to a zero

Declassified and Approved For Release 2013/03/01 : CIA-RDP10-02196R000300100005-6

Declassified and Approved For Release 2013/03/01 : CIA-RDP10-02196R000300100005-6

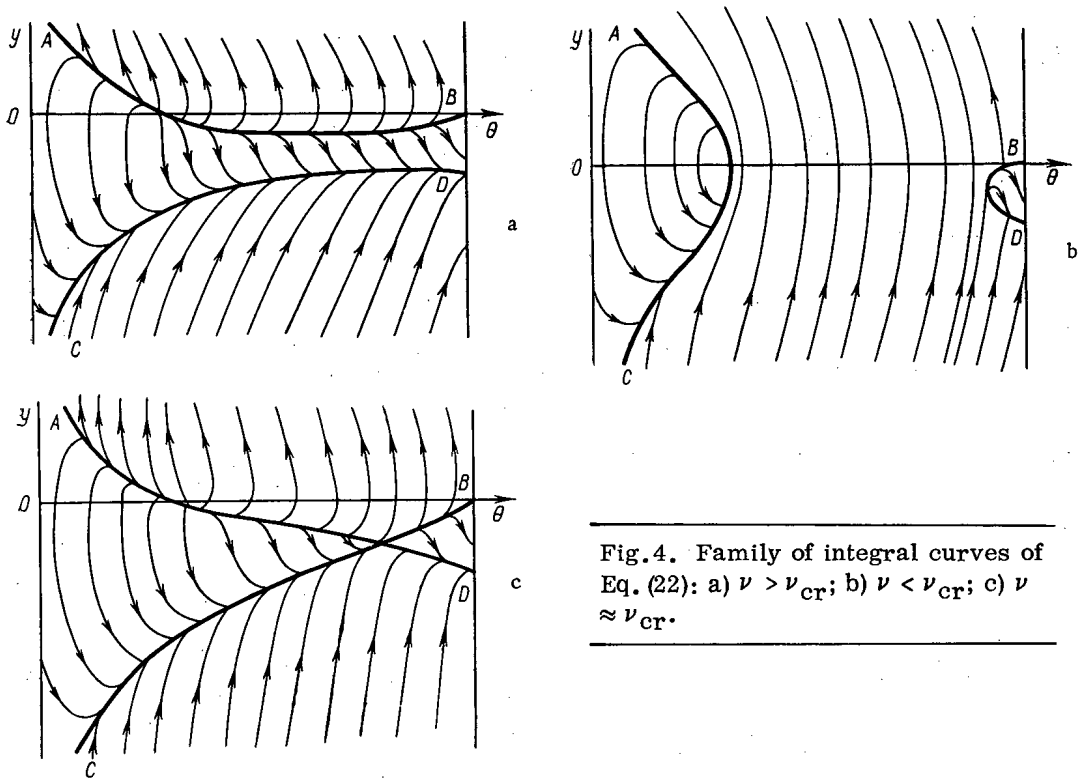

Fig. 4. Family of integral curves of Eq. (22): a) $\nu > \nu_{cr}$; b) $\nu < \nu_{cr}$; c) $\nu \approx \nu_{cr}$.

energy flux. On the other hand, a fair distance behind the leading edge of the wave, in the region in which thermal equilibrium is assumed to exist, the following two conditions must be satisfied: $\theta = 1$ and $\theta_\xi = 0$. These are readily seen to be equivalent. Thus in the region in which $\theta \approx 1$ there is essentially one boundary condition.

From Eq. (7) and the boundary conditions we may derive the condition for the existence of a thermonuclear wave of combustion, its velocity, and also the condition of thermal equilibrium behind the leading edge of the wave.

Approximate Method of Solution

Thus the problem amounts to the solution of an ordinary differential equation (7) (nonlinear and nonhomogeneous). An analytical solution over the whole range of variation of the argument ξ is hardly possible. However, we may make use of an approximate method by seeking the solution in two limiting regions: $\theta \ll 1$ and $\theta \approx 1$; the resultant solutions may be matched in the intermediate region at $\theta \approx 1/2$. At the matching point two conditions clearly have to be satisfied; the two solutions must be equal and so must their derivatives (otherwise the condition of continuity imposed on the energy flux is infringed).

Solution of the Equation in the Region $\theta \ll 1$. As already mentioned, immediately in front of the wave we take $\theta = 0$. At the origin of the wave front the plasma clearly undergoes heating, mainly by virtue of the heat arriving from the neighboring hotter region (intrinsic heat generation is as yet quite small here). The heat arrives as a result of conduction; any heating due to the absorption of the intrinsic plasma radiation may be neglected. The flow of heat not only heats the plasma but also compensates the losses due to radiation and heat conduction to the walls and neighboring colder regions.

Neglecting the right-hand side of (7), describing the heat losses and intrinsic heat generation, by comparison with the first term on the left, describing the thermal flux from the hotter region, we have

$$(\theta^{k_\parallel}\theta_\xi)_\xi + \nu\theta_\xi = 0. \tag{8}$$

The solution of this equation satisfying the boundary conditions is

$$\theta = (-k_\parallel \nu \xi)^{-1/k_\parallel}. \tag{9}$$

Declassified and Approved For Release 2013/03/01 : CIA-RDP10-02196R000300100005-6

Declassified and Approved For Release 2013/03/01 : CIA-RDP10-02196R000300100005-6

The minus sign occurs because owing to the coordinate system chosen the region $\theta > 0$ corresponds to negative ξ, so that the quantity in the brackets is positive. Substituting the solution into Eq. (7) we readily see that in the absence of marked radiation losses the right-hand side of (7) may indeed be neglected. In the presence of such losses we may only neglect this for $k_{\parallel} > 5/2$. In the case $k_{\parallel} = 5/2$ the solution has the same power dependence on ξ as that given by (9) if in the latter we take $k_{\parallel} = 5/2$:

$$\theta = (-q_+\xi)^{2/5}, \tag{10}$$

but with a different factor in front of ξ, one allowing for the radiant energy losses

$$q_+ = \frac{5}{4}\nu + \sqrt{\frac{25}{16}(\nu)^2 + \frac{25}{4}\phi_R(1)}. \tag{11}$$

We see from the resultant solutions that the wave front is curved (Fig. 2) on approaching the point $\xi = 0$: $\theta_\xi|_{\xi\to 0} \to -\infty$.

Solution of the Equation in the Region $\theta \approx 1$. In this case we may certainly not neglect any term on the right of Eq. (7); however, the equation may be greatly simplified by introducing a new function z in accordance with

$$z = 1 - \theta \ll 1 \tag{12}$$

and then expanding the terms of Eq. (7) with respect to z.

If we carry out such an expansion with respect to z in (7) and retain the first nonvanishing terms, we obtain

$$z_{\xi\xi} + \nu z_\xi + \phi'_\theta(1)\, z = 0. \tag{13}$$

Here we also allow for the fact that a fair distance behind the leading edge of the wave the condition of thermal equilibrium has to be satisfied for $\theta = 1$

$$\phi|_{\theta=1} = 0. \tag{14}$$

The general solution of (13) takes the form

$$z = C_+ e^{p_+\xi} + C_- e^{p_-\xi}, \tag{15}$$

where p_+, p_- are the roots of the characteristic equation

$$p_\pm = -\frac{\nu}{2} \pm \sqrt{\left(\frac{\nu}{2}\right)^2 - \phi'_\theta(1)}. \tag{16}$$

Since on approaching the region of thermal equilibrium $\theta \to 1$, and hence we should have $z \to 0$, we must take $C_- = 0$. For the exponential associated with C_+ to fall on moving away from the leading edge in the high-temperature direction, we require $p_+ > 0$, and this can only occur if

$$\phi'_\theta(1) < 0. \tag{17}$$

From physical considerations it is easy to see that for $\phi'_\theta(1) > 0$ there can be neither stable thermal equilibrium behind the leading edge of the wave [1] nor even a combustion wave at all. If $\phi'_\theta(1) < 0$ there can only be a cooling wave. We may convince ourselves of this by considering that the cooling wave corresponds to $\nu < 0$ (it must clearly travel in a direction opposite to the wave of combustion); then $p_+ > 0$. An additional condition for the existence of a cooling wave, as indicated by (10) and (11), is the existence of radiation losses.

Finally for the region $\theta \approx 1$ we obtain the solution

$$\theta = 1 - C_+ e^{p_+\xi}. \tag{18}$$

The constant in (18) cannot be determined from the boundary conditions, since in the region $\theta \approx 1$ there is essentially only one boundary condition, which has already been used in determining C_-.

Matching of the Solutions and Velocity of the Wave. As already mentioned at the beginning of the section, the solutions have to be matched at $\theta \approx 1/2$, i.e., where the intrinsic heat generation is small, but not so much so as to be negligible by comparison with the flow of heat from the hotter region. At the matching point two conditions arising from the continuity of the temperature and its derivative have to be satisfied. From the first condition we find the integration constant C_+ and from the second the velocity of the wave.

Declassified and Approved For Release 2013/03/01 : CIA-RDP10-02196R000300100005-6

Declassified and Approved For Release 2013/03/01 : CIA-RDP10-02196R000300100005-6

The simplest expression for the velocity of the wave is obtained when the radiation losses are insignificant (in the region $T > 10^8$°K in which a combustion wave is possible, this is in fact so). If $k \geq 5/2$ we have for the wave velocity

$$w = \alpha \frac{\beta T_0^{k_\parallel}}{mC_p} \frac{\sqrt{|\phi'(1)|}}{n_0 d}. \tag{19}$$

Here w is the velocity of the leading edge of the wave with respect to the hot material, i.e., $w = w'(n_0'/n_0)$; the numerical factor in general depends on the power index $k_\parallel$. Comparison with the exact solution obtained numerically shows that (19) correctly describes the change in wave velocity if $\alpha = 1$.

If we then use the relation between $n_0 d$ and T_0 imposed by the condition of thermal equilibrium behind the leading edge of the wave, we may find the velocity of the wave as a function of T_0. For the case in which thermal contact of the plasma with the walls is effected by the ions (a fairly strong magnetic field being applied parallel to the walls) while heat is transferred along the system by the electrons in accordance with Eq. (4), in which $k_\parallel = 5/2$, this relationship is illustrated in Fig. 3. The velocity of the wave rises quite quickly with increasing temperature, but still remains below the velocity of sound up to temperatures of $\sim 4.10^9$°K.

Study of the Problem by the Phase-Plane Method

The phase-plane method [4] easily enables us to draw conclusions regarding the possible existence of a thermonuclear combustion wave and also to make a quantitative estimate of the wave velocity. Furthermore this method is useful in that it clearly demonstrates the uniqueness of the resultant solution.

Introducing the phase variable $y(\theta) = \theta_\xi$, we transform the original Eq. (7) to the form

$$y^2 + \nu \frac{y}{k_\parallel \theta^{k_\parallel - 1}} + \frac{\phi(\theta)}{k_\parallel \theta^{k_\parallel - 1}} = -\frac{1}{k_\parallel} \theta y y_\theta, \tag{20}$$

where $\phi(\theta)$ is the thermal source function including the generation of heat, and also the loss of heat at the walls and by radiation. If we then use the functions

$$y_\pm(\theta) = -\frac{\nu}{k_\parallel \theta^{k_\parallel - 1}} \pm \sqrt{\left(\frac{\nu}{k_\parallel \theta^{k_\parallel - 1}}\right)^2 - \frac{\phi(\theta)}{k_\parallel \theta^{k_\parallel - 1}}}, \tag{21}$$

that is, the roots of Eq. (20) without the right-hand side, the latter may be transformed into

$$y_\theta = -\frac{k_\parallel}{\theta y} [y - y_+(\theta)][y - y_-(\theta)]. \tag{22}$$

The family of integral curves relating to Eq. (22) for $k_\parallel = 5/2$ is shown schematically in Fig. 4. The thick lines represent the functions $y = y_\pm(\theta)$. It is quite easy to show from the results of the previous section that the desired intergral curve for $\theta \ll 1$ is linearly related to $y_-(\theta)$ thus: $y(\theta) \approx c y_-(\theta)$; the proportionality factor $c > 1$. For $\theta \approx 1$ also we have a linear relation $y = c y_+(\theta)$, but here $c < 1$. Thus the integral curve representing the solution of the problem should proceed below the special curve $y_-(\theta)$ for $\theta \ll 1$ and above $y_+(\theta)$ for $\theta \approx 1$. The course of the integral curves varies considerably with the relation between ν and ν_{cr} where ν_{cr} is the value of ν, for which the expression under the root in (21) is not negative for any θ from the range [0, 1].

Figure 4a corresponds to $\nu > \nu_{cr}$. The integral curve satisfying the boundary condition $\theta = 1$, $\theta_\xi = 0$ for $\xi = -\infty$ should arise from the point at which $\theta = 1$; $y = 0$ (point B). We see from Fig. 4a that the required integral curves connecting the "cold" ($\theta \to 0$, $\theta_\xi \to 0$) and "hot" states of the material are nonexistent in this particular case.

Figure 4b shows the integral curves for $\nu < \nu_{cr}$. We see from this figure that in this case also there are no integral curves satisfying the conditions of the problem.

The integral curve (BC) does, however, exist for $\nu \approx \nu_{cr}$ (Fig. 4c). From this we find the velocity of the wave, which agrees qualitatively with the value obtained by the approximate method in the previous section. The necessary condition for the existence of a thermal combustion wave is also confirmed, namely, that the derivative of the right-hand side of Eq. (7) should be negative at temperatures close to the maximum temperature in the plasma.

Declassified and Approved For Release 2013/03/01 : CIA-RDP10-02196R000300100005-6

Declassified and Approved For Release 2013/03/01 : CIA-RDP10-02196R000300100005-6

We may thus conclude from the foregoing analysis that a combustion wave can only occur in a thermonuclear plasma for plasma parameters which make the temperature derivative of the effective heat source (including the energy effect of the fusion reaction and the heat losses associated with radiation and transfer to the walls) negative. This criterion is simultaneously the condition for the stability of the thermal equilibrium in plasma between walls [1]. The foregoing solution with the monotonic wave profile (Fig. 2) is the only one; there are no other types of wave in the present case.

Under different conditions waves of other structures may possibly arise. Thus it was shown in [5] by a numerical technique that in an unbounded plasma in which the plasma had no thermal contact with any walls a combustion wave of the space-periodic type was quite possible.

LITERATURE CITED

1. A. F. Nastoyashchii, At. Énerg., 32, 43 (1972).
2. L. D. Landau and E. M. Lifshits, Mechanics of Continuous Media [in Russian], Gostekhteorizdat, Moscow (1945).
3. L. A. Artsimovich, Controlled Thermonuclear Reactions [in Russian], Fizmatgiz, Moscow (1961).
4. N. N. Bogolyubov and Yu. A. Mitropol'skii, Asymptotic Methods in the Theory of Nonlinear Oscillations [in Russian], Fizmatgiz, Moscow (1958).
5. S. Alikhanov and I. Konkashbaev, Nucl. Fusion, 11, 119 (1971).

Declassified and Approved For Release 2013/03/01 : CIA-RDP10-02196R000300100005-6

Declassified and Approved For Release 2013/03/01 : CIA-RDP10-02196R000300100005-6

ELEMENTARY SOLUTION OF THE NEUTRON TRANSPORT EQUATION WITH ANISOTROPIC SCATTERING

N. V. Sultanov

UDC 539.125.52

The usefulness of a system of elementary solutions of Boltzmann's equation when considering neutron-transport problems was demonstrated in [1]. Assuming plane geometry and isotropic scattering, a complete system of elementary solutions of the one-velocity steady-state Boltzmann equation was there derived, the distribution function $\Psi(x, \mu)$ depending on two variables. The case of anisotropic scattering was studied in [2, 3].

In certain problems of practical interest one has to solve the Boltzmann equation for a distribution function depending on three variables (for example, in considering the oblique incidence of a parallel neutron beam on a plate, or in setting up a system of elementary equations possessing cylindrical symmetry from a system of elementary plane solutions [4]). In this case new solutions appear, allowing for azimuthal deviations from symmetry. The case of isotropic scattering was considered in [4].

We shall now study the case of anisotropic scattering. The scattering indicatrix is expressed in the form of a finite series in Legendre polynomials:

$$f(\Omega\Omega') = \frac{1}{4\pi}\sum_{k=0}^{N} b_k P_k(\Omega\Omega'). \tag{1}$$

Whereas in the isotropic approximation the solutions responsible for the azimuthal asymmetry have only a continuous spectrum of ν values, in the anisotropic case the new solutions with numbers $m \leq N$ acquire a discrete spectrum of ν_i^m. In order to find the ν_i^m transcendental characteristic equations will be obtained in this paper. The number of ν_i^m will be estimated. We shall also demonstrate the orthogonality and completeness of the resultant system of elementary solutions.

The system of plane elementary solutions thus obtained is suitable for modifying the computer program "Praktinets" also used for calculating the cell characteristics in the linear-anisotropic approximation. We shall calculate several cells by means of this modified program.

System of Plane Elementary Solutions. The one-velocity Boltzmann equation for the distribution function $\Psi(x, \mu, \varphi)$ in plane geometry takes the form

$$\mu\frac{\partial\Psi(x, \mu, \varphi)}{\partial x} + \Psi(x, \mu, \varphi) = c\int f(\Omega\Omega')\,\Psi(x, \Omega')\,d\Omega', \tag{2}$$

where c is the number of secondary neutrons per collision; x is the distance measured in neutron free paths.

We shall seek a solution in the form of a plane wave:

$$\Psi(x, \mu, \varphi) = e^{-x/\nu}\Phi(\nu, \mu, \varphi), \tag{3}$$

where ν is a complex number. Substituting (3) into (2) we obtain an equation for $\Phi(\nu, \mu, \varphi)$:

$$\left(1 - \frac{\mu}{\nu}\right)\Phi(\nu, \Omega) = c\int f(\Omega\Omega')\,\Phi(\nu, \Omega')\,d\Omega'. \tag{4}$$

We use proposition (1) and the addition theorem for Legendre polynomials twice [5]. Then (4) takes the form

Translated from Atomnaya Énergiya, Vol. 32, No. 6, pp. 457–462, June, 1972. Original article submitted July 19, 1971.

© 1972 Consultants Bureau, a division of Plenum Publishing Corporation, 227 West 17th Street, New York, N. Y. 10011. All rights reserved. This article cannot be reproduced for any purpose whatsoever without permission of the publisher. A copy of this article is available from the publisher for $15.00.

Declassified and Approved For Release 2013/03/01 : CIA-RDP10-02196R000300100005-6

Declassified and Approved For Release 2013/03/01 : CIA-RDP10-02196R000300100005-6

TABLE 1. Results of the Calculation of Some Cell Characteristics

Number of cell	Characteristic	Approximation					
		isotropic		linear-anisotropic		transport	
		G_1	G_3	G_1	G_3	G_1	G_3
1	$\bar{\Phi}_2/\bar{\Phi}_1$	1,550	1,548	1,488	1,487	1,511	1,513
	Θ	0,9189	0,9190	0,9219	0,9220	0,9208	0,9207
2	$\bar{\Phi}_2/\bar{\Phi}_1$	1,296	1,273	1,296	1,273	1,296	1,281
	$\bar{\Phi}_3/\bar{\Phi}_1$	1,713	1,661	1,651	1,599	1,674	1,630
	Θ	0,8749	0,8779	0,8778	0,8808	0,8767	0,8791
3	$\bar{\Phi}_2/\bar{\Phi}_1$	1,598	1,581	1,501	1,484	1,509	1,496
	Φ_3/Φ_1	2,322	2,297	2,127	2,102	2,142	2,113
	Θ	0,7964	0,7983	0,8092	0,8110	0,8082	0,8101

Note: Φ_i is the mean flux in the i-th zone; G_N is the number of the approximation [7].

$$\left(1-\frac{\mu}{\nu}\right)\Phi(\nu,\mu,\varphi)=\frac{c}{4\pi}\int_{-1}^{1}\int_{0}^{2\pi}\sum_{m'=0}^{N}\left[\sum_{\kappa=m'}^{N}b_\kappa\frac{(\kappa-m')!}{(\kappa+m')!}P_\kappa^{m'}(\mu')P_\kappa^{m'}(\mu)\right][e^{im'(\varphi-\varphi')}+e^{-im'(\varphi-\varphi')}]\Phi(\nu,\mu',\varphi')\,d\mu'\,d\varphi'. \quad (5)$$

Here μ, μ' are the projections of Ω and Ω' respectively on the x axis; φ, φ' are the azimuthal angles of Ω, Ω' in a plane perpendicular to the x axis.

Let us expand $\Phi(\nu, \mu, \varphi)$ in an orthogonal system of functions $e^{in\varphi}$, where $n = 0, \pm1, \pm2, \ldots$

$$\Phi(\nu,\mu,\varphi)=\sum_{n=-\infty}^{\infty}\Phi^n(\nu,\mu,\varphi)=\sum_{n=-\infty}^{\infty}\Phi^n(\nu,\mu)\,e^{in\varphi}. \quad (6)$$

Substituting (6) into (5) and integrating the right-hand side of the resultant equation with respect to φ', we obtain

$$\left(1-\frac{\mu}{\nu}\right)\sum_{n=-\infty}^{\infty}\Phi^n(\nu,\mu)\,e^{in\varphi}=\frac{c}{2}\sum_{m'=0}^{N}\left[\sum_{\kappa=m'}^{N}b_\kappa\frac{(\kappa-m')!}{(\kappa+m')!}P_\kappa^{m'}(\mu)\int_{-1}^{1}P_\kappa^{m'}(\mu)\Phi^n(\nu,\mu)\,d\mu\right](e^{im'\varphi}\delta_{m',n}+e^{-im'\varphi}\delta_{-m',n}), \quad (7)$$

where δ_{mn} is the Kronecker symbol.

Multiplying both sides of Eq. (7) by $e^{im\varphi}$, where $m = 0, \pm1, \pm2, \ldots$, and integrating over all φ, we obtain an infinite system of equations for $\Phi^m(\nu, \mu)$.

For the case $|m| \leq N$ we have

$$\left(1-\frac{\mu}{\nu}\right)\Phi^m(\nu,\mu)=\frac{c}{2}\sum_{\kappa=|m|}^{N}b_\kappa\frac{(\kappa-|m|)!}{(\kappa+|m|)!}P_\kappa^{|m|}(\mu)\,h_\kappa^{|m|}(\nu), \quad (8)$$

where

$$h_\kappa^{|m|}(\nu)=\int_{-1}^{1}P_\kappa^{|m|}(\mu)\,\Phi^m(\nu,\mu)\,d\mu. \quad (9)$$

Clearly for $\Phi^m(\nu, \mu)$ and $\Phi^{-m}(\nu, \mu)$ we obtain identical equations.

For $m = 0$ Eq. (8) takes the form

$$(\nu-\mu)\,\Phi^0(\nu,\mu)=\frac{c\nu}{2}\sum_{\kappa=0}^{N}b_\kappa P_\kappa(\mu)\,h_\kappa^0(\nu).$$

This was studied in detail in [3]. Subsequently we shall consider equations with $m \geq 0$.

The relation between the $h_\kappa^m(\nu)$ ($m \leq \kappa \leq N$) may be found on multiplying both sides of Eq. (8) by $(2\kappa + 1)$ $P_\kappa^m(\mu)$, integrating them over all μ allowing for the normalization of the associated Legendre polynomials

Declassified and Approved For Release 2013/03/01 : CIA-RDP10-02196R000300100005-6

Declassified and Approved For Release 2013/03/01 : CIA-RDP10-02196R000300100005-6

and the recurrence relations between them [5]:

$$\nu[(2\kappa+1)-cb_\kappa]\,h_\kappa^m(\nu)-(\kappa-m+1)\,h_{\kappa+1}^m(\nu)-(\kappa+m)\,h_{\kappa-1}^m(\nu)=0, \tag{10}$$

where $h_{m-1}^m(\nu)=0$. We see from this equation that $h_\kappa^m(\nu)(\kappa>m)$ are expressed in terms of $h_m^m(\nu)$. For convenience we introduce the normalization

$$h_m^m(\nu)=1. \tag{11}$$

Then the $h_\kappa^m(\nu)$ are polynomials of order $(\kappa-m)$ with the following properties:

$$h_\kappa^m(-\nu)=(-1)^{\kappa-m}h_\kappa^m(\nu);\quad [h_\kappa^m(\nu^*)]^*=h_\kappa^m(\nu), \tag{12}$$

where the sign "*" denotes the complex conjugate quantity.

The first four polynomials $h_\kappa^m(\nu)$ have the following form:

$$h_m^m(\nu)=1;\quad h_{m+1}^m(\nu)=[(2m+1)-cb_m]\,\nu;$$
$$h_{m+2}^m(\nu)=\frac{1}{2}\{[(2m+3)-cb_{m+1}][(2m+1)-cb_m]\,\nu^2-(2m+1)\};$$
$$h_{m+3}^m(\nu)=\frac{1}{6}\{[(2m+5)-cb_{m+2}][(2m+3)-cb_{m+1}][(2m+1)-cb_m]\,\nu^3-(2m+1)\times[(2m+5)-cb_{m+2}]\,\nu-4(m+1)[(2m+1)-cb_m]\,\nu\}. \tag{13}$$

We see from these expressions that for certain values of c and b_κ the order of the polynomials may be lower than $(\kappa-m)$.

The general solution of Eq. (8) will take the form

$$\Phi^m(\nu,\mu)=\frac{c\nu}{2}P\frac{\sum_{\kappa=m}^{N}\frac{(\kappa-m)!}{(\kappa+m)!}b_\kappa P_\kappa^m(\mu)\,h_\kappa^m(\nu)}{(\nu-\mu)}+\lambda^m(\nu)\,\delta(\nu-\mu), \tag{14}$$

where P denotes the principal Cauchy value on integrating the expression incorporating the function $\Phi^m(\nu,\mu)$; $\lambda^m(\nu)$ is a function of ν [see (23)].

For the case $|m|>N$ we have

$$\left(1-\frac{\mu}{\nu}\right)\Phi^m(\nu,\mu)=0. \tag{15}$$

The solution of this equation will have the form

$$\Phi^m(\nu,\mu)=\delta(\nu-\mu). \tag{16}$$

In future we shall consider the case $0\le m\le N$. For $\nu\overline{\in}[-1,1]$ Eq. (14) becomes

$$\Phi^m(\nu,\mu)=\frac{c\nu}{2}\cdot\frac{\sum_{\kappa=m}^{N}\frac{(\kappa-m)!}{(\kappa+m)!}b_\kappa h_\kappa^m(\nu)\,P_\kappa^m(\mu)}{(\nu-\mu)}. \tag{17}$$

Multiplying (17) by $P_m^m(\mu)$, integrating over all μ, and remembering (9) and (11), we obtain a transcendental equation for finding the discrete values of ν:

$$1=\frac{c\nu}{2}\sum_{\kappa=m}^{N}\frac{(\kappa-m)!}{(\kappa+m)!}b_\kappa h_\kappa^m(\nu)\int_{-1}^{1}\frac{P_\kappa^m(\mu)\,P_m^m(\mu)}{\nu-\mu}d\mu. \tag{18}$$

Let us transform Eq. (18) remembering the relations of [5]:

$$P_m^m(\mu)=(-1)^m(1-\mu^2)^{m/2}(2m-1)!!;$$
$$\int_{-1}^{1}\frac{(1-\mu^2)^{m/2}P_\kappa^m(\mu)}{z-\mu}d\mu=(-1)^m\,2\,(z^2-1)^{m/2}\,Q_\kappa^m(z), \tag{19}$$

where $Q_\kappa^m(z)$ is a Legendre function of the second order, analytical in the expanded complex plane with a cut at $[-1,1]$.

Let us give a number of expressions for $Q_\kappa^m(z)(z\overline{\in}[-1,1])$ [5] which we shall use subsequently:

$$Q_\kappa^m(z)=(z^2-1)^{\frac{m}{2}}\frac{d^mQ_\kappa(z)}{dz^m}; \tag{20}$$

Declassified and Approved For Release 2013/03/01 : CIA-RDP10-02196R000300100005-6

Declassified and Approved For Release 2013/03/01 : CIA-RDP10-02196R000300100005-6

$$Q_\kappa(z) = P_\kappa(z)\, Q_0(z) - W_{\kappa-1}(z), \tag{21}$$

where $W_{\kappa-1}$ is a polynomial of order $(\kappa - 1)$ and

$$Q_0(z) = \frac{1}{2} \ln \frac{z-1}{z+1}.$$

Equation (18) takes the form

$$1 = cz \sum_{\kappa=m}^{N} b_\kappa (2m-1)!! \, \frac{(\kappa-m)!}{(\kappa+m)!} (z^2-1)^{\frac{m}{2}} h_\kappa^m(z)\, Q_\kappa^m(z). \tag{22}$$

For $\nu \in [-1, 1]$ we operate on Eq. (14) in the same way as on (17). Using the relation

$$P \int_{-1}^{1} \frac{(1-\mu^2)^{m/2} P_n^m(\mu)\, d\mu}{\nu - \mu} = (-1)^m 2P\,[(1-\nu^2)^{m/2} Q_n^m(\nu)],$$

we obtain

$$\lambda^m(\nu) = \frac{1}{P_m^m(\nu)} \left\{ 1 - (-1)^m c\nu \sum_{\kappa=m}^{N} b_\kappa \frac{(\kappa-m)!}{(\kappa+m)!}\, h_\kappa^m(\nu)\, P\,[P_m^m(\nu)\, Q_\kappa^m(\nu)] \right\}. \tag{23}$$

We introduce a new function

$$\Omega^m(z) = R^m(z) - czN^m(z)\, Q_0(z), \tag{24}$$

where $R^m(z)$ and $M^m(z)$ are polynomials of order 2N:

$$R^m(z) = 1 - cz \sum_{\kappa=m}^{N} b_\kappa (2m-1)!! \, \frac{(\kappa-m)!}{(\kappa+m)!}\, h_\kappa^m(z)\, (z^2-1)^m \left[\sum_{n=0}^{m-1} \frac{d^n P_\kappa(z)}{dz^n} \cdot \frac{d^{m-n} Q_0(z)}{dz^{m-n}} - \frac{d^m W_{\kappa-1}(z)}{dz^m} \right]; \tag{25}$$

$$N^m(z) = \sum_{\kappa=m}^{N} b_\kappa (2m-1)!! \, \frac{(\kappa-m)!}{(\kappa+m)!}\, h_\kappa^m(z)\, (z^2-1)^m \, \frac{d^m P_\kappa(z)}{dz^m}. \tag{26}$$

Here $\Omega^m(z)$ is an analytical function in the expanded complex plane with a cut at $[-1, 1]$ since it consists of the sum of the products of analytical functions [see (22)].†

With the introduction of the function $\Omega^m(z)$ Eqs. (22) and (23) respectively take the form

$$\Omega^m(z) = 0; \tag{27}$$

$$\lambda^m(\nu) = \frac{P\Omega^m(\nu)}{P_m^m(\nu)}. \tag{28}$$

From the definition of $\Omega^m(z)$ and the properties of $h_\kappa^m(z)$ and the derivatives $P_\kappa(z)$, $Q_0(z)$, and $W_{\kappa-1}(z)$ it may be shown that if ν_i^m is a root of Eq. (27) then $-\nu_i^m$, $\pm\nu_i^{m*}$ are roots of the same equation,‡ i.e., the roots of Eq. (27) occur in fours $\pm\nu_i^m$, $\pm\nu_i^{m*}$, if ν_i^m is a complex number, and in pairs if ν_i^m is a real or purely imaginary number. Let the number of roots of Eq. (27) be $2M^m$. Then the solutions of Eq. (8) may be written in the form:

for $\nu \in [-1, 1]$ for $|m| \le N$

$$\Phi^m(\pm\nu_i^m, \mu) = \frac{c(\pm\nu_i^m)}{2(\pm\nu_i^m - \mu)} \sum_{\kappa=|m|}^{N} \frac{(\kappa-|m|)!}{(\kappa+|m|)!}\, b_\kappa h_\kappa^{|m|}(\pm\nu_i^m)\, P_\kappa^{|m|}(\mu) \tag{29}$$

$$(\text{here} \quad i = 1, 2, \ldots, M^m);$$

for $|m| > N$

$$\Phi^m(\nu, \mu) = 0; \tag{30}$$

for $\nu \in [-1, 1]$ for $|m| \le N$

†It follows from the definition of $Q_\kappa^m(z)$ in Eq. (20) and $h_\kappa^m(z)$ in Eq. (13) that $Q_\kappa^m(z) \sim z^{-k-1}$, $h_\kappa^m(z) \sim z^{\kappa-m}$, and $(z^2-1)^{(m/2)} \sim z^m$ as $z \to \infty$. Then each term of Eq. (22) $zQ_\kappa^m(z)\, h_n^m(z)\, (z^2-1)^{(m/2)} \sim 1$ as $z \to \infty$, i.e., $\Omega^m(z)$ is bounded as $z \to \infty$, and hence analytical.

‡This was established for the first time in [6].

Declassified and Approved For Release 2013/03/01 : CIA-RDP10-02196R000300100005-6

Declassified and Approved For Release 2013/03/01 : CIA-RDP10-02196R000300100005-6

$$\Phi^m(\nu, \mu) = P\frac{c\nu}{2(\nu-\mu)}\sum_{\varkappa=|m|}^{N}\frac{(\varkappa-|m|)!}{(\varkappa+|m|)!}b_\varkappa h_\varkappa^{|m|}(\nu)\,P_\varkappa^{|m|}(\mu) + \frac{P\Omega^m(\nu)}{P_{|m|}^{m}(\nu)}\,\delta(\nu-\mu); \tag{31}$$

for $|m| > N$

$$\Phi^m(\nu, \mu) = \delta(\nu-\mu). \tag{32}$$

The complete solution of the Boltzmann equation (2) takes the form

$$\Psi(x, \mu, \varphi) = \sum_{m=-\infty}^{\infty} S_\nu a^m(\nu)\,\Phi^m(\nu, \mu)\,e^{-\frac{x}{\nu}+im\varphi}, \tag{33}$$

where

$$S_\nu f(\nu) = \sum_{\varkappa=-M^m}^{M^m} f(\nu_\varkappa) + \int_{-1}^{1} f(\nu)\,d\nu.$$

The coefficients $a^m(\nu)$ are determined from the boundary conditions.

Number of Discrete Elementary Functions. The function $\Omega^m(z)$ is an analytical function in the expanded complex plane with a cut along a section of the real axis $[-1, 1]$ without any singularities. Hence the number of roots of this function may be determined by means of the principal of the argument

$$2M^m = \frac{1}{2\pi}\Delta_c \arg \Omega^m(z), \tag{34}$$

where the contour c passes around the section $[-1, 1]$.

Carrying out operations analogous to those of [3], for the case in which $\Omega^{m+}(\nu)$ and $\Omega^{m-}(\nu)$ are not equal to zero in the section $[-1, 1]$, i.e.,

$$S^m(\nu) = [P\Omega^m(\nu)]^2 + \left[\frac{\pi c\nu}{2}N^m(\nu)\right]^2 \neq 0 \tag{35}$$

we obtain for $\nu \in [-1, 1]$,

$$M^m = \frac{1}{\pi}\arg \Omega^{m+}(1). \tag{36}$$

Here the signs ± relate to values of the function above and below the cut respectively.

Let us estimate the number of discrete values of ν_i^m. Since $N^m(\nu)$ is an even polynomial of order 2N, the number of roots of the polynomial $\nu N^m(\nu)$ in the section [0, 1] cannot exceed N + 1; there is no less than one root for $\nu = 0$ and no less than m roots for $\nu = 1$ (see Eq. (26)).

Thus

$$m+1 \leqslant M^m \leqslant N+1, \tag{37}$$

where $m \leq N$.

For the case in which $S^m(\nu) = 0$ inequality (37) takes the form

$$m+1 \leqslant M^m + l^m \leqslant N+1,$$

where M^m is determined from Eq. (36) and l^m is the sum of the number of common roots of the polynomials $N^m(z)$ and $R^m(z)$ in the section [0, 1].

Orthogonality and Completeness of the System of Elementary Functions. Let us write the equations for $\Phi^m(\nu, \mu, \varphi)$ and $\Phi^{n*}(\nu', \mu, \varphi)$ in the form:

$$\left(1-\frac{\mu}{\nu}\right)\Phi^m(\nu, \mu, \varphi) = \frac{c}{2}\sum_{\varkappa=|m|}^{N}\frac{(\varkappa-|m|)!}{(\varkappa+|m|)!}P_\varkappa^{|m|}(\mu)\,h_\varkappa^{|m|}(\nu)\,e^{im\varphi};$$

$$\left(1-\frac{\mu}{\nu}\right)\Phi^{n*}(\nu', \mu, \varphi) = \frac{c}{2}\sum_{\varkappa=|n|}^{N}\frac{(\varkappa-|n|)!}{(\varkappa+|n|)!}P_\varkappa^{|n|}(\mu)\,h_\varkappa^{|n|}(\nu')\,e^{-in\varphi}.$$

Let us multiply the first equation by $\Phi^{n*}(\nu', \mu, \varphi)$, and the second by $\Phi^m(\nu, \mu, \varphi)$, and integrate both over all μ and φ. Using the definition of $h_\varkappa^m(\nu)$, and subtracting the first equation from the second, we have:

Declassified and Approved For Release 2013/03/01 : CIA-RDP10-02196R000300100005-6

Declassified and Approved For Release 2013/03/01 : CIA-RDP10-02196R000300100005-6

$$\left(\frac{1}{\nu}-\frac{1}{\nu'}\right)\int_0^{2\pi}\int_{-1}^{1}\mu\Phi^m(\nu,\mu,\varphi)\,\Phi^{n*}(\nu',\mu,\varphi)\,d\mu\,d\varphi=0.$$

Hence for the two elementary functions $\Phi^m(\nu, \mu, \varphi)$ with different m and $\nu \neq \nu'$ (here ν may take both discrete and continuous values) we have

$$\int_{-1}^{1}\int_0^{2\pi}\mu\Phi^m(\nu,\mu,\varphi)\,\Phi^{n*}(\nu',\mu,\varphi)\,d\mu\,d\varphi=0.$$

The norms of the elementary functions $\Phi^m(\nu, \mu, \varphi)$ may be found by direct integration. For discrete values of ν_i^m we obtain

$$N_r^m(\pm\nu_i^m)=\int_0^{2\pi}\int_{-1}^{1}\mu\Phi^m(\pm\nu_i^m,\mu,\varphi)\,\Phi^{m*}(\pm\nu_i^m,\mu,\varphi)\,d\mu\,d\varphi=\pm 2\pi c\nu_i^m\left\{\frac{c(\nu_i^m)^2}{2[(\nu_i^m)^2-1]}\sum_{\kappa=m}^{N}\sum_{n=m}^{N}\frac{(\kappa-m)!}{(\kappa+m)!}\right.$$

$$\times\frac{(n-m)}{(n+m)}\,b_\kappa b_n h_\kappa^m(\nu_i^m)\,h_n^m(\nu_i^m)\,r_{\kappa n}-\frac{1}{2}\sum_{\kappa=m}^{N}\frac{(\kappa-m)!}{(\kappa+m)!}\,b_\kappa[h_\kappa^m(\nu_i^m)]^2$$

$$-\nu_i^m\sum_{\substack{\kappa=m\\ \kappa-\text{odd}}}^{N}\frac{(\kappa-m)!}{(\kappa+m)!}\,b_\kappa h_\kappa^m(\nu_i^m)\sum_{\substack{n=m\\ n-\text{even},\,>m}}^{\kappa-1}(2n+1)\,h_n^m(\nu_i^m)$$

$$\left.-\nu_i^m\sum_{\substack{\kappa=m\\ \kappa-\text{even}}}^{N}\frac{(\kappa-m)!}{(\kappa+m)!}\,b_\kappa h_\kappa^m(\nu_i^m)\sum_{\substack{n=m\\ n-\text{odd}\,>m}}^{\kappa-1}(2n+1)\,h_n^m(\nu_i^m)\right\},\qquad(38)$$

where

$$r_{\kappa n}\begin{cases}1, & \text{when } (\kappa+n)-\text{even},\\ \nu_i^m, & \text{when } (\kappa+n)-\text{odd}.\end{cases}$$

In calculating the norms of the functions $\Phi^m(\nu, \mu, \varphi)$ for continuous values of ν we used the Poisson–Bertrand equation:

$$\int_0^{2\pi}\int_{-1}^{1}\mu\Phi^m(\nu,\mu,\varphi)\int_{-1}^{1}Q(\eta)\,\Phi^{m*}(\nu,\mu,\varphi)\,d\eta\,d\mu\,d\varphi=N_r^m(\nu)\,Q(\nu),\qquad(39)$$

where $N_r^m(\nu)=\nu\left\{\left[\frac{P\Omega^m(\nu)}{P_m^m(\nu)}\right]^2+\left[\frac{c\pi\nu}{2}\cdot\frac{N^m(\nu)}{P_m^m(\nu)}\right]^2\right\}$ and $Q(\eta)$ is an arbitrary function for $\nu\in[-1, 1]$, satisfying the Gelder condition in the same range of ν values.

Let us establish that the resultant system of plane elementary solutions (29), (31), and (32) is complete, i.e., any function $f(\mu, \varphi)$ defined in the interval $a \le \mu \le b$, $c \le \varphi \le d$, where $-1 \le a < b \le 1$, $0 \le c < d \le 2\pi$, may be expanded with respect to this system.

Let the function $f(\mu, \varphi)$ be expanded in a descending Fourier series with respect to the functions [8]

$$e^{\frac{im\pi\varphi}{c-d}},\qquad(40)$$

where $m = 0, \pm1, \pm2, \ldots$, in the section [c, d] and satisfies the condition H* [9] in the interval (a, b), i.e., for any μ_1 and μ_2 out of the interval (a, b) the condition

$$|f(\mu_2,\varphi)-f(\mu_1,\varphi)|\le c(\varphi)\,|\mu_2-\mu_1|^\alpha\qquad(41)$$

is satisfied, where $c(\varphi)$ is a positive function integrable in the section [c, d] and α is a positive constant ($\alpha < 1$). In addition to this, around the ends a and b $f(\mu, \varphi)$ behaves as

$$f(\mu,\varphi)=\frac{f^*(\mu,\varphi)}{|\mu-u|^\beta},\quad 0\le\beta<1.\qquad(42)$$

Here $f^*(\mu, \varphi)$ is a function satisfying condition (41) in the section $[a, b]$, u is one of the ends of $[a, b]$: a or b.

Declassified and Approved For Release 2013/03/01 : CIA-RDP10-02196R000300100005-6

Declassified and Approved For Release 2013/03/01 : CIA-RDP10-02196R000300100005-6

Many interesting physical problems satisfy conditions (40-42).

The system of plane elementary solutions is complete if the integral equation

$$f(\mu, \varphi) = \sum_{m=-\infty}^{\infty} S_{\nu} a^m(\nu)\, \Phi^m(\nu, \mu)\, e^{\frac{im\pi\varphi}{c-d}}, \tag{43}$$

where $a \leq \nu \leq b$ has a unique solution.

Expanding $f(\mu, \varphi)$ with respect to the system of functions $e^{in\pi\varphi/(c-d)}$ we transform from the integral equation (43) to a system of integral equations for the function $f^m(\mu)$:

$$f^m(\mu) = S_{\nu} a^m(\nu)\, \Phi^m(\nu, \mu),$$

where $m = 0, \pm 1, \pm 2 \ldots$

We obtain the condition H* for the functions $f^m(\mu)$ by using conditions (41) and (42):

$$|f^m(\mu_2) - f^m(\mu_1)| = \left| \frac{1}{c-d} \int_c^d [f(\mu_2, \varphi) - f(\mu_1, \varphi)]\, e^{\frac{im\pi\varphi}{c-d}} d\varphi \right|$$

$$\leqslant \frac{1}{c-d} \int_c^d |f(\mu_2, \varphi) - f(\mu_1, \varphi)|\, \left| e^{\frac{im\pi\varphi}{c-d}} \right| d\varphi \leqslant c_1 |\mu_2 - \mu_1|^{\alpha}, \tag{45}$$

where $c_1 = \int_c^d c(\varphi)\, d\varphi/(c-d)$.

Analogously we may find how $f^m(\mu)$ behave around the ends of the section $[a, b]$:

$$f^m(\mu) = \frac{f^{*m}(\mu)}{|\mu - u|^{\beta}}, \quad 0 \leqslant \beta < 1. \tag{46}$$

The uniqueness of the solution of the integral equation (44) in the section $[a, b]$ is proved in the same way as in [3]. The coefficients $f^m(\mu)$ uniquely determine the function $f(\mu, \varphi)$ [8].

Thus the completeness of the system of plane elementary solutions is established.

Calculation of Cylindrical Cells. The complete system of plane elementary solutions thus obtained was used in order to modify the program "Praktinets" by means of which the characteristics of a cell may be calculated even in the linear-anisotropic approximation. Using the modified "Praktinets" program we calculated three cells: in the isotropic (zero term retained in expansion of the scattering indicatrix), linear-anisotropic, and transport [Σ_S replaced by $\Sigma_S(1 - \bar{\mu})$] approximations. The cells were chosen from the condition that the scattering anisotropy should have a considerable effect on the thermal-neutron use factor in the cells. The results of the calculations are presented in Table 1.

The original data were: for cell 1 – $r_1 = 0.199$ cm; $r_2 = 0.525$ cm; $\mu_1 = 0$; q_1† = 0; $\Sigma_1 = 2.601$ cm^{-1}; $\Sigma_1^a = 2.052$ cm^{-1}; $\mu_2 = 0.3$; $q_2 = 1$; $\Sigma_2 = 3.470$ cm^{-1}; $\Sigma_2^a = 0.0196$ cm^{-1}. For cell 2 – $r_1 = 0.169$ cm; $r_2 = 0.199$ cm; $r_3 = 0.525$ cm; $\mu_1 = 0$; $q_1 = 0.0170$; $\Sigma_1 = 3.211$ cm^{-1}; $\Sigma_1^a = 2.755$ cm^{-1}; $\mu_2 = 0$; $q_2 = 0.0319$; $\Sigma_2 = 1.115$ cm^{-1}; $\Sigma_2^a = 0.221$ cm^{-1}; $\mu_3 = 0.3$; $q_3 = 3.256$; $\Sigma_3 = 3.511$ cm^{-1}; $\Sigma_3^a = 0.020$ cm^{-1}. For cell 3 – $r_1 = 1.3$ cm; $r_2 = 1.7$ cm; $r_3 = 11.90$ cm; $\mu_1 = 0$; $q_1 = 0$; $\Sigma_1 = 0.720$ cm^{-1}; $\Sigma_1^a = 0.320$ cm^{-1}; $\mu_2 = 0.3$; $q_2 = 22.75$; $\Sigma_2 = 2.878$ cm^{-1}; $\Sigma_2^a = 0.020$ cm^{-1}; $\mu_3 = 0.056$; $q_3 = 1$; $\Sigma_3 = 0.39331$ cm^{-1}; $\Sigma_3^a = 0.00031$ cm^{-1}.

We see from Table 1 that the values of θ calculated on the isotropic and linear-anisotropic approximations differ by –0.32% (–0.32%)‡, –0.33% (–0.33%), and –1.6% (–1.6%), while the values calculated in the transport and linear-anisotropic approximations differ by –0.14% (–0.11%), –0.19% (–0.12%), and –0.11% (–0.12%) for cells 1, 2, and 3. In a uranium–graphite cell with a light-water coolant (cell 3) the transport approximation accounts for almost the whole influence of the scattering anisotropy on θ.

The author wishes to thank N. I. Laletin for proposing this theme and for useful discussions, and also V. I. Lebedev for valuable comments.

†q is the density of the neutron source.

‡The difference for the G_1 approximation is given in brackets.

Declassified and Approved For Release 2013/03/01 : CIA-RDP10-02196R000300100005-6

Declassified and Approved For Release 2013/03/01 : CIA-RDP10-02196R000300100005-6

LITERATURE CITED

1. K. Case, Ann. Phys., 9, 1 (1960).
2. R. Zelazny et al., Ann. Phys., 16, 69 (1961).
3. I. Mika, Nucl. Sci. and Engng., 11, 415 (1961).
4. N. I. Laletin, At. Energ., 26, 370 (1969).
5. I. S. Gradshtein and I. M. Ryzhik, Tables of Integrals, Sums, Series, and Products [in Russian], Fizmatgiz, Moscow (1963).
6. K. Case and P. Zweifel, Linear Transport Theory, Addison–Wesley (1967).
7. N. I. Laletin, Preprint IAE-1828 (1969).
8. G. M. Fikhtengol'ts, Course of Differential and Integral Calculus [in Russian], Vol. 3, Fizmatgiz, Moscow (1969).
9. N. I. Muekhelishvili, Singular Integral Equations [in Russian], Gostekhizdat, Moscow (1946).

Declassified and Approved For Release 2013/03/01 : CIA-RDP10-02196R000300100005-6

Declassified and Approved For Release 2013/03/01 : CIA-RDP10-02196R000300100005-6

ON ESTIMATING THE COST OF PROCESSING LIQUID RADIOACTIVE WASTE

B. S. Pavlov-Verevkin and M. F. Krasnaya

UDC 338.621.039.7.14

The fundamental economic index in the operation of chemical water-purifying plants is the cost of processing 1 m^3 of waste water. This quantity depends on the processing technology adopted, the level of automation of the process, the cost of the reagents employed, and so on. In order to estimate the effects of these factors which determine the cost of processing waste water, let us consider the corresponding data relating to the water-purifying stations of various countries characterized by different powers and different processing techniques. These data are presented in Table 1, in which lines 1, 2, 4-7-9, 11-13 are taken from [1], lines 6 and 12 from [2]. The same data are also presented in Fig. 1.

Despite the great difference in the processing technologies adopted in different water-purifying stations (from evaporation to controlled ejection without processing), all the points in the figure groups neatly around a straight line, the equation of which may be approximately written

$$\lg C = -0.777 \lg Q + 4.222, \tag{1}$$

if the cost is expressed in dollars/m^3 or

$$\lg C = -0.777 \lg Q + 4.176, \tag{1a}$$

in roubles/m^3.

Since we have considered data relating to water-purifying installations in different countries, this line expresses a kind of "world-average" cost of processing water in relation to the productivity of each station. Thus the dependence of cost on the productivity of the installation may be traced quite clearly.

Attention should be drawn to the fact that the real costs of treatment may lie either above or below the mean cost line. If we consider the position of corresponding points relative to the world-average cost, taking account of the technological procedure of treating the water used in each station, we see that the more complex the technology the higher is the cost of treatment.

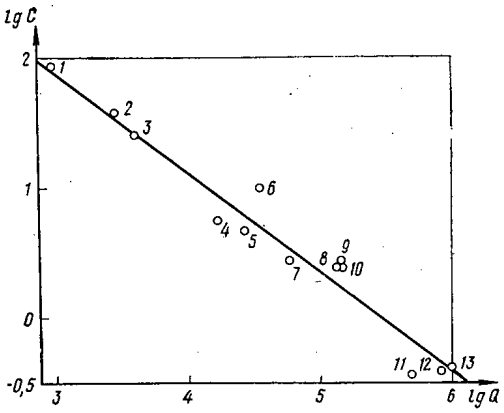

Fig. 1. Cost of treating waste water in dollars/m^3 (C) as a function of the annual output (Q) of the purifying plants (the numbers of the points correspond to the numbers of the lines in Table 1).

Thus evaporation (point 1), two-stage chemical purification (point 2), the successive use of two or more stages of purification (points 6, 8-10) raise the cost of treatment by comparison with the average cost for the particular output of the station. For example, stations using evaporation to purify all the water (point 1) spend 5-7 dollars/m^3 more on processing than indicated by Eq. (1).

On the other hand, the decantation of some (points 4 and 5) or all (points 11 and 12) the waste without processing reduces the cost of treatment.

Thus for various productivities of water-purifying stations the cost of treatment is determined primarily by the productivity, and for equal productivities by the technological procedures employed, on which the cost of the reagents also depends. For estimating the efficiency of the automation of the process there are as yet no comparable data.

Translated from Atomnaya Énergiya, Vol. 32, No. 6, pp. 463-464, June, 1972. Original article submitted September 23, 1971.

© 1972 Consultants Bureau, a division of Plenum Publishing Corporation, 227 West 17th Street, New York, N. Y. 10011. All rights reserved. This article cannot be reproduced for any purpose whatsoever without permission of the publisher. A copy of this article is available from the publisher for $15.00.

Declassified and Approved For Release 2013/03/01 : CIA-RDP10-02196R000300100005-6

Declassified and Approved For Release 2013/03/01 : CIA-RDP10-02196R000300100005-6

TABLE 1. Productivity, Cost of Processing, and Methods of Purifying Water at Various Waste-Deactivation Stations

Serial number	Undertaking	Productivity Q, m^3/year	lg Q	Cost of purification C, dollars/m^2	lg G	Method of purification and removal
1	2	3	4	5	6	7
1	Grenoble, France	950	2.978	88.0	1.945	Evaporation, still residues cemented
2	Karlsruhe, West Germany	3000	3.477	38.3	1.583	Two-stage chemical purification, pulp filtered, residue enclosed in barrels
3	Chemical water-purifying equipment of a radiochemical laboratory	4000	3.602	25.3	1.403	One two-stage chemical purification, condensed pulp stored in tanks
4	Studwig, Sweden	17000	4.230	5.7	0.756	Monitoring, ejection into the sea, or evaporation, still residues kept in vessels
5	Tokai-Mura, Japan	27700	4.443	4.7	0.672	Monitoring, ejection into the sea, 50% waste purified by ion exchange and electrolysis, regenerates evaporated, concentrate cemented
6	Leningrad Station, USSR	36000	4.556	10.33	1.014	Coagulation, evaporation, purification completed by ion exchange
7	Mole, Belgium	62500	4.796	2.7	0.431	Chemical purification with subsequent ion exchange, pulp bitumenized
8	Harwell, England	137000	5.137	2.4	0.380	Chemical purification, sorption in vermiculite, pulp condensed and buried
9	Moscow Purification Station, USSR (1966 data)	150000	5.176	2.7	0.431	Coagulation, two-stage ion-exchange purification, regenerates evaporated. Liquid concentrate conveyed to burial station (cost of transport not considered)
10	Moscow Purification Station, USSR (1970 data)	150000	5.176	2.43	0.386	The same
11	Argonne, USA	500000	5.699	0.37	−0.432	Large volumes of low-activity waste (10^{-10}- 10^{-8} Ci/liter) removed without processing, sometimes after preliminary holding
12	Oak Ridge, USA	850000	5.929	0.38	−0.420	
13	Harwell, England	1000000	6.000	0.41	−0.387	

We calculated the cost of the deactivation of waste water from a radiochemical laboratory in water-purifying installations with a productivity of 4000 m^3/yr. We allowed for all the expenses specified in [1] in order to obtain data comparable with Table 1. In 1970 the cost of deactivation was 22.80 roubles/m^3 or 25.3 dollars/m^3, regarding 1 dollar as equal to 0.90 roubles. We see from Fig. 1 (point 3) that this cost is also close to the world average, but slightly below it, since for a productivity of 4000 m^3/yr the latter equals 26.5 dollars/m^3 by Eq. (1). The low cost is due to the fact that the deactivation of the low-activity water from a radiochemical laboratory is achieved by a single chemical precipitation, and only in rare cases (less than 2% of the total volume) is a second similar treatment required.

Naturally the coefficients of Eq. (1) obtained from a comparison of a small number of data may require refinement; however, until a broader base of comparison has been attained these may reasonably be used in order to estimate the expenses required for the treatment of radioactive waste water.

The equation thus obtained may also be used for a comparative estimate of the economic efficiency of water-purifying stations of different powers, for which a direct comparison of the cost of treating the water is impossible. In this case we may compare the cost of treating the water at each stage with the values obtained from Eq. (1) and draw conclusions on the basis of this comparison.

LITERATURE CITED

1. V. M. Sedov, At. Énerg., 23, 173 (1967).
2. A. N. Kondrat'ev et al., Management of Low and Intermediate Level Radioactive Wastes, IAEA, Vienna (1970), p. 297.

Declassified and Approved For Release 2013/03/01 : CIA-RDP10-02196R000300100005-6

Declassified and Approved For Release 2013/03/01 : CIA-RDP10-02196R000300100005-6

TISSUE DOSES FROM HIGH-ENERGY NUCLEONS

I. M. Dmitrievskii, Ya. I. Kabakov,
E. L. Potemkin, and V. V. Frolov

UDC 539.12.08

At the present time, there is practically no data on the dose characteristics of nucleons with energies greater than 3 GeV needed for manned space flight. Existing calculations of tissue doses are mainly based on Monte Carlo calculations and have been carried out for nucleons with energies up to 2-3 GeV [1, 2]. The extension of such techniques to higher energies runs into considerable difficulty because of the lack of information about the differential characteristics of nuclear interactions between nucleons and the elements in tissue and because of the considerable increase in machine time needed to carry out such calculations.

It should be pointed out that the idea of "dose" embodies an averaged characteristic of the effect of radiation on matter and consideration of many details of the interaction (Monte Carlo program) with subsequent averaging is not always justified. Using average characteristics of a nuclear interaction for a solution of this problem is completely permissible. Such an approach reduces the volume of computation considerably and is justified by the fact that existing nuclear interaction theory and experiment give the most reliable data for precisely these average characteristics. Such an approach was proposed earlier for the calculation of doses from nucleons with energies to 2 GeV [3]. The extension of this method to higher energies is the purpose of this paper.

Computational Method. The absorbed dose and the dose equivalent for nucleons was calculated for a phantom in the form of a uniform slab 30 cm thick having infinite transverse dimensions. Tissue composition corresponded to $H_{140}C_{21}N_3O_{57}$. Tissue density was assumed to be 1 g/cm^3. It was assumed that the homogeneous tissue phantom was irradiated on one side of the slab by a normally incident, uniform beam of nucleons.

In the general case, penetration of particles through matter is described by a system of integro-differential equations similar to the well-known kinetic or transport equation. An energy distribution function

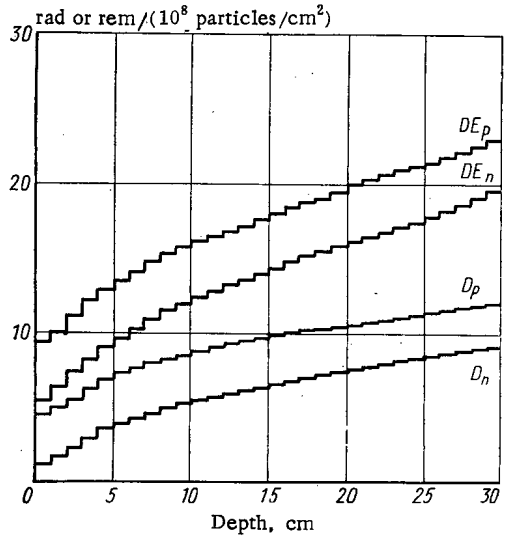

Fig. 1. Absorbed dose D and dose equivalent DE for 3 GeV protons and neutrons.

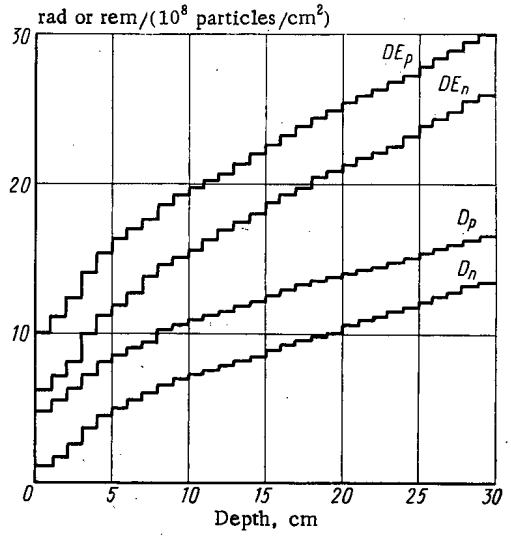

Fig. 2. The same as Fig. 1 for 5 GeV particles.

Translated from Atomnaya Énergiya, Vol. 32, No. 6, pp. 465-470, June, 1972. Original article submitted October 7, 1971; revision submitted December 30, 1971.

© 1972 Consultants Bureau, a division of Plenum Publishing Corporation, 227 West 17th Street, New York, N. Y. 10011. All rights reserved. This article cannot be reproduced for any purpose whatsoever without permission of the publisher. A copy of this article is available from the publisher for $15.00.

Declassified and Approved For Release 2013/03/01 : CIA-RDP10-02196R000300100005-6

Declassified and Approved For Release 2013/03/01 : CIA-RDP10-02196R000300100005-6

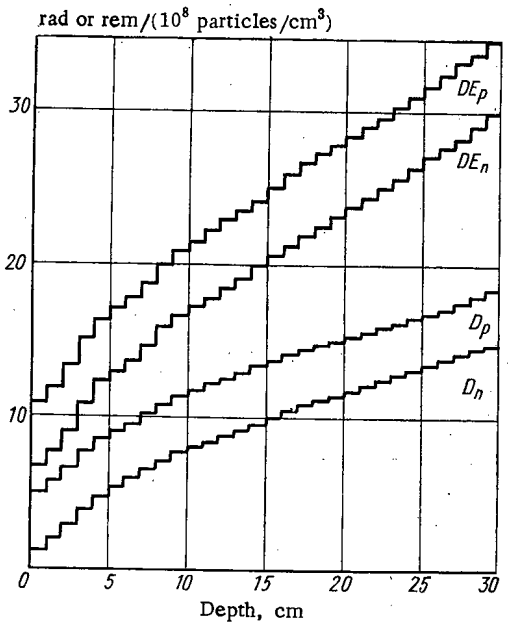

Fig. 3. The same as Fig. 1 for 10 GeV particles.

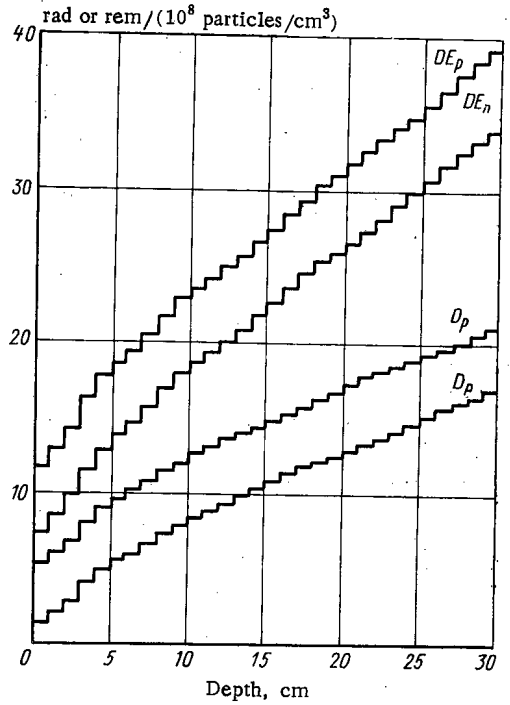

Fig. 4. The same as Fig. 1 for 20 GeV particles.

for cascade particles with energies above 0.4 GeV was obtained from the solution of the kinetic equation. To convert from the distribution function found for the cascade particles to a dose distribution, a method was used which was proposed in [3] and which was based, as has already been mentioned, on the use of average characteristics of a nuclear interaction.

Experimental and theoretical data show that secondary fast cascade particles emerging from the nucleus are mainly contained within a narrow cone around the direction of the incident particle. This situation makes it possible to reduce the problem to a one-dimensional problem (straight-ahead approximation). Calculations made in [4] show good agreement between dose distributions calculated by the straight-ahead approximation and those obtained by detailed Monte Carlo calculations for 0.1 GeV protons. With an increase in incident particle energy, the straight-ahead approximation becomes increasingly more accurate.

To solve the equation, the following additional assumptions were also made:

1) the inelastic interaction cross section for nucleons and mesons is independent of particle energy;

2) stopping powers are constant for all charged particles;

3) the change in energy of primary and cascade particles because of elastic scattering by nuclei is insignificant;

4) neutral pions decay at the point of creation and do not participate in the nuclear cascade process;

5) the difference between positively and negatively changed particles is small;

6) the decay probability for charged pions is insignificant.

Under these assumptions, the equation system for the nuclear cascade process is written as

$$\frac{d}{dx} n_i(E, x) + \Sigma_i n_i(E, x) = \sum_{\kappa} \int_{E}^{E_0} \frac{d\Sigma_{i\kappa}(E', E)}{dE'} n_\kappa(E', x)\, dE',$$

where $n_i(E, x)$ is the distribution function for particles of the i-th kind having an energy E; Σ_i is the macroscopic cross section for interactions between particles of the i-th kind and nuclei in tissue; and $d\Sigma_{ik}(E', E)/dE'$ is the differential cross section for the production of particles of the i-th kind having an energy E from the interaction with tissue nuclei of particles of the k-th kind having an energy E'.

Declassified and Approved For Release 2013/03/01 : CIA-RDP10-02196R000300100005-6

Declassified and Approved For Release 2013/03/01 : CIA-RDP10-02196R000300100005-6

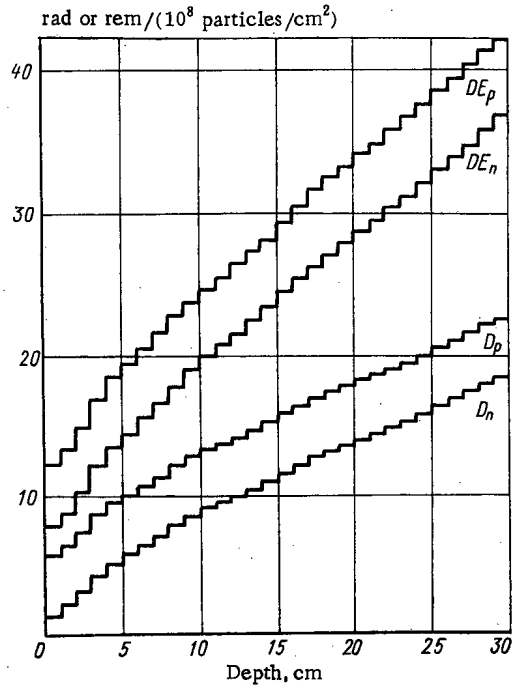

Fig. 5

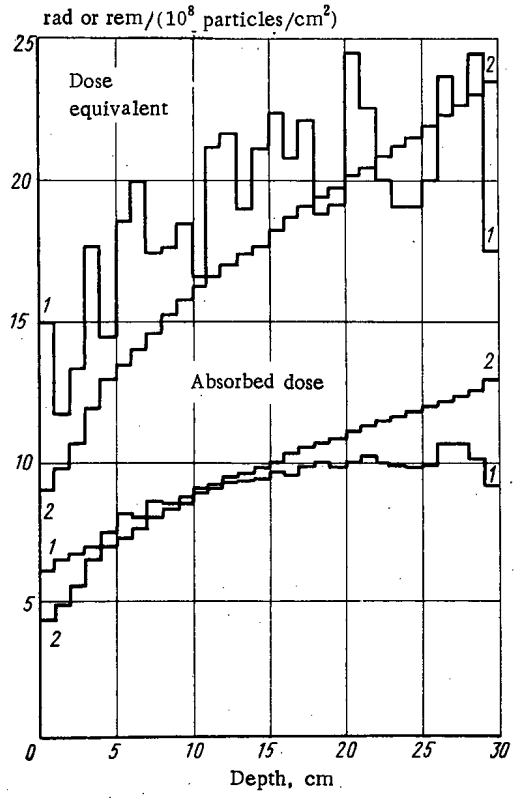

Fig. 6

Fig. 5. The same as Fig. 1 for 30 GeV particles.

Fig. 6. Comparison of depth dose distributions for 3 GeV protons calculated in [2] (curve 1) with similar data obtained in the present work (curve 2).

In solving the equation system, differential cross sections given by the Trilling formulas [5] were used for the primary proton. The calculations were made under the assumption that the secondary particle spectrum was the same for pion–nucleus and nucleon–nucleus interactions. Since the ratio $d/\lambda_i \leqslant 3/8$ (d is phantom dimension and $\lambda_i = 1/\Sigma_i$) is rather small for this problem, the equation system was solved by successive approximation, keeping the first three terms. The error because of cutoff of succeeding terms in the iteration series was no greater than 1%.

The transformation from the resultant distribution of cascade particles to a dose distribution was performed in the following manner. In the calculations, it is convenient to represent the total dose in the form of a sum

$$D = D_1 + D_2 + D_3,$$

where D_1 is the dose resulting from the energy deposited by ionization loss of charged cascade particles with energies above 0.4 GeV; D_2 is the dose resulting from energy transferred by cascade particles with energies below 0.4 GeV through ionization loss and nuclear interaction; and D_3 is the dose resulting from energy transferred by particles formed in the evaporative stage of cascade particle interaction.

The first term in this sum was computed from the equation

$$D_1(x) = \sum_i \int_{0.4\,\text{GeV}}^{E_0} n_i(E, x) \left(\frac{dE}{dx}\right)_{\text{ion}} dE$$

using ionization losses calculated by the Bethe–Bloch formula. Consideration of the effect of δ-rays, which are formed during the penetration of high-energy charged particles, on dose distribution by a method similar to that described in [6] shows that this effect reduces the value of D_1 by 20% at the surface and by 10% at a depth of 5 cm. Considering the comparatively small contribution of D_1 to the total dose, this effect can be neglected. In transforming from absorbed dose to dose equivalent, a quality factor of one was used in calculations of D_1.

Declassified and Approved For Release 2013/03/01 : CIA-RDP10-02196R000300100005-6

Declassified and Approved For Release 2013/03/01 : CIA-RDP10-02196R000300100005-6

In the calculation of D_2, it was assumed that this part of the dose was determined mainly by the total number of cascade particles with energies below 0.4 GeV; the effect of the shape of their spectral distribution is not critical. In addition, use was made of the experimental fact that the number of cascade nucleons with energies less than 0.4 GeV and their average energy is independent of the energy of the primary particles in the high-energy region (from several GeV to 10^3 GeV) [7]. On this basis, the spectrum of cascade nucleons with energies below 0.4 GeV given in [8] was used in the calculations.

The pion energy spectrum was determined by the Trilling formula. The calculation of D_2 was carried out in the straight-ahead approximation using the equation

$$D_2(x) = \sum_i \sum_\kappa \int_{0.4\,\text{GeV}}^{E_0} \int_0^x dx' \int_0^{0.4\,\text{GeV}} \frac{d\Sigma_{i\kappa}(E', E)}{dE'} n_i(E, x') D_\kappa(x - x', E)\, dE',$$

where E is the energy of cascade particles above 0.4 GeV, $D_k(x, E')$ is the dose distribution for particles of the k-th kind, and $d\Sigma_{ik}(E', E)/dE'$ is the energy spectrum of particles with energies up to 0.4 GeV for incident particles of energy E.

Data on the distributions of absorbed dose and dose equivalent from nucleons below 0.4 GeV were taken from [9, 10].

In the calculation of D_3, a basic characteristic of the evaporative stage of nuclear interaction was used – an average excitation energy which is only slightly dependent on the energy of the incident nucleons. A significant rise in average excitation energy with increase in incident particle energy pointed out in some theoretical papers is contradicted by experimental data [11] on the constancy of dense tracks and of the average energy of individual types of evaporated particles obtained in studies of nuclear collisions in emulsions.

We assumed the average excitation energy to be constant and equal to 30 MeV for incident nucleons and 50 MeV for pions [8, 9, 12-14]. In calculating the quality factor for radiation arising in the evaporative stage of a nuclear interaction, use was made of the fact that the composition of this radiation is independent of the energy of the incident nucleons. The quality factor was calculated by taking into account the composition and energy spectra of evaporated particles on the basis of experimental data for the reaction of 660 MeV protons with C^{12} [15, 16].

Since mainly low-energy, short-range particles are emitted in the evaporative stage of an interaction, it was assumed that the energy deposited was absorbed locally:

$$D_3(x) = \sum_i \int_{0.4\,\text{Гэв}}^{E_0} n_i(E, x)\, \Sigma_i E_i^*\, dE,$$

where E_i^* is the average excitation energy of the residual nucleus formed by the interaction between cascade particles of the i-th kind with energies above 0.4 GeV and nuclei in tissue.

As mentioned above, it was assumed in the calculations that π^0 mesons formed in a cascade decay into two γ-quanta. The contribution to the dose because of the resulting electron–photon shower was calculated by using the dose distribution for γ-rays [17] and their distribution function obtained from the equation for the nuclear cascade process.

Since the recoil nuclei which are produced in elastic scattering are absorbed locally, their contribution to the dose will be determined by the average recoil energy and the distribution function for the cascade particles.

The average nuclear recoil energy was calculated from the angular distributions of elastically scattered particles [18] using the well-known relativistic relations between angle and energy. The quality factor was assumed to be 20 for the nuclei C^{12}, N^{14}, and O^{16}; for the hydrogen nucleus, it was assumed to be 1.5 (on the basis of dependence on the linear energy transfer of the radiation).

Results of the Calculation. Calculations of depth dose distribution for the absorbed dose and the dose equivalent were carried out by the proposed method for nucleons with energies of 3, 5, 10, 20, and 30 GeV. Some of the results are shown in Figs. 1-5. The results show that the absorbed dose and the dose equivalent increase with depth in the slab for both protons and neutrons of the energies mentioned, reaching a maximum value at the end of the slab.

Declassified and Approved For Release 2013/03/01 : CIA-RDP10-02196R000300100005-6

Declassified and Approved For Release 2013/03/01 : CIA-RDP10-02196R000300100005-6

The most rapid increase with depth is observed in the first 5-10 cm at the surface of the slab with subsequent reduction in curvature; this results from the attainment of equilibrium for the low-energy portion of the cascade protons, which have a range close to the slab dimension.

As the energy increases, the maximum and average tissue doses also increase; however, this rise is comparatively small. For an increase in energy from 3 to 30 GeV, the absorbed dose and dose equivalent increase by a factor of 1.8 for protons and 1.9 for neutrons.

The quality factor, calculated as the ratio of the maximum dose equivalent to the maximum absorbed dose, is practically constant in the nucleon energy range from 3 to 30 GeV and is 2 for neutrons and 1.9 for protons.

Comparison with Other Results. Since there are no theoretical or experimental papers on the determination of dose distribution from nucleons with energies above 3 GeV, our results were compared with the results of Monte Carlo calculations [2] for 3 GeV nucleons. Such a comparison with the results of the detailed calculations carried out in [2] is of interest because the proposed method of calculation is an approximate one. The comparison shown in Fig. 6 is evidence of acceptable agreement. The few discrepancies are apparently the result of lack of consideration of the angular distribution of cascade nucleons with energies below 0.4 GeV.

A comparison of our data with experimental data for 2.9 GeV protons [19] reveals the overestimate of absorbed dose at the edge of the slab common to all theoretical papers which may possibly be the result of some systematic property of the experiments or a lack of completely identical geometries for both theory and experiment.

In conclusion, we point out the need for expansion of theoretical and experimental work on the determination of tissue dose from high-energy particles, paying particular attention to experiments on the depth distribution of dose equivalent and quality factor, and to calculations at high energies and for other geometrics including consideration of tissue inhomogeneity.

LITERATURE CITED

1. H. Wright et al., Health Phys., 16, 13 (1969).
2. R. Alsmiller et al., ORNL-TM-2924 (1970).
3. I. M. Dmitrievskii, E. L. Potemkin, and V. V. Frolov, in: Dosimetry and Physics of Accelerator Shielding [in Russian] (JINR-16-4888), JINR, Dubna (1970).
4. R. Alsmiller et al., NASA SP-71-1965 (1965).
5. J. Ranft, Nucl. Instrum. and Methods, 48, 133 (1967).
6. R. Vora et al., Health Phys., 16, 139 (1968).
7. V. S. Murzin and L. N. Sarycheva, Cosmic Rays and Their Interactions [in Russian], Atomizdat, Moscow (1968), p. 106.
8. F. P. Denisov et al., FIAN Preprint A-3 (1962).
9. J. Turner et al., Health Phys., 10, 783 (1964).
10. C. Zerbv et al., Nucl. Instrum. and Methods, 36, 125 (1965).
11. See [7], p. 110.
12. V. S. Barashenkov et al., JINR Preprint P2-5118 (1970).
13. V. S. Barashenkov et al., JINR Preprint P2-5963 (1971).
14. E. Gross, UCRL 3300 (1956).
15. A. P. Zhdanov et al., Zh. Éksp. i Teor. Fiz., 37, 392 (1959).
16. P. N. Fedotov, Dissertation [in Russian], Leningrad (1961).
17. H. Beck, Nucl. Instrum. and Methods, 78, 333 (1970).
18. J. Ranft, Nucl. Instrum. and Methods, 32, 65 (1965).
19. L. Phillips et al., Nucleonics, 21, 55 (1963).

Declassified and Approved For Release 2013/03/01 : CIA-RDP10-02196R000300100005-6

Declassified and Approved For Release 2013/03/01 : CIA-RDP10-02196R000300100005-6

COMPUTATION OF THERMAL CONSTRICTION RESISTANCE IN THE PRESENCE OF CONTACT OF LAMINAS WASHED BY HEAT TRANSFER AGENT

V. V. Kharitonov, L. S. Kokorev, and V. K. Yurenko

UDC 621.039.517

The thermal conductivity in the presence of contact of the core with the casing of the fuel element of a nuclear reactor is made up of the conductivity of the actual contact and the conductivity of the medium in the gap.* The constriction resistance, i.e., the inverse of the conductivity of the actual contact, is usually taken in the computations to be the same as in the case of contact of semiinfinite bodies. The mathematical analysis of the effect of the thickness of the casing and the conditions of external heat exchange on the thermal constriction resistance $R_c = (\vartheta_c/q)(\lambda/b)$ shows that the effect can be significant for thin-walled casings (in annular or laminar fuel elements), especially for strip contacts. Here q is the nominal heat flux, W/m^2; ϑ_c is the temperature thrust caused by the constriction of the lines of heat flow toward the sites of actual contact, °C; λ is the thermal conductivity of the material of the case, W/m·deg; b is the halfwidth (radius) or the equivalent cell.

In this case the thermal constriction resistance is equal to the sum $R_\infty + \Delta R$, i.e., the effect of the resistance corresponding to the contact of semiinfinite bodies

$$R_\infty = \begin{cases} -\frac{2}{\pi} \ln \sin \frac{\pi}{2} \eta & \text{for strip,} \\ \frac{8}{3\pi} \frac{(1-\eta)^{3/2}}{\eta} & \text{for spot,} \end{cases}$$

and the correction reflecting the effect of the thickness and the external heat exchange, which is computed numerically by the following formulas:

$$\Delta R = \begin{cases} \frac{2}{\pi} \frac{(1-\operatorname{th} \pi\delta)(\pi\delta - Bi)}{Bi + \pi\delta \operatorname{th} \pi\delta} (1-\eta)^{3/2} (1+e^{-8\delta}) & \\ 2 \frac{(1-\operatorname{th} 3.8\delta)(3.8\delta - Bi)}{Bi + 3.8\delta \operatorname{th} 3.8\delta} (1-\eta)^2 & \text{for spot.} \end{cases} \quad \text{for strip;}$$

$$\delta = l/b \geqslant 0.1; \quad \eta = a/b \leqslant 0.4; \quad 0 \leqslant Bi \leqslant \infty.$$

Here $Bi = \alpha l/\lambda$ is Biot number, in which α is the heat-transfer coefficient, W/m^2·deg; a is the halfwidth or radius of the area of contact. In the range of values of the thickness corresponding to $\delta = l/b > 0.1$ (2b is the distance between contact strips or spots) for any value of Biot number and for relative area of contact $\eta \leq 0.4$ these expressions give an error less than 15%.

This correction rapidly decreases in absolute value with the increase in the thickness of the body. The correction can be neglected for all values of Biot number and relative area of contact with an error not exceeding 10%, if the thickness of the casing exceeds 1/3 of the distance between the contact strips or spots.

By way of illustration of the results an example is given: for the contact of two casings of equal thickness $\delta = 0.1$ when $\lambda = 25$ W/m·deg, $q = 10^5$ W/m^2, $\eta = 0.02$ and for undulation step $b = 2.5 \cdot 10^{-3}$ m the temperature drop at the contact for Bi equal to 0.1 and 10 is 60 and 32°C, respectively, i.e., the values differ by a factor of two.

*N. N. Del'vin et al., see the following article.

Translated from Atomnaya Énergiya, Vol. 32, No. 6, p. 471, June, 1972. Original article submitted June 12, 1971.

© 1972 Consultants Bureau, a division of Plenum Publishing Corporation, 227 West 17th Street, New York, N. Y. 10011. All rights reserved. This article cannot be reproduced for any purpose whatsoever without permission of the publisher. A copy of this article is available from the publisher for $15.00.

Declassified and Approved For Release 2013/03/01 : CIA-RDP10-02196R000300100005-6

Declassified and Approved For Release 2013/03/01 : CIA-RDP10-02196R000300100005-6

CONTACT CONDUCTIVITY OF CYLINDRICAL BODIES IN DENSE AND RAREFIED GASEOUS MEDIA

N. N. Del'vin, L. S. Kokorev,
Ya. A. Bychko, and E. K. Shmachkov

UDC 621.039.517.5

In the computation of the total value of the contact conductivity α_c between the core and the casing of fuel elements of a nuclear reactor problems appear that are related to the role of the dependence of the conductivity of the actual contact α_a on the temperature field in the fuel element and the presence of the gaseous medium in the gaps between the contacts. The characteristics of the relation between the contact pressure and the conductivity are investigated in [1] for different regimes of fitting and operation of the fuel elements.

This article shows what is the contribution of the conductivity of the gaseous medium α_g^{eff} in the total contact conductivity between the heat-releasing core and the casing cooled by the heat-transfer agent, and how its magnitude depends on the degree of rarefaction of the gas.

Results of investigations aimed at the solution of these problems in relation to the conditions of fuel elements in a nuclear reactor are not available in the literature; the only works considering the effect of gas pressure on α_g^{eff} are [2, 3].

The first problem is solved on an analog computer USM-1. The properties of the medium filling the gap are varied and also the profile of this gap. It is found that the total contact conductivity can be calculated from the formula

$$\alpha_c = \alpha_a + \alpha_g^{eff}$$

with an error not exceeding 15%.

The effective conductivity α_{go}^{eff} for a dense gaseous medium in the gap can be approximated by the equation (up to $\eta \leq 0.4$)

$$\alpha_{go}^{eff} = \frac{\lambda_{go}}{\delta_{eff}} = \frac{\lambda_{go}}{\bar{\delta}(1-\eta)(1-\varepsilon)},$$

where λ_{go} is the coefficient of thermal conductivity of the continuous gas; η, ε are respectively the relative values of the area of the actual contact and the proximity of the bodies; $\bar{\delta}$ is the mean height of the gap.

Using well-known results of the molecular–kinetic theory of gases we obtain the equation for the function Ψ determining the dependence of α_g^{eff} on the degree of rarefaction of the gas:

$$\Psi = \frac{\alpha_g^{eff}}{\alpha_{go}^{eff}} = 1 - \exp\left(-\frac{1}{Kn_0}\right),$$

where $Kn_0 = \Lambda/\delta_{eff}$ is Knudsen number; Λ is the mean free path of gas molecules in infinite space.

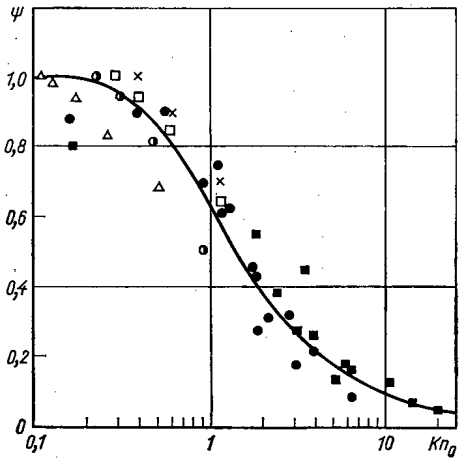

Fig. 1. Dependence of the effective conductivity of gaseous interlayer on the degree of rarefaction of the gas: ——) computed from the equation

$$\Psi = \frac{\alpha_g^{eff}}{\alpha_{go}^{eff}} = 1 - \exp\left(-\frac{1}{Kn_0}\right).$$

Data of the present article for argon: ●) δ = const; ■) zirconium grade 30. Data of [3] for aluminum–aluminum contact: ×) air; ◑) hydrogen; □) helium; for uranium–aluminum contact: △) hydrogen.

Translated from Atomnaya Énergiya, Vol. 32, No. 6, pp. 471-472, June, 1972. Original article submitted August 20, 1971.

Declassified and Approved For Release 2013/03/01 : CIA-RDP10-02196R000300100005-6

Declassified and Approved For Release 2013/03/01 : CIA-RDP10-02196R000300100005-6

An experimental verification of the proposed analytical dependence has also been carried out in conditions of an annular gap filled by a gas, and for direct contact of cylindrical core and casing. The measurements were made in the nonstationary thermal regime using induction method of heating the core.

The experimental results obtained here and available in the literature are satisfactorily described by the function $\Psi(Kn_0)$ (see Fig. 1). The average difference between the computed and experimental results is ±20%.

LITERATURE CITED

1. N. N. Del'vin and L. S. Kokarev, in: Problems of Thermal Physics of Nuclear Reactors [in Russian], Vol. 3, Atomizdat, Moscow (1971), p. 62.
2. R. S. Prasolov, "Toward computation of resistance of zone of contact of solids," At. Énerg., 24, 86 (1968).
3. F. Boeschoten and E. Van Der Held, Physica, 23, No. 1, 37 (1957).

A METHOD FOR OPTIMIZING CERTAIN CHARACTERISTICS OF METAL – WATER SHIELDS

Yu. N. Borisov, A. A. Gordeev, and O. Ya. Shakh

UDC 621.039.538.7

We describe a calculational method for optimizing heterogeneous shields in one-dimensional cylindrical geometry. The shields consist of alternating layers of light (neutron shielding) and heavy components.

The spatial and energy distributions of neutrons are calculated by a multigroup method similar to that described in [1]. The change of dose rate components resulting from γ-rays at each step of the iterative optimization process is described by an exponential kernel. This procedure is justified if the following assumptions are satisfied:

1) The layers of neutron shielding between the layers of the heavy component must be thick enough for the equilibrium neutron spectrum to be established in them.

2) In neutron shielding materials the condition $\mu < \Sigma_r$ must be satisfied, where μ is the total gamma attenuation coefficient and Σ_r is the cross section for the removal of neutrons from the leading group.

TABLE 1. Comparison of Optimum Characteristics of a Three-Layer Iron–Water Shield

Composition	Weight, kg/cm	Thickness, cm	D_N	D_{cap}	D_{core}
From data in [2]	1160	265	0.14	0.57	0.29
From our data	1133	272	0.07	0.59	0.34

Note: D_N, D_{cap}, and D_{core} are respectively the neutron component of the dose rate and the contributions of capture gamma radiation from the shield and direct gamma radiation from the core.

The total dose can be written as a function of the shield parameters – the layer thicknesses d_i and their distances x_i from the center of the core:

$$D = f(d_i, x_i). \quad (1)$$

The optimization of the weight or thickness (volume) of a shield is reduced to the problem of finding the thicknesses d_i which minimize the functions describing the weight or thickness of the shield:

$$P = \varphi_1(d_i, x_i); \quad (2)$$

$$T = \varphi_2(d_i, x_i) \quad (3)$$

Translated from Atomnaya Énergiya, Vol. 32, No. 6, pp. 472–473, June, 1972. Original article submitted August 31, 1971; revision submitted January 20, 1972.

Declassified and Approved For Release 2013/03/01 : CIA-RDP10-02196R000300100005-6

Declassified and Approved For Release 2013/03/01 : CIA-RDP10-02196R000300100005-6

under the condition

$$D(d_i, x_i) - D_0 = 0, \tag{4}$$

where D_0 is the given total dose rate at the shield surface. By using the methods of undetermined Lagrangian multipliers the optimization calculation is reduced to the problem of finding the roots of a system of nonlinear algebraic equations:

$$f_i(\mathbf{Z}) = 0 \quad \text{for } i = 1, 2, \ldots, N, \tag{5}$$

where **Z** is the vector whose components are the dimensionless shield parameters. Equations (5) are solved by a combination of Newton's method and the method of steepest descents. This significantly improves the convergence of the iterative process.

Table 1 compares the characteristics of optimum shields calculated both by the more accurate method based on the use of a maximum principle and the nonlinear theory of small perturbations [2], and the method presented here.

LITERATURE CITED

1. A. P. Veselkin et al., in: Dosimetry and Shielding Problems [in Russian], Vol. 5, Atomizdat, Moscow (1966).
2. A. P. Suvorov and R. T. Fedorenko, in: Problems in the Physics of Reactor Shielding [in Russian], Vol. 3, Atomizdat, Moscow (1969).

MULTIGROUP HETEROGENEOUS DESCRIPTION OF A ROD OF FINITE RADIUS

S. S. Gorodkov

UDC 621.039.521

In the Feinberg–Galanin method, proposed for calculating heterogeneous reactors, rods were simulated by filamentary isotropic source-sinks. This model works well for thin rods when the neutron flux at the surface of a rod is practically independent of the azimuthal angle. Later the concept of a dipole moment of a rod was introduced to take account of the first harmonic in the thermal neutron distribution and to try to account for the nonuniformity of the distribution of intermediate energy neutrons at the surface of the rod in the age-diffusion approximation.

We solve the problem of simulating a rod by a filamentary source when the neutron distribution in the moderator is described by a system of multigroup diffusion equations. The analytic solution of this system is found in two forms. The first and simpler form can be used for few-group calculations, while the second more complicated form permits computer calculations for a large number of groups. On the basis of the interpretation of the free coefficients in the analytical solution it is shown that an actual rod with specified characteristics can be simulated by a collection of singular sources, proportional to various derivatives of the δ-function.

The source strengths depend linearly on the corresponding derivatives of the external neutron distribution at the location of a rod. The coefficients in this relation, the so-called heterogeneous constants, can be calculated uniquely, e.g., from the albedo characteristics of the rod. Trial calculations were performed for 26 groups. A very simple method is proposed for obtaining few-group heterogeneous constants from the multigroup calculations.

Translated from Atomnaya Énergiya, Vol. 32, No. 6, p. 473, June, 1972. Original article submitted September 13, 1971; revision submitted February 8, 1972.

Declassified and Approved For Release 2013/03/01 : CIA-RDP10-02196R000300100005-6

Declassified and Approved For Release 2013/03/01 : CIA-RDP10-02196R000300100005-6

GASTHERMAL DISINTEGRATION OF FUEL ELEMENTS OF A WATER-COOLED WATER-MODERATED POWER REACTOR WITH SEPARATION OF FUEL

A. T. Ageenkov and V. F. Savel'ev

UDC 621.039.54

The object of the present work is to search for and develop a simple and efficient method of disintegration of fuel elements of power reactors before chemical regeneration making it possible to open the fuel element without mechanical division and to separate the nuclear fuel from the constructional material of the casing.

Based on the study of the changes in the mechanical and physicochemical properties of the zirconium casing of fuel elements of a water-cooled water-moderated power reactor (WWPR) during interaction with hydrogen a two-state process of gasthermal disintegration of fuel elements has been proposed and investigated on laboratory and enlarged scale. The hydrogenation operation was carried out at a temperature of 650-770°C and the pressure of hydrogen ±0.2 gauge atmosphere. The hydrogenated fuel elements were treated at a temperature of 400-500°C in air or oxygen.

Fig. 1. Product of regeneration of fuel element: a) fragments of hydrogenated casing; b) powder of uranous–uranic oxide.

As a result of hydrogenation the zirconium casing absorbs 1.8-1.95% weight of hydrogen, the diameter of the casing increases by 5-6.5%, fissures appear in it, and the hermeticity of the fuel elements is impaired; the material of the casing becomes brittle and its strength is lowered by a factor of 30-40. In the subsequent oxidation treatment oxygen penetrates into the fuel element through the fissures and interacts with UO_2. As a result of the transformation $3UO_2 + O_2 = U_3O_8$, which occurs with an increase of the volume by 30%, the fuel exerts pressure on the inner wall of the casing of the fuel element. The weakened brittle casing breaks up into pieces of 3-50 mm size. The core of the fuel is transformed into powder of uranous–uranic oxide with particle size of the order of a few microns.

The method of hydrogen–oxygen disintegration of fuel elements with the separation of the fuel from the material of the casing was checked on a test equipment. Fuel elements of VVER-1 (WWPR) were subjected to regeneration. A complete disintegration of the casing of the fuel elements occurred and briquets of uranium dioxide were formed in all tests. The separation of the fuel and the material of the casing was accomplished in the equipment on a steel grid with the mesh size equal to 1.5 mm. The powder of uranous–uranic oxide and the fragments of the casing were collected in separate bins. The fuel thus obtained contained less than 0.1% zirconium. Uranium remaining on the surface of the casing material was 0.02-0.05%. After deactivation of the casing in nitric acid the loss of uranium was reduced to 0.003-0.005%.

Translated from Atomnaya Énergiya, Vol. 32, No. 6, p. 474, June, 1972. Original article submitted September 30, 1971; revision submitted January 1, 1972.

Declassified and Approved For Release 2013/03/01 : CIA-RDP10-02196R000300100005-6

Declassified and Approved For Release 2013/03/01 : CIA-RDP10-02196R000300100005-6

EXPERIMENTAL INVESTIGATION OF CONTACT HEAT EXCHANGE BETWEEN COAXIAL CYLINDRICAL CASINGS IN VACUUM

I. I. Novikov, L. S. Kokorev, and N. N. Del'vin

UDC 621.039.517.5

In composite cylindrical constructions the contact pressure depends on the temperature drop between the inner and outer cylinders, and hence, on the contact thermal resistance R_c. Therefore, in the computation of the contact heat exchange in constructions with independent heat release (for example, in fuel elements in reactors) it is convenient to use the thermal load q as the defining parameter.

The functional relation $R_c(q)$ shows a significant dependence on the installation conditions, the ratio of the thermal expansion coefficients (α) of the materials of the core and the casing, and also on the form of their deformations [1].

The present work is devoted to the experimental investigation of this dependence in vacuum conditions for a single bulge in the longitudinal undulation of the core. It was found in the experiments that: a) for the ratio $(\alpha_2/\alpha_1) \leq 1$ (subscript 1 refers to the core, 2 to the casing) the contact thermal resistance decreases with the increase in the thermal load; the limit of the change in the contact pressure ($p_{c\infty}$) is due to plastic deformation of the casing, after which the curve of $R'_c(Q)$ irreversibly shifts toward increasing R'_c (the total contact thermal resistance R'_c and the thermal load Q are determined in the experiments); b) for $(\alpha_2/\alpha_1) > 1$ $p_{c\infty}$ is determined by the set of construction characteristics [1]; if the initial pressure $p_{c0} > p_{c\infty}$ (due to tight installation), then on increasing the thermal load p_c decreases tending to $p_{c\infty}$, while the values of R'_c increase. For $p_{c0} < p_{c\infty}$ the reverse pattern is observed. In all cases the installation with gap increases the contact thermal resistance appreciably.

The obtained experimental results are in satisfactory agreement with the computational results [1] which have the following form for the conditions of the present experiment:

$$\frac{p'_c - p'_{c0}}{r_1\gamma'} = Q\alpha_1 R'_c; \tag{1}$$

$$\frac{p'_{c0}}{\gamma'} = r_1\alpha_1(T_2 - T_{10}) - r_2\alpha_2(T_2 - T_{20}); \tag{2}$$

$$p'_c \leqslant p'_{\max}\ (\sigma_T); \tag{3}$$

$$R'_c = Cp'^{-n}_c; \tag{4}$$

$$T_2 = T_\gamma + Q/h'_\gamma \tag{5}$$

Here (1) is the equation of the cylindrical contact and reflects the interrelationship between the instantaneous value of the contact pressure p'_c and the values of R'_c and Q; p'_{c0} is the initial pressure for Q = 0 and isothermal heating of the construction to a temperature T_2; T_{10} and T_{20} are the temperatures of unstressed contact; C and n are constants (these were determined from the experimental data); σ_T is the yield point; h'_γ is the total coefficient of heat transfer; T_γ is the temperature of the heat-transfer agent:

$$\gamma' = \left(\frac{r_1^2\beta_1}{E_1\delta_1} + \frac{r_2^2\beta_2}{E_2\delta_2}\right)^{-1}, \text{ where } \beta_i = [3(1-\nu_i^2)]^{1/4}(r_1\delta_1)^{-1/2},\ i = 1;\ 2;$$

r, δ are respectively the radius of the core surface and the thickness of the casing; E is the modulus of elasticity; ν is Poisson's coefficient.

LITERATURE CITED

1. N. N. Del'vin and L. S. Kokorev, in: Problems of Thermal Physics of Nuclear Reactors [in Russian], Vol. 3, Atomizdat, Moscow (1971), p. 62.

Translated from Atomnaya Énergiya, Vol. 32, No. 6, pp. 474-475, June, 1972. Original article submitted November 15, 1971.

Declassified and Approved For Release 2013/03/01 : CIA-RDP10-02196R000300100005-6

Declassified and Approved For Release 2013/03/01 : CIA-RDP10-02196R000300100005-6

LETTERS TO THE EDITOR

POSSIBILITY OF NEGLECTING ELASTIC SCATTERING IN CALCULATING THE VELOCITIES OF NUCLEAR REACTIONS IN A UNIFORM SPHERE

V. K. Kapyshev and V. I. Sakharov

UDC 539.125.52

In describing nuclear-physical processes due to high-energy neutrons (neutron energy equal to several MeV or over) elastic scattering is sometimes neglected owing to its severe anisotropy. Let us examine the permissibility of this neglect when calculating the velocities of nuclear reactions in a uniform sphere due to a monoenergetic neutron flux $\Psi(r, \mu)$ from a point source of unit strength in the center of the sphere. In other words, if the reaction under consideration is characterized by a macroscopic cross section Σ_i, then we require to determine the error in calculating the functional

$$Q_i = \int_{V_R} \int_{4\pi} \Sigma_i \Psi(r, \mu)\, dV\, d\Omega, \tag{1}$$

where V_R is the volume of the sphere of radius R. The solution of this problem is important when calculating the velocities of nuclear reactions in the shell of a hypothetical thermonuclear reactor due to neutrons arising from the fusion of deuterium and tritium.

In order to solve this problem we use the theory of small perturbations set out by Marchuk and Orlov in [1].

The neutron flux $\Psi(r, \mu)$ is the solution of the one-velocity Boltzmann equation

$$\mu \frac{\partial \Psi}{\partial r} + \frac{1-\mu^2}{r} \cdot \frac{\partial \Psi}{\partial \mu} + \Sigma_T \Psi = \Sigma_s \int_{4\pi} \Psi(r, \mu')\, g(\mu_0)\, d\Omega' + \frac{\delta(r)}{4\pi r^2}; \tag{2}$$

$$\Psi(R, \mu) = 0; \quad \mu \leqslant 0,$$

where $\Sigma_T = \Sigma_S + \Sigma_a$ is the total macroscopic cross section; Σ_S and Σ_a are the macroscopic scattering and absorption cross sections. The remaining notation is as in [2].

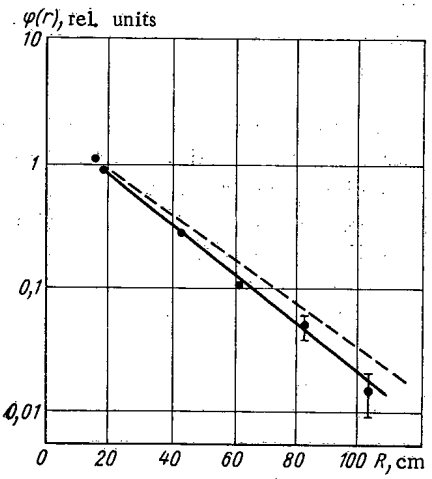

Fig. 1. Calculated (– – –) and experimental (———) neutron distribution in an infinite medium of boron carbide.

Translated from Atomnaya Énergiya, Vol. 32, No. 6, pp. 477–478, June, 1972. Original article submitted April 15, 1971.

© 1972 Consultants Bureau, a division of Plenum Publishing Corporation, 227 West 17th Street, New York, N. Y. 10011. All rights reserved. This article cannot be reproduced for any purpose whatsoever without permission of the publisher. A copy of this article is available from the publisher for $15.00.

Declassified and Approved For Release 2013/03/01 : CIA-RDP10-02196R000300100005-6

Declassified and Approved For Release 2013/03/01 : CIA-RDP10-02196R000300100005-6

The neglect of elastic scattering means that in Eq. (2) we reject the term

$$\delta L(\Psi) = -\Sigma_s \Psi + \Sigma_s \int_{4\pi} \Psi(r, \mu')\, g(\mu_0)\, d\Omega. \tag{3}$$

Without this term Eq. (2) may be regarded as an unperturbed equation, with a solution

$$\Psi_0(r, \mu) = \frac{\exp(-\Sigma_a r)}{4\pi r^2}\, \delta(1-\mu). \tag{4}$$

Correspondingly the perturbation (3) has the form

$$\delta L(\Psi_0) = \Sigma_s \frac{\exp(-\Sigma_a r)}{4\pi r^2} [-\delta(1-\mu) + g(\mu)]. \tag{5}$$

Let us now calculate the error in determining the quantity (1) which appears on neglecting (3). For this purpose we find the neutron value function $\Psi^+(\mathbf{r}, \mu)$ with respect to the functional (1). This function is the solution of an equation the left-hand side of which is the operator of the unperturbed equation, while the right-hand side contains a quantity numerically equal to $(-\Sigma_i)$:

$$\mu \frac{\partial \Psi^+}{\partial r} + \frac{(1-\mu^2)}{r} \cdot \frac{\partial \Psi^+}{\partial \mu} - \Sigma_a \Psi^+ = -\Sigma_i;$$
$$\Psi^+(R, \mu) = 0;\ \mu > 0.$$

By making a change of variables [1]

$$x = r\mu,\ y = r\sqrt{1-\mu^2}$$

we reduce this to an ordinary differential equation

$$\frac{\partial \Psi^+}{\partial x} - \Sigma_a \Psi^+ = -\Sigma_i;$$
$$\Psi^+(-\sqrt{R^2-y^2},\ y) = 0;\ 0 \leqslant y \leqslant R.$$

The solution of this equation takes the form

$$\Psi^+(r, \mu) = \Sigma_i \int_0^{-r\mu + R\sqrt{1-\left(\frac{r}{R}\right)^2(1-\mu^2)}} \exp(-\Sigma_a \rho)\, d\rho$$

$$= \frac{\Sigma_i}{\Sigma_a} \left\{1 - \exp\left[-\Sigma_a\left(-r\mu + R\sqrt{1-\left(\frac{r}{R}\right)^2(1-\mu^2)}\right)\right]\right\}. \tag{6}$$

Using Eqs. (5) and (6) we find the error δQ_i in the calculation of the functional (1):

$$\delta Q_i = \int_{V_R} \int_{4\pi} [\delta L(\Psi_0)\, \Psi_i^+(r, \mu)]\, dV\, d\Omega = -\frac{\Sigma_s \Sigma_i}{\Sigma_a} \int_0^R \frac{\exp(-\Sigma_a r)}{r^2} \int_{-1}^{+1} [\delta(1-\mu) - g(\mu)]$$
$$\times \left\{1 - \exp\left[-\Sigma_a\left(-r\mu + R\sqrt{1-\left(\frac{r}{R}\right)^2(1-\mu^2)}\right)\right]\right\} d\mu r^2\, dr. \tag{7}$$

We note that the resultant equation (7) may be used if the perturbation (3) is small. This occurs if, for example, the elastic scattering of the neutrons takes place (as a result of anisotropy) close to the direction of their initial approach. Then by expanding the second factor in the integrand in series in powers of $(1-\mu)$ we obtain

$$1 - \exp\left[-\Sigma_a\left(-r\mu + R\sqrt{1-\left(\frac{r}{R}\right)^2(1-\mu^2)}\right)\right] = \exp(-\Sigma_a(R-r)) \left\{1 - \Sigma_a r\left(1-\frac{r}{R}\right)(1-\mu)\right.$$
$$\left. - \Sigma_a\left[r_a\left(1-\frac{r}{R}\right) + R\left(\frac{r}{R}\right)^2\right]\frac{(1-\mu^2)}{2} \cdots\right\}.$$

Confining attention to the first two terms and substituting the resultant expression in (7), after integration we obtain

$$\delta Q_i = \Sigma_i \Sigma_s \left[\frac{R^2}{6} \exp(-\Sigma_a R)\right]\left[1 - \int_{-1}^{+1} \mu g(\mu)\, d\mu\right]. \tag{8}$$

As indicated by physical considerations, the error in fact tends to zero when R tends either to zero or to infinity. The maximum error occurs for $R = 2/\Sigma_a$.

Declassified and Approved For Release 2013/03/01 : CIA-RDP10-02196R000300100005-6

Declassified and Approved For Release 2013/03/01 : CIA-RDP10-02196R000300100005-6

By way of example let us consider a lead sphere with 14.06 MeV neutrons coming from a monoenergetic point source. Then according to [3]

$$1-\int_{-1}^{+1}\mu g(\mu)\,d\mu=0.1;\quad \frac{\Sigma_T-\Sigma_a}{\Sigma_T}=0.36.$$

In this case the error in determining the rate of absorption of the neutrons in the whole sphere reaches its maximum for R = 11.78 and equals $\delta Q_i = 0.006$. If in order to calculate the functional (1) we use Eq. (8), then $Q_a = 0.865$, i.e., the error in determining Q_a is 0.7%.

The permissibility of neglecting elastic scattering is confirmed experimentally. Using copper indicators with the reaction $Cu^{63}(n, 2n)Cu^{62}$, the distribution of neutrons from a point neutron source of energy 14.1 MeV in an infinite boron carbide sphere was studied in [4]. Since in this case the anisotropy of elastic scattering was also large, while the cross section of the reaction $Cu^{63}(n, 2n)Cu^{62}$ for energies below 14.1 MeV was small, on neglecting the elastic scattering the neutron flux of this energy should be given by Eq. (4). In Fig. 1 the continuous curve gives the flux $\varphi_1(r)$ measured with a copper detector in relative units:

$$\varphi_1(r)=\frac{\varphi_1(r)\,4\pi r^2}{\varphi_1(r_1)\,4\pi r_1^2},$$

where r_1 = 6 cm. The broken curve represents the function

$$\varphi_2(r)=\frac{4\pi r^2\int_{-1}^{+1}\frac{\exp[-(\Sigma_T-\Sigma_s)r]}{4\pi r^2}\delta(1-\mu)\,d\mu}{\exp[-(\Sigma_T-\Sigma_s)r_1]}.$$

The calculated curve may be considered close to the experimental curve on allowing for the accuracy of the experiments as well as the accuracy of determining the inelastic scattering cross section. The course of the experimental curve (exponential fall) confirms the validity of the neglect of elastic scattering.

LITERATURE CITED

1. G. I. Marchuk and V. V. Orlov, in: Neutron Physics [in Russian], Gosatomizdat, Moscow (1961), p. 31.
2. G. I. Marchuk, Numerical Methods of Calculating the Energy of Reactors [in Russian], Atomizdat, Moscow (1958).
3. I. V. Gordeev, D. A. Kardashev, and A. V. Malyshev, Nuclear-Physical Constants [in Russian], Gosatomizdat, Moscow (1963).
4. S. P. Belov et al., At. Énerg., 6, 663 (1959).

Declassified and Approved For Release 2013/03/01 : CIA-RDP10-02196R000300100005-6

Declassified and Approved For Release 2013/03/01 : CIA-RDP10-02196R000300100005-6

FUSIBILITY DIAGRAMS OF SYSTEMS INVOLVING LITHIUM CHLORIDE, URANIUM TRICHLORIDE, AND URANIUM TETRACHLORIDE

V. N. Desyatnik, N. N. Kurbatov,
S. P. Raspopin, and I. I. Trifonov

UDC 546.791.6:131.34

The use of melted salts as electrolytes in obtaining metals by electrolysis makes it necessary to study the fusibility diagrams of binary and ternary systems. In the present article we shall discuss the results of investigations conducted on binary and ternary systems involving uranium trichloride, uranium tetrachloride, and lithium chloride.

The binary systems $LiCl-UCl_3$ and $LiCl-UCl_4$ have been studied previously [1]. However, a check revealed some discrepancies between the published data and the results of the investigation. The phase diagram of the binary system UCl_3-UCl_4 was published in [2].

In order to conduct the experiment, we prepared pure initial substances [3, 4]. The uranium tetrachloride had an atomic ratio of [Cl]: [U] = 4.01 and a melting point of 590 ± 2°C. The uranium trichloride

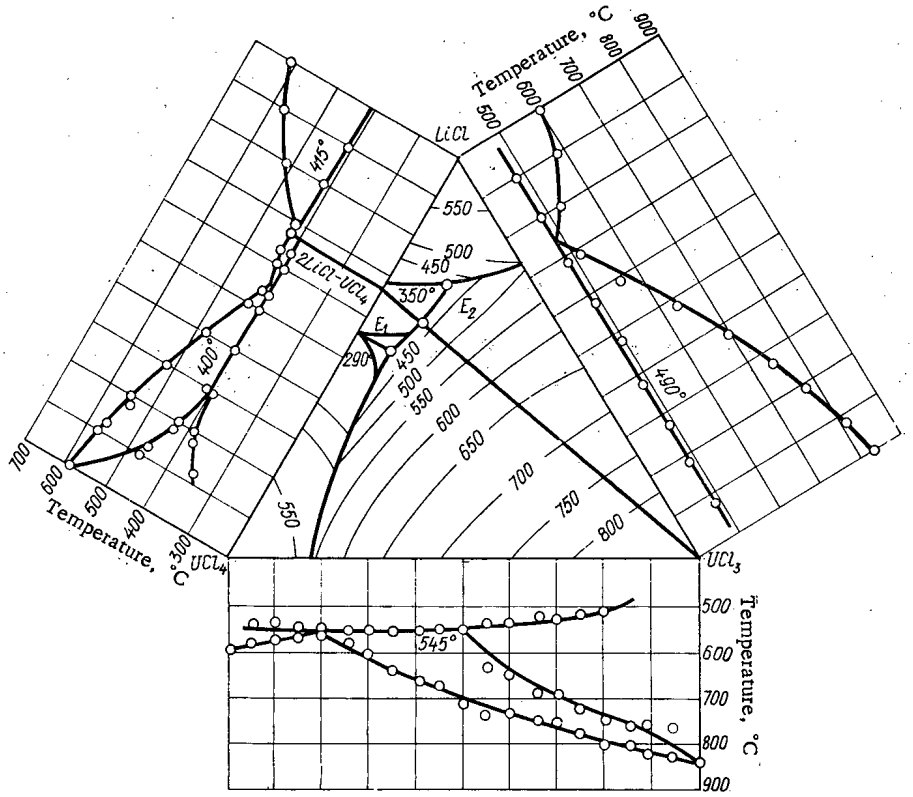

Fig. 1. Fusibility diagram of the system $LiCl-UCl_3-UCl_4$ and the corresponding phase diagrams of the binary systems.

Translated from Atomnaya Énergiya, Vol. 32, No. 6, pp. 479-480, June, 1972. Original article submitted June 9, 1971.

© 1972 Consultants Bureau, a division of Plenum Publishing Corporation, 227 West 17th Street, New York, N. Y. 10011. All rights reserved. This article cannot be reproduced for any purpose whatsoever without permission of the publisher. A copy of this article is available from the publisher for $15.00.

Declassified and Approved For Release 2013/03/01 : CIA-RDP10-02196R000300100005-6

Declassified and Approved For Release 2013/03/01 : CIA-RDP10-02196R000300100005-6

prepared from the tetrachloride thus obtained [3] had an atomic ratio of [Cl] : [U] = 3.02 and a melting point of 835 ± 2°C. Anhydrous LiCl was obtained by dehydrating OSCh brand lithium chloride in a vacuum at temperatures of 50, 100, and 300°C, maintaining it at each temperature for 4-5 h. After this the lithium chloride was heated to 750°C, and gaseous chlorine obtained by the electrolysis of lead chloride was bubbled through the melt for 30-60 min. After the chlorine had been bubbled through, the melt was slowly cooled for 2 h in a vacuum. The resulting LiCl was analyzed for chlorine and lithium content; these were found to be stoichiometric within the limits of error. The melting point of this LiCl was 605 ± 2°C, which is in good agreement with the published value [5].

The starting materials were kept in a dry chamber, since they are extremely hygroscopic.

The binary and ternary systems were studied by the method of differential thermal analysis, with the cooling curves recorded at a rate of 5-8 deg/min on an NTR-62M recorder.

The binary system $LiCl-UCl_3$ plotted on the basis of our investigations is characterized by one eutectic with a melting point of 490 ± 2°C at a UCl_3 content of 26.5 mole % (see Fig. 1), which is in good agreement with the results of [1]. In the binary system $LiCl-UCl_4$ we found two eutectics at UCl_4 content values of 31.00 and 44.00 mole %, having melting points of 415 ± 2 and 400 ± 2°C, respectively, and the compound $2LiCl \cdot UCl_4$, which melted congruently at 430 ± 2°C. Unlike [1], which does not contain any investigation of the UCl_4 = 75-100 mole % region, our study revealed the existence of a UCl_4-UCl_3 solid solution. In the ternary system $LiCl-UCl_3-UCl_4$ (see Fig. 1) we studied 10 temperature sections passing through the vertex of the concentration triangle (corresponding to the composition LiCl) and the opposite side. In this system we found four crystallization fields: UCl_4, $2LiCl \cdot UCl_4$, LiCl, and UCl_3. The quasibinary cut $UCl_3-2LiCl \cdot UCl_4$ divides the system into two secondary simple eutectic systems. The eutectic points (E_1) formed by the crystallization fields UCl_4, $2LiCl \cdot UCl_4$, and UCl_3 is characterized by a melting point of 290 ± 2°C and corresponds to a composition of 50.00 mole % LiCl, 10.00 mole % UCl_3, and 40.00 mole % UCl_4. The crystallization fields $2LiCl \cdot UCl_4$, LiCl, and UCl_3 converge, forming a eutectic (E_2) with a melting point of 350 ± 2°C, corresponding to a composition of 68.00 mole % LiCl, 13.00 mole % UCl_3, and 19.00 mole % UCl_4.

LITERATURE CITED

1. Reactor Handbook, Vol. 1, Materials, New York (1960), p. 425.
2. V. N. Desyatnik et al., Atomnaya Énergiya, 26, 549 (1969).
3. J. J. Katz and E. Rabinovitch, The Chemistry of Uranium [Russian translation], Izd-vo Inostr. Lit., Moscow (1954).
4. V. N. Desyatnik, I. F. Nichkov, and S. P. Raspopin, Izv. Vuzov. Tsvetnaya Metallurgiya, No. 5, 95 (1969).
5. Handbook of Melted Salts [Russian translation], A. G. Morachevskii (editor), Khimiya, Moscow (1971).

Declassified and Approved For Release 2013/03/01 : CIA-RDP10-02196R000300100005-6

Declassified and Approved For Release 2013/03/01 : CIA-RDP10-02196R000300100005-6

OPTIMIZATION OF A REACTOR FOR PHYSICAL INVESTIGATIONS BY MEANS OF FUEL PROFILING

T. S. Zaritskaya, Yu. V. Petrov,
A. P. Rudik, and É. G. Sakhnovskii

UDC 621.039.51

In [1] a functional of the following form was proposed for estimating the reactor component of the cost of obtaining information in experiments in a stationary reactor:

$$I=\frac{P}{\Phi(r_{\max})}\left(\frac{1}{yG}+\frac{1}{P}\right), \tag{1}$$

where P is the power of the reactor; y is the average burnup of the fuel elements at the time of their removal; $\Phi(r)$ is the flux of thermal neutrons; r_{max} is the maximum point of the function $\Phi(r)$ in the reflector; G is a given constant. It would be of interest to find a distribution of nuclear fuel in the volume of the reactor active zone such that the functional (1) will be a minimum.

For a qualitative investigation of the solution, let us consider the simplest model of this problem. We shall confine our attention to the case in which the nonuniformity of the burnup may be neglected. We select a plane symmetric reactor with an active zone of halfwidth R and a reflector of thickness Δ. We assume that the structural materials (including the moderator) are uniformly distributed through the volume of the reactor and that their properties are constant both in the active zone ($0 \leq r \leq R$) and in the reflector ($R \leq r \leq R+\Delta$). If we assume that resonance absorption and neutron capture in the slowing-down process are insignificant, the system of equations for the thermal-neutron flux $\Phi(r)$ and the fast-neutron flux $\varphi(r)$ in the active zone can be written in a two-group diffusion approximation as follows:

$$\Phi''-\frac{1+u}{L_0^2}\Phi+\frac{D}{\tau}\varphi=0,\quad \varphi''-\frac{1}{\tau}\varphi+\frac{\eta u}{DL_0^2}\Phi=0, \tag{2}$$

where $D = D_f/D_t$ is the ratio of the diffusion coefficient of the fast group to that of the thermal group; L_0 is the diffusion length when absorption in the uranium is disregarded; τ and η are, respectively, the square of the slowing-down length and the effective number of generated fast neutrons per capture in the uranium. The equations for the neutron fluxes in the reflector can be obtained from the system (2) if in that system we take $u \equiv 0$ and replace L_0, τ, and D by the reflector constants L_*, τ_*, and D_*.

The function u(r) is the ratio of the macroscopic cross sections of absorption of the uranium and the structural materials and is proportional to the uranium concentration, which is not known in advance. However, it is subject to the following technological and heat-engineering limitations:

$$0 \leqslant u(r) \leqslant U_{\max};\quad \Phi(r)\,u(r) \leqslant q_{\max}. \tag{3}$$

We must determine the function u(r) in such a way as to minimize the functional (1).

TABLE 1. Behavior of $\Phi(r)$ and u(r)

r, cm	0	10	20	30	40	50	55
$\Phi(r)$	1,25	1,24	1,22	1,21	1,17	1,29	1,49
$u(r)$	0,80	0,81	0,82	0,83	0,86	0,78	0,67

The problem formulated here was investigated as a nonclassical problem of the calculus of variations by using Pontryagin's maximum principle [2] and by the method of Lagrangian multipliers [3]; in the first case it is convenient to reduce it to a problem of minimum reactor power for a given maximum flux in the reflector, and in the second case, to the problem of maximizing the neutron flux in the reflector for a given reactor power. Since Eqs. (2) are

Translated from Atomnaya Énergiya, Vol. 32, No. 6, pp. 480-481, June, 1972. Original article submitted June 15, 1971.

© 1972 Consultants Bureau, a division of Plenum Publishing Corporation, 227 West 17th Street, New York, N. Y. 10011. All rights reserved. This article cannot be reproduced for any purpose whatsoever without permission of the publisher. A copy of this article is available from the publisher for $15.00.

Declassified and Approved For Release 2013/03/01 : CIA-RDP10-02196R000300100005-6

Declassified and Approved For Release 2013/03/01 : CIA-RDP10-02196R000300100005-6

linear and their coefficients are linear functions of the control function, it is easy to show [4, 5] that the only admissible values of the function u(r) are the boundaries of its region of variation. Thus, the active zone of a reactor which is optimal in the sense under discussion can consist of segments of three and only three types: $u(r) = U_{max}$; $u(r) = q_{max}/\Phi(r)$; and $u(r) = 0$. The optimal combination of such segments of the active zone will obviously depend either on the given maximum neutron flux in the reflector (in the first approach) or on the given power (in the second approach). If we exclude from consideration all active-zone combinations which include segments with $u(r) = 0$, i.e., if we look for a solution in the class of continuous functions, then we can trace how combinations which we suspect may be optimal depend on the given power (or on the maximum reflector neutron flux).

For small power values P the heat-engineering limitation will be satisfied everywhere in [0, R], and the only possible combination will be one with $u(r) = U_{max}$ everywhere in [0, R]. As the power increases, there will be an increase in $\Phi(r)$ as well, so that for some power value P_1 (in the case of research reactors we shall assume, for the sake of definiteness, that $L_0 \ll L_*$ and $\tau_* \ll L_*^2$) we will find $\Phi(R) = q_{max}/U_{max}$. For $P > P_1$ and $u(r) = U_{max}$ we would have at the boundary with the reflector a segment with $\Phi(r) > q_{max}/U_{max}$, on which the heat-engineering limitation would be violated. Therefore if $P > P_1$, the optimal distribution must be one with $u(r) = U_{max}$ at the center of the reactor and $u(r) = q_{max}/\Phi(r)$ at the boundary with the reflector. As the power increases further, at $P = P_2 > P_1$ we will find $\Phi(0) = q_{max}/U_{max}$, and for $P_1 > P_2$ the optimal combination would be one with segments $u(r) = q_{max}/\Phi(r)$ at the center and at the edge and with a segment $u(r) = U_{max}$ between them. Lastly, at a power value of $P = P_3 > P_2$ the segment with $u(r) = U_{max}$ will shrink to a point, and when $P \geq P_3$, the optimal combination will be one with $u(r) = q_{max}/\Phi(r)$ everywhere in the active zone.

Numerical calculations† confirmed that in the cases indicated the necessary condition for optimality of the system under consideration is satisfied. The calculations were carried out for $\eta = 2.3$, $L_0 = 169$ cm^2, $L_*^2 = 10^4$ cm^2, $\tau = \tau_* = 144$ cm^2, $\Delta = 200$ cm, and equal diffusion coefficients in the active zone and in the reflector; $\Phi(r)$ was normalized so as to make $q_{max} = 1$.

Table 1 shows for purposes of illustration the variation of $\Phi(r)$ and $u(r)$ for the case in which $P \geq P_3$ and R = 55 cm. Then the maximum thermal-neutron flux is $\Phi(r) \approx 1.84$, and the value of r for this maximum is $r_{max} \approx 71$ cm. When $P > P_3$, we find that, as was to be expected, the neutron flux $\Phi(r_{max})$ increases slightly, and the distance $r_{max} - R$ becomes very slightly smaller. Thus, as R varies from 55 cm to 75 cm, we find that $\Phi(r_{max})$ and $r_{max} - R$ change only in the fourth decimal place.

Thus, for every reactor with known active-zone and reflector constants and with given values of U_{max} and q_{max} there are three characteristic parameters: the power values P_1, P_2, and P_3 [or the values of the neutron flux $\Phi(r_{max})$], which are the boundaries of the regions in which the above combinations exist. To each value of the power P there corresponds its particular optimal combination. Among all such combinations, we must find the one which will minimize the functional (1). The minimum of this functional will be determined after a specific value of yG is given.

LITERATURE CITED

1. A. N. Erykalov and Yu. V. Petrov, Atomnaya Énergiya, 25, 52 (1968).
2. L. S. Pontryagin et al., The Mathematical Theory of Optimal Processes [in Russian], Fizmatgiz, Moscow (1959).
3. V. A. Troitskii, Prikl. Mat. i Mekhan., 26, 29 (1962).
4. T. S. Zaritskaya and A. P. Rudik, Atomnaya Énergiya, 22, 6 (1967).
5. É. G. Sakhnovskii, Atomnaya Énergiya, 29, 201 (1970.

†The calculations were carried out by V. P. Glushakov.

Declassified and Approved For Release 2013/03/01 : CIA-RDP10-02196R000300100005-6

Declassified and Approved For Release 2013/03/01 : CIA-RDP10-02196R000300100005-6

USE OF SOLID TRACK DETECTORS IN REACTOR EXPERIMENTS

V. A. Kuznetsov, A. I. Mogil'ner,
V. P. Koroleva, V. S. Samovarov,
and L. A. Chernov

UDC 539.1.074.88

In recent years solid track detectors [1-3] are being increasingly used for recording fission products and charged particles in nuclear physics and the physics of reactors. The high sensitivity and recording efficiency, small sizes and small inserted perturbation are the advantages of the solid detectors, which are especially valuable for measurements on critical assemblies with close grids and low neutron fluxes. The aim of the present work consists in the development of the procedure of recording nitrocellulose α-particles from the reactions $B^{10}(n, \alpha)Li^7$, $Li^6(n, \alpha)T$ and fission products of U^{235} with the use of mica, a selection of suitable materials for recording, investigation of their characteristics and etching regimes, and also the application of the procedure in experiments on reactors.

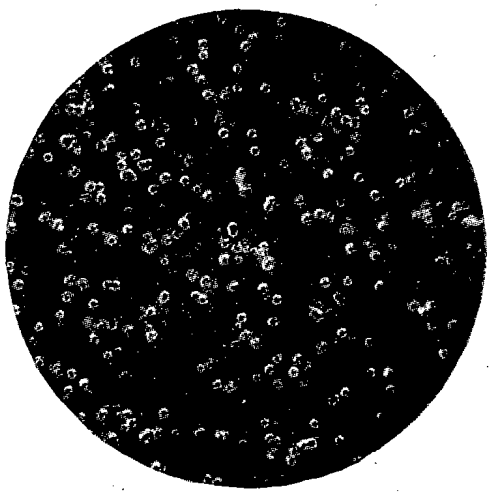

Fig. 1. Photographs of tracks of α-particles of B^{10} layer in nitrocellulose.

Nitrocellulose. For recording α-particles from B^{10} and Li^6 cinematographic films A2 and VCh and x-ray films RF-3, RF-5 with nitrocellulose base were used. Aqueous solutions of sodium or potassium hydroxide was used as the chemical solvent in etching. Tracks of α-particles with 20-30 μ size were examined after etching on an MIM-7 microscope with an amplification of 130. The photographs of the tracks of α-particles of B^{10} layer and the dependences of the sizes of the tracks on the etching time (for the two solvents), the temperature, the concentration of the solvent, and the energy of the α-particles are shown in Figs. 1-5. The following regimes

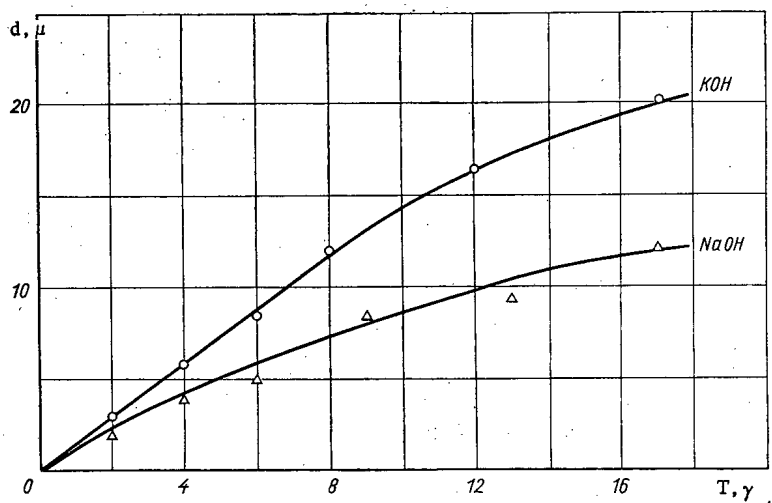

Fig. 2. Dependence of the sizes of tracks of α-particles of B^{10} layer on the etching time of nitrocellulose in different chemical solvents (t = 20°C, concentration 20%).

Translated from Atomnaya Énergiya, Vol. 32, No. 6, pp. 481-483, June, 1972. Original article submitted July 7, 1971; revision submitted January 12, 1972.

© 1972 Consultants Bureau, a division of Plenum Publishing Corporation, 227 West 17th Street, New York, N. Y. 10011. All rights reserved. This article cannot be reproduced for any purpose whatsoever without permission of the publisher. A copy of this article is available from the publisher for $15.00.

Declassified and Approved For Release 2013/03/01 : CIA-RDP10-02196R000300100005-6

Declassified and Approved For Release 2013/03/01 : CIA-RDP10-02196R000300100005-6

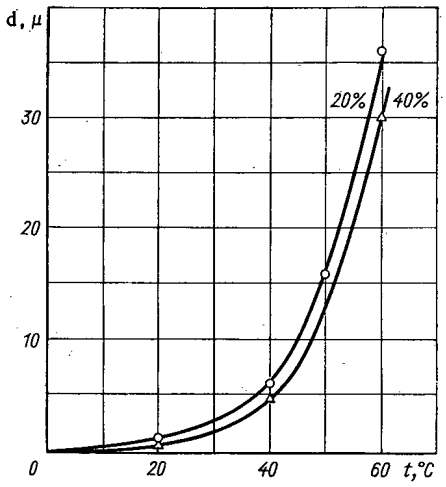

Fig. 3

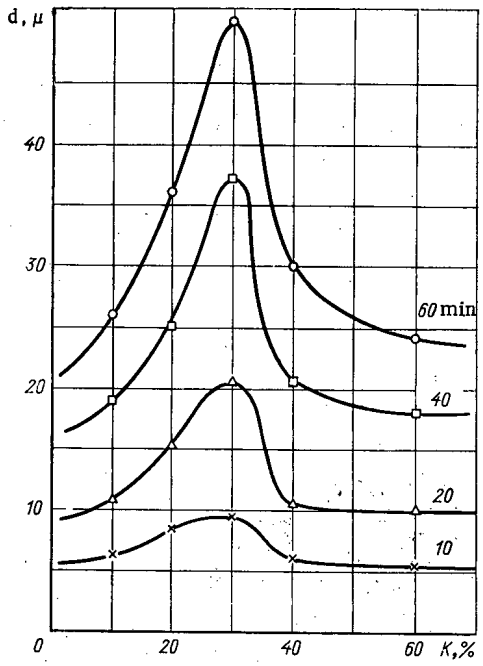

Fig. 4

Fig. 3. Dependence of the sizes of the tracks of α-particles of B^{10} layer on the temperature of the solvent NaOH for concentrations of 20 and 40% (etching time 1 h).

Fig. 4. Dependence of the sizes of the tracks of α-particles of B^{10} layer on the concentration of the solvent NaOH at t = 60°C for different etching times.

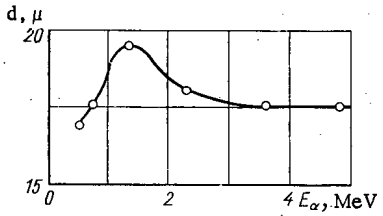

Fig. 5. Dependence of the sizes of the tracks on the energy of α-particles (solvent NaOH, concentration 30%, t = 60°C, etching time 15 min).

of etching can be recommended for nitrocellulose: solvent NaOH, concentration 30%, t^0 = 60°C, T_{etch} = 15 min.

Mica. Fission products were recorded by mica. Mica was etched before irradiation in order to separate the background tracks present in it from the tracks of fission in the reactor according to the sizes.

The photographs of the tracks of the fission products of U^{235} layer along with the background tracks (large rhombuses) are shown in Fig. 6. For the etching of mica a 40% HF solution was used (t = 60°C, T_{etch} = 30 min).

Indicator Layers. Samples of nitrocellulose and mica were irradiated in the reactor closely set against indicator layers of B^{10}, Li^6, U^{235}. The layers of boron and lithium having thickness of 0.05 mg/cm^2 were prepared by vacuum coating on copper backing. The layer of U^{235} of 90% enrichment had a thickness of 0.2 mg/cm^2 and was deposited on a titanium backing. Besides this a 0.035 mm thick metallic uranium foil was used.

Measurements. The measurements were made at the PF-4F8 assembly [4] with a compensating rod of boron carbide at the center; the diameter of the rod was 19.2 mm. The relative distribution of the density of absorption of neutrons along the radius of the rod was measured in the middle plane of the reactor with the use of nitrocellulose and semiconductor silicon counter. The results are shown in Fig. 7. The errors in the measurement by nitrocellulose are insignificant (~1%) and, therefore, are not indicated in the figure.

It is known that the ratios of neutron reaction cross sections for certain isotopes can serve as a sensitive characteristic of the neutron spectrum in a reactor. Irradiating nitrocellulose together with B^{10} and Li^6 layers, and mica with U^{235} layer at a fixed point in the reactor (at the midpoint of the radius of the active zone in the midplane of the reactor), and also in a thermal column, one can obtain the spectral indices: $\bar{\sigma}(B^{10})/\bar{\sigma}_f(U^5)$ = 3.53 ± 0.07 for ionization chambers, and $\bar{\sigma}(B^{10})/\bar{\sigma}_f(Li^6)$ = 4.01 ± 0.12 for track detectors. In the

Declassified and Approved For Release 2013/03/01 : CIA-RDP10-02196R000300100005-6

Declassified and Approved For Release 2013/03/01 : CIA-RDP10-02196R000300100005-6

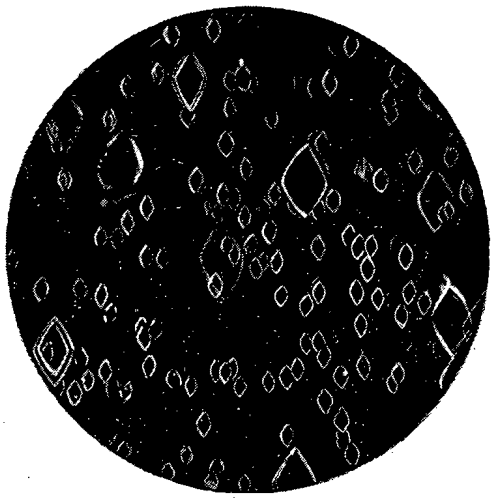

Fig. 6

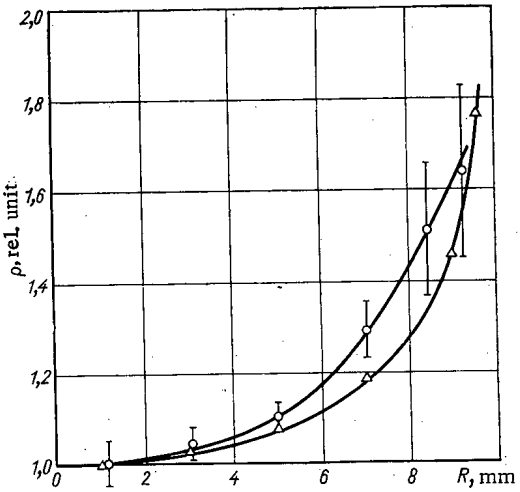

Fig. 7

Fig. 6. Photograph of tracks of fission products of U^{235} layer in mica.

Fig. 7. Distribution of density of absorption of neutrons ρ along the radius of the boron carbide rod, measured by nitrocellulose (Δ) and semiconductor Au–Si counter (○).

calculation we have made use of the cross section of the reaction (n, α) on B^{10} and Li^6 for thermal neutrons [5] and the cross section of fission of U^{235} for thermal neutrons [6]. The range of problems, that can be solved with the use of solid detectors, can be significantly extended by using different indicator layers.

LITERATURE CITED

1. R. Fleischer, P. Price, and R. Walker, Ann. Rev. Nucl. Sci., 15, 1 (1965).
2. Kh. Abdulaev et al., Pribory i Tekh. Éksperim., No. 6, 64 (1968).
3. G. Somogyi, Atomki Közlemenyek, 8 Kötet, 3szam (1966), p. 218.
4. A. I. Mogil'ner et al., Atomnaya Énergiya, 24, 42 (1968).
5. I. V. Gordeev et al., Nuclear-Physical Constants [in Russian], Gosatomizdat, Moscow (1963).
6. J. Stehn et al., Neutron Cross Section, BNL-325, Second Edition, Supplement No. 2, Vol. III (1965).

Declassified and Approved For Release 2013/03/01 : CIA-RDP10-02196R000300100005-6

Declassified and Approved For Release 2013/03/01 : CIA-RDP10-02196R000300100005-6

A NEW INTERMETALLIC COMPOUND IN A ZIRCONIUM – IRON SYSTEM

Yu. F. Babikova, V. I. Filippov, and I. I. Shtan'

UDC 546.831.72:669.017.12:539.172.3

Zirconium is utilized extensively in atomic technology in the capacity of structural materials. One of the primary additions to alloys of zirconium, improving its corrosion resistance, is iron. For the study of the processes involved in the oxidation of zirconium alloys containing iron, it is important to know the phase diagram for the zirconium–iron system which at the present time is not sufficiently well known. Thus, the published phase diagrams for the zirconium–iron system [1] contain only one intermetallic compound $ZrFe_2$ being a Laves phase with a $MgCu_2$ structure, discovered by means of x-ray and metallographic methods [2, 3]. There has been speculation [4-6] concerning the existence of other intermetallic compounds, including Zr_4Fe, Zr_2Fe, and Zr_3Fe_2. However, these speculations have not been confirmed because the phase diagrams from [1] were employed in studies on the physicochemical properties of zirconium [7, 8].

For the purpose of discovering possible intermetallic compounds, we investigated zirconium alloys containing iron using the method of nuclear γ-resonance (NGR) over a wide range of iron concentrations (0.4-57 wt.%).

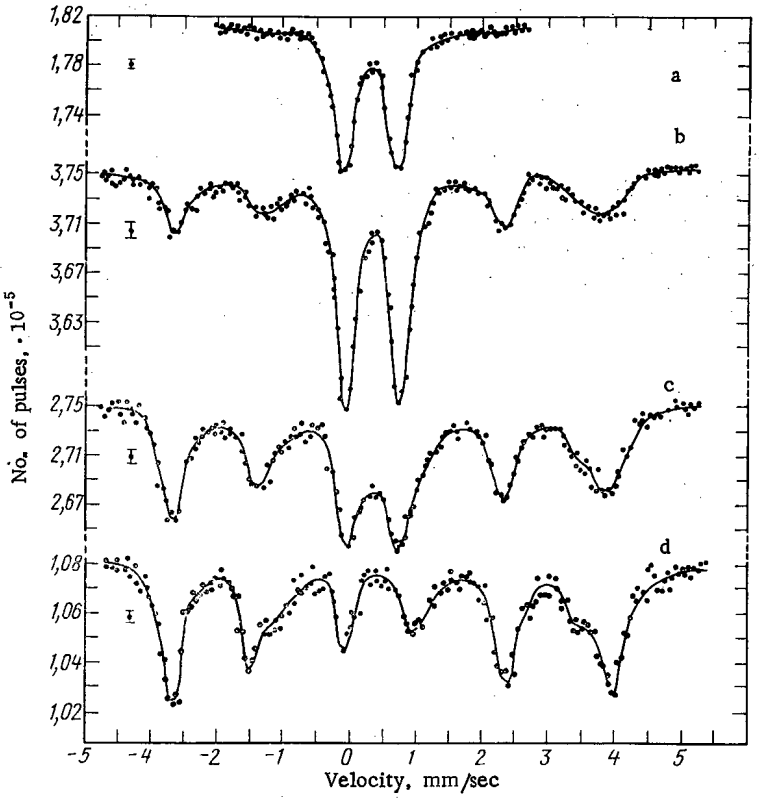

Fig. 1. Resonance absorption spectra recorded at T = 300°K for zirconium–iron alloys with iron content: a) 24 wt.%; b) 26.15 wt.%; c) 37.15 wt.%; d) 55.15 wt.%.

Translated from Atomnaya Énergiya, Vol. 32, No. 6, pp. 484-485, June, 1972. Original article submitted July 12, 1971.

© 1972 Consultants Bureau, a division of Plenum Publishing Corporation, 227 West 17th Street, New York, N. Y. 10011. All rights reserved. This article cannot be reproduced for any purpose whatsoever without permission of the publisher. A copy of this article is available from the publisher for $15.00.

Declassified and Approved For Release 2013/03/01 : CIA-RDP10-02196R000300100005-6

Declassified and Approved For Release 2013/03/01 : CIA-RDP10-02196R000300100005-6

The alloys were prepared by the fusion of zirconium iodide containing iron in an electric arc furnace with an unconsumed electrode in an atmosphere of purified argon. After homogenization by annealing, a part of the alloy was rolled into 20-60 μ thick foil, while some was converted to powder.

The homogenized annealed foil and powder were placed in a quartz ampoule in a vacuum of 10^{-5}-$5 \cdot 10^{-6}$ mm Hg. The foils and alloys, from which powders for filters were prepared, as well as the powders themselves, were annealed at a temperature of 780°C for 50 h. After annealing, the foils served as absorbers. Absorbers were also made from the powder by depositing it, mixed with an alcoholic solution of the BF-2 cement, on an aluminum backing. Sample-absorbers have been prepared with iron content of 0.4; 1.0; 1.5; 2.2; 5.6; 13; 17; 24; 26.15; 28; 37.15; 45; 55.15; 57 wt.%.

Resonance absorption spectra were recorded by an electrodynamic apparatus with a constant acceleration, operating on time behavior. After amplification and discrimination, the registered pulses were stored in a PA-256 analyzer. Co^{57} inserted in platinum was used as a radiation source. The NGR spectrometer was calibrated with respect to the standard spectra of $\alpha = Fe_2O_3$, sodium nitroprusside, and Armco iron. The isomeric shifts were determined relative to the Co^{57} in platinum source.

The resonance absorption spectra, obtained at T = 300°K, are represented in Fig. 1. The NGR spectra for absorbers containing 0.4-24 wt.% of iron appear as a well resolved hyperfine splitting in the 4.2-1050°K range. At 300°K, the quadrupole splitting $\Delta E = 0.89 \pm 0.01$ mm/sec (see Fig. 1a). The isomeric shift δ within this interval does not vary with the composition or with the annealing time and temperature, and for T = 300°K, $\delta = 685 \pm 0.005$ mm/sec.

For alloys, in which the concentration of iron exceeded 24 wt.%, the absorption spectra represent a superposition of lines of magnetic hyperfine and quadrupole splitting (see Fig. 1b, c).

In proportion to the increase in the iron concentration above 24 wt.% in alloys, the line intensities of the magnetic hyperfine splitting are increased, and with an iron concentration equal to 55.15 wt.%, the resonance absorption spectrum consists only of lines of magnetic hyperfine splitting (see Fig. 1d).

The effective magnetic fields H_{eff} at the nuclei in alloys of zirconium containing iron over the entire range of concentrations (25-57 wt.%) have the same value and are equal to 204 ± 10 kOe, that with great accuracy coincides with the effective magnetic fields in the intermetallic compound $ZrFe_2$ [9-11].

According to the phase diagram [1], the solubility of iron in zirconium is 0.02% at a temperature of 800°C. Therefore, as has been shown by autoradiographical and microstructural studies [12], short-duration annealing (during 3 h at 800°C) also results in complete separation of the iron in the form of an intermetallic compound.

The experimental data confirms that upon annealing the iron separates out in the form of intermetallic compounds. This follows from the fact that, for alloys containing up to 24 wt.% of iron, the isomeric shift does not vary with the duration of the annealing or the composition. The observed spectra indicate the presence in a zirconium–iron (25-57 wt.%) system of two compounds. One of these compounds is the intermetal $ZrFe_2$ having NGR spectra with a magnetic hyperfine structure [9-11] (see Fig. 1b, c). The other compound has a resonance absorption spectrum in the form of the lines in the quadrupole splitting superimposed on the lines of the $ZrFe_2$. Its isomeric shift agrees with the isomeric shift found in alloys containing up to 24 wt.% of iron. This indicates the fact that the lines of quadrupole splitting in all of the alloys investigated corresponds to the same unknown intermetallic compound. Thus, with iron content in the alloys up to 24 wt.% only one unknown intermetallic compound separates out, while with an iron content greater than 24 wt.% this same intermetal separates out along with $ZrFe_2$. The quantity of unknown intermetal in alloys containing more than 24 wt.% of iron decreases in proportion to the approach to a stoichiometric composition for the $ZrFe_2$. This follows from the fact that the line intensities of the quadrupole splitting decrease (see Fig. 1b-d).

Because there is only one unknown intermetallic compound in zirconium–iron alloys with iron content up to 24% by weight, while both the unknown compound and $ZrFe_2$ are found in alloys containing more than 24 wt.% of iron, then, consequently, the unknown compound has a stoichiometric composition of Zr_2Fe which corresponds to an alloy of Zr + 24 wt.% of Fe (33 at.%).

Thus, in alloys of zirconium containing iron over the 0.4-24 wt.% range there is a single intermetallic compound: Zr_2Fe; while over the 25-55.15 wt.% range of iron content, there are two compounds: Zr_2Fe and $ZrFe_2$.

Declassified and Approved For Release 2013/03/01 : CIA-RDP10-02196R000300100005-6

Declassified and Approved For Release 2013/03/01 : CIA-RDP10-02196R000300100005-6

The observed broadening of the lines in the magnetic hyperfine splitting (see Fig. 1b–d) is explained by the presence, in an elementary unit of the $ZrFe_2$ compound, of two types of iron atoms, for which the angles between the axis and the axially symmetric gradients of the electric and magnetic fields equal: $\theta_1 = 0°$, $\theta_2 = 70°32'$ [11].

LITERATURE CITED

1. M. Khansen and K. Anderko, The Structure of Binary Alloys [in Russian], Metallurgizdat, Moscow (1962).
2. E. Hayes et al., Trans. Amer. Soc. Metals, 43, 888 (1951).
3. L. Tanner and D. Levinson, Trans. Met. Soc., AIME, 215, 1066 (1959).
4. V. Vogel and W. Gottingen, Arch. Eisenhuttenwesen, 5, 387 (1932).
5. H. Wallbaum, Arch, Eisenhuttenwesen, 14, 521 (1941).
6. Atomic Energy Review, Vol. 1, IAEA, Vienna (1963), p. 152.
7. I. L. Ivanov, Physicochemical Properties of Zirconium [in Russian], Nauka, Moscow (1967).
8. A. S. Berezhnoi, Multicomponent Systems of Oxides [in Russian], Naukova Dumka, Kiev (1970).
9. G. Wertheim and V. Iaccarino, Phys. Rev., 135, A51 (1964).
10. S. Komura and N. Shikasano, J. Phys. Soc. Japan, 18, 323 (1963).
11. W. Wallace and J. Epstein, J. Chem. Phys., 35, 238 (1961).
12. P. L. Gruzin, G. G. Ryabova, and G. B. Fedorov, At. Énerg., 8, 58 (1960).

Declassified and Approved For Release 2013/03/01 : CIA-RDP10-02196R000300100005-6

Declassified and Approved For Release 2013/03/01 : CIA-RDP10-02196R000300100005-6

MEASUREMENT OF THE NEUTRON SPECTRUM AT THE OUTLET OF THE HORIZONTAL CHANNELS IN A HEAVY WATER REACTOR AND THE SM-2 REACTOR BY THE TIME OF FLIGHT METHOD

S. M. Kalebin, M. Adib,
G. V. Rukolaine, O. M. Gudkov,
T. S. Belanova, N. G. Kocherygin,
and S. N. Nikol'skii

UDC 621.039.524

The research reactor SM-2 (Scientific-Research Institute of Aviation Instruments) has important features in the arrangement of its core [1] and is distinguished by high neutron flux ($\sim 2 \cdot 10^{15}$ neutrons/cm^2 · sec). This reactor's neutron spectrum was measured at the outlet of a horizontal channel, and the results are given in this article. For comparison, analogous measurements were made on the Institute of Theoretical and Experimental Physics (ITÉF) thermal heavy-water reactor [2]. Neutron choppers with a magnetic suspension [3] and identical detectors, i.e., boron counters SNM-5 with a BF_3 pressure $\approx$ 230 mm Hg, were used in both cases. These detectors fulfilled the requirements of a "sensitive" detector, and their efficiency was proportional to 1/v with good accuracy, where v is the neutron velocity. Measurement of the spectrum on the ITÉF reactor was done prior to its reconstruction [4], using a crystal spectrometer.

In the thermal energy region, the neutron spectrum was compared with a Maxwellian distribution. In order to do this, a computer was used to fit the experimental data, by the method of least squares, to an expression of the form

$$N(\lambda) = \frac{\varepsilon}{\lambda^{\alpha}} \lambda_0^3 e^{-\left(\frac{\lambda_0}{\lambda}\right)^2} = \Phi(\lambda)\, \lambda d\lambda,$$

where $N(\lambda)$ is the number of counts in the channels of the time analyzer (corrected for the analyzer's counting loss, for the chopper's transmission function, etc.); λ is the neutron wavelength; λ_0 is the neutron wavelength corresponding to the most probable neutron velocity; and $\Phi(\lambda)$ is the neutron flux. The constants ε, λ_0, and α were assigned values giving the best possible agreement between the expression and the experimental data.

The thermal neutron temperature T was found from the equation

$$T = \frac{949.6}{2\lambda_{\max}^2},$$

where λ_{max} is the neutron wavelength corresponding to the maximum in the experimental distribution.

On the ITÉF reactor, the neutron spectrum was measured at the outlet of horizontal channel No. 4 for three circulating-heavy-water (moderator) temperatures. The water temperatures at the core outlet were 43 ± 1, 49 ± 1, and 64 ± 1°C, and at the inlet, 23 ± 1, 31 ± 1, and 45 ± 1°C, respectively. In all cases it was established that the neutron distribution in the thermal energy region virtually does not differ from the Maxwellian (α = 3.960 ± 0.014). The neutron temperatures were 65 ± 4, 68 ± 4, and 83 ± 4°C, respectively. As may be seen, the neutron temperature varies with the moderator temperature, and exceeds the latter by ~ 20°C.

The experimental neutron spectrum for a moderator temperature of 43°C is given in Fig. 1 (the results are corrected for the chopper's transmission function, the analyzer's counting loss, etc.). The results

Translated from Atomnaya Énergiya, Vol. 32, No. 6, pp. 485-487, June, 1972. Original article submitted July 22, 1971; revision submitted December 30, 1971.

© 1972 Consultants Bureau, a division of Plenum Publishing Corporation, 227 West 17th Street, New York, N. Y. 10011. All rights reserved. This article cannot be reproduced for any purpose whatsoever without permission of the publisher. A copy of this article is available from the publisher for $15.00.

Declassified and Approved For Release 2013/03/01 : CIA-RDP10-02196R000300100005-6

Declassified and Approved For Release 2013/03/01 : CIA-RDP10-02196R000300100005-6

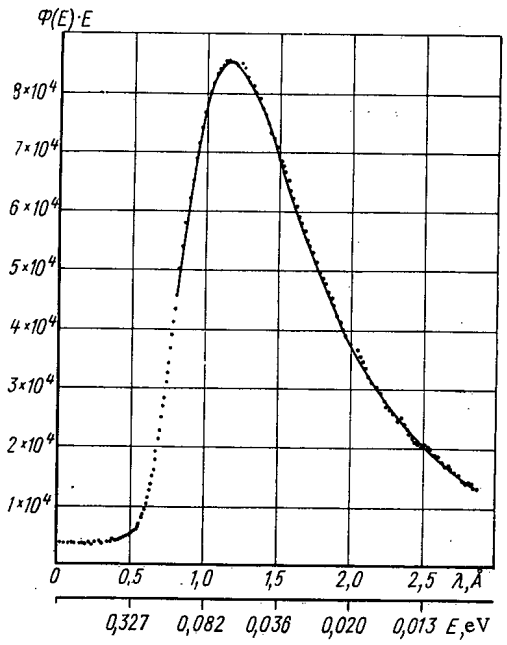

Fig. 1

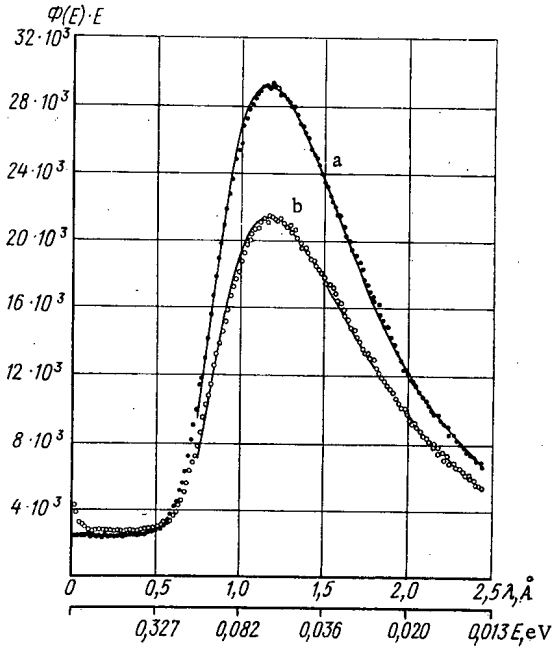

Fig. 2

Fig. 1. Neutron spectrum of the ITÉF reactor. The solid line is the result of calculation by the method of least squares, using a computer.

Fig. 2. Neutron spectrum of the SM-2 reactor: a) with beryllium; b) without beryllium. The solid line is the results of calculation by the method of least squares, using a computer.

of the spectrum calculation done by computer are shown with a solid line. The results of measurement in the resonance energy region are given in the figure in addition to the Maxwellian part of the spectrum. It may be seen that for an energy of ~0.5 eV and higher, the spectrum of the neutrons emerging from the ITÉF reactor's horizontal channel is proportional to 1/E, where E is the neutron energy.

The neutron spectrum of the SM-2 reactor was measured at the outlet of horizontal channel No. 1 for two cases. In the first case, there was a 7 cm thickness of beryllium between the reactor core and the channel, the reactor power was 75 MW, and the cooling-water temperature was 64 ± 1°C and 95 ± 1°C at core entry and exit, respectively. The results are presented in Fig. 2a. It was found by computer that the thermal neutron spectrum at the channel outlet corresponds to a Maxwellian distribution (α = 4.020 ± 0.017) at a neutron temperature of 86 ± 4°C. We note that the neutron temperature was lower than the cooling-water temperature at core exit. This testifies to the fact that the neutron spectrum is formed by the light water between this channel and the reactor core. The temperature of this water is apparently close to that of the coolant at reactor entry.

In the second case, the spectrum was measured without beryllium (Fig. 2b). The reactor power was 65 MW and the cooling-water temperature was 60 ± 1°C and 89 ± 1°C at entry and exit, respectively. In this case also, the neutron spectrum was close to Maxwellian (α = 3.800 ± 0.017). The neutron temperature, which was 79 ± 4°C, exceeded the water temperature at entry by ~19°C.

In the resonance energy region, the neutron spectrum, measured without beryllium, deviates from the 1/E law. This difference is, for example, ~8% for an energy of ~14 eV, and ~30% for an energy of ~400 eV.

The difference in the ratio of the thermal neutron flux to the resonance neutron flux is noteworthy. In the ITÉF reactor, this ratio is ~25 (see Fig. 1), whereas in the SM-2 reactor with beryllium it is ~12, and without beryllium, ~8 (see Fig. 2). It also follows from the experiments that in the presence of beryllium the thermal neutron flux increases by ~25%, while the resonance neutron flux diminishes by the same percentage.

The spectrum of the neutrons emerging from the horizontal channel of the SM-2 reactor is strongly affected by the light water between the core and the end of the channel (the thickness of the water layer is

Declassified and Approved For Release 2013/03/01 : CIA-RDP10-02196R000300100005-6

Declassified and Approved For Release 2013/03/01 : CIA-RDP10-02196R000300100005-6

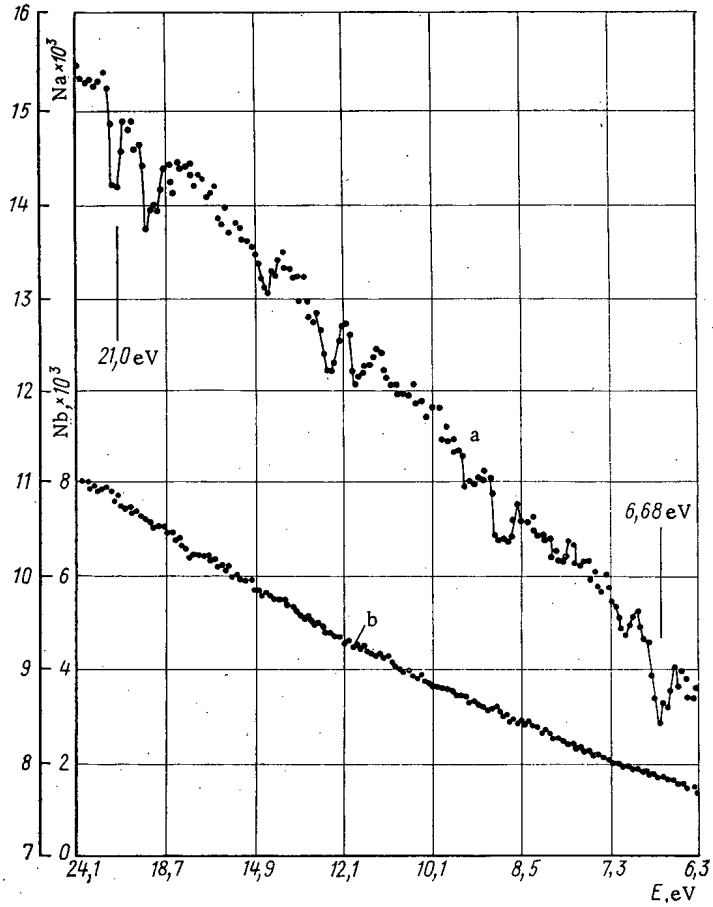

Fig. 3. Neutron counting rate in the energy region 6-25 eV: a) ITÉF reactor; b) SM-2 reactor.

~2 cm). This effect is illustrated in Fig. 3, giving the neutron counting rates, which were obtained with high resolution (the data were not corrected for the chopper's transmission function). In the ITÉF reactor, the end of the horizontal channel is separated from the core by a layer of heavy water ~2 cm in thickness, and in the SM-2 reactor, by a layer of light water of the same thickness. Enrichment of the fuel in U^{235} is approximately the same in both reactors, i.e., 80% in the heavy-water reactor and 90% in the SM-2 reactor [4]. However, traces of the strongest resonance levels of U^{235} (7.1, 8.8, 9.26, 11.65, 12.4, 14.65, and 19.64 eV) and of U^{238} (6.68 and 21.0 eV) were found in the neutron spectrum of the ITÉF reactor, but not in that of the SM-2 reactor. The light water noticeably "softens" the spectrum of the neutrons emerging from the horizontal channel of the SM-2 reactor. Therefore, on the basis of the measurements with and without beryllium, it may be surmised that the resonance neutron spectrum in the core deviates even more from the function 1/E.

The authors are indebted to Yu. G. Abov, Yu. S. Zamyatina, and V. N. Nefedova for their interest in the work, and to T. I. Belova and T. Denisova for the mathematical treatment of the experimental results.

LITERATURE CITED

1. S. M. Feinberg et al., Third Geneva Conference (1964), Report No. 320.
2. A. I. Alikhanov et al., Proc. Intern. Conf. Peaceful Uses of Atomic Energy (Geneva, 1955), Vol. 2, U.N. (1955), p. 331.
3. S. M. Kalebin, G. V. Rukolaine, and M. Adib, Pribory i Tekh. Éksperim., 3, 79 (1970).
4. V. V. Goncharov, At. Énerg., 17, 258 (1964).

Declassified and Approved For Release 2013/03/01 : CIA-RDP10-02196R000300100005-6

Declassified and Approved For Release 2013/03/01 : CIA-RDP10-02196R000300100005-6

STUDY OF THE DISPERSION (PARTICLE-SIZE) COMPOSITION OF RADIOACTIVE AEROSOLS IN THE LAYER OF AIR CLOSE TO THE EARTH

B. I. Ogorodnikov, O. G. Skotnikova,
V. I. Skitovich, L. S. Soldaeva,
and I. E. Konstantinov

UDC 551.508.957

Information as to the particle-size distribution of radioactive aerosols is important in order to study processes taking place during nuclear explosions, the propagation of radioactive substances in the atmosphere, the development of collective and individual shielding methods, and so on. Since the concentrations of radioactive aerosols in the layers of air close to the Earth are usually small, the use of impactors, thermal precipitators, electrical settlers, centrifuges, and other instruments for determining the particle sizes of aerosols encounters serious methodical and experimental difficulties. In the present investigation we used multilayer filters made of fibrous materials of the FP type [1].

Using simulated single-dispersion aerosols with particle radii 0.05–0.5 μ we studied the filtering characteristics of FPA-70-0.12, FPP-70-0.25, and LFS-2 materials distinguished from one another by the diameter of the fibers and the thickness of the layer. In order to obtain particles of radius 0.05 μ we used selenium and in order to obtain larger particles stearic acid. The breakthrough of the aerosols K, equal to the ratio of the number of particles after passing through the filter to the number before it, was

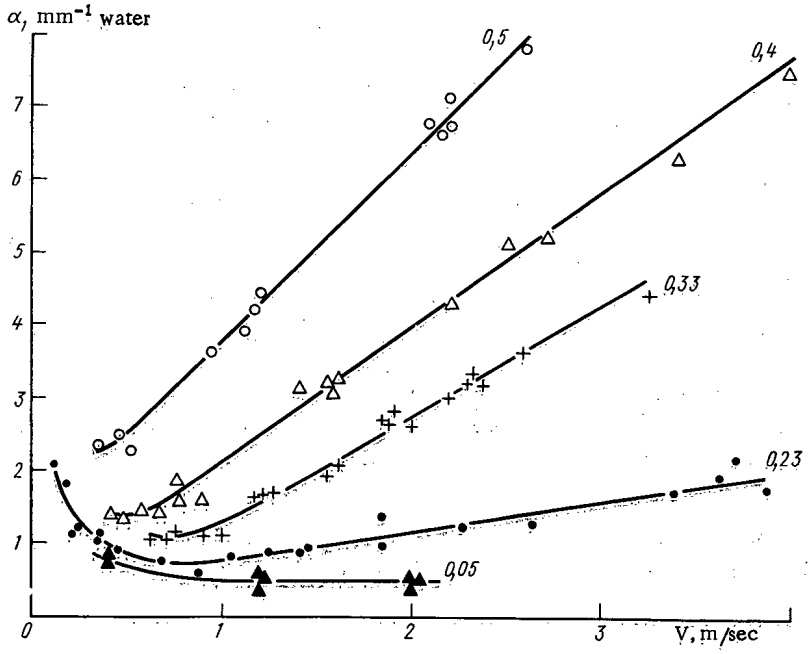

Fig. 1. Dependence of the filtering coefficient of FPP-70-0.25 on the rate of filtration for particles of different sizes. (Figures on the curves give the radius of the particles in μ.)

Translated from Atomnaya Énergiya, Vol. 32, No. 6, pp. 488–489, June, 1972. Original article submitted August 12, 1971; revision submitted November 22, 1971.

© 1972 Consultants Bureau, a division of Plenum Publishing Corporation, 227 West 17th Street, New York, N. Y. 10011. All rights reserved. This article cannot be reproduced for any purpose whatsoever without permission of the publisher. A copy of this article is available from the publisher for $15.00.

Declassified and Approved For Release 2013/03/01 : CIA-RDP10-02196R000300100005-6

Declassified and Approved For Release 2013/03/01 : CIA-RDP10-02196R000300100005-6

TABLE 1. Size Distribution of Radioactive Particles, % (Averaged over two to four samples)*

Particle size, μ	Zr^{95}	Nb^{95}	Ce^{144}	Be^{7}	Ru^{103}	Rh^{106}	Cs^{137}
$r < 0,2$	38,5	43	18,7	70	76,6	50,5	65,8
$0,2 < r < 0,3$	53,7	51	45,2	29,5	23,4	34,8	34,2
$0,3 < r < 0,5$	7,8	2,0	34,7	0,5		14,7	
$r > 0,5$			1,5				

*Particle density taken as 2 g/cm^3.

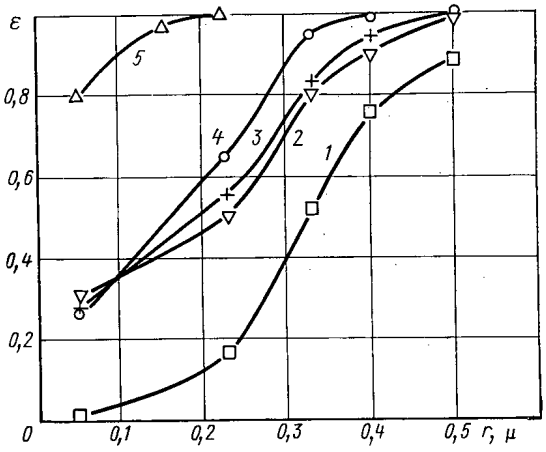

Fig. 2. Dependence of the aerosol trapping efficiency on particle radius (v in m/sec): 1) FPA-70-0.12, v = 1.0; 2) FPP-70-0.25, v = 0.75; 3) FPP-70-0.25, v = 1.0; 4) FPP-70-0.25, v = 1.8; 5) LFS-2, v = 1.0.

determined nephelometrically. Figure 1 shows the dependence of the filtering coefficient $\alpha = -\log K/[\Delta p]$ (here $[\Delta p]$ is the resistance of the filter for a velocity of 1 cm/sec) on the rate of filtration for FPP-70-0.25. Analogous results were obtained for FPA-70-0.12.

For velocities up to 40-60 cm/sec the aerosols are mainly trapped as a result of the diffusive settling of the particles and direct capture. With increasing velocity inertial settling begins, and above 100 cm/sec α becomes proportional to the square of the particle radius. In the filtering velocity range studied LFS-2 trapped the graded aerosols almost completely (Fig. 2).

Samples of air close to the ground (60-70 thousand m^3) were taken in Podmoskov in April-May, 1970 on days in which there was no fallout. The area of the filter was 0.5 m^2 and the rate of filtration 0.75-1.8 m/sec. The number of layers was 3-4. After air had ceased passing through, each layer of the filter was compressed into tablets ~3 cm in diameter and measured in a semiconductor γ-spectrometer with a Ge–Li detector 20 cm^3 in volume. The resolution of the spectrometer was 1%, the measuring time for each layer 5 h, the activity 10^{-9}-10^{-10} Ci.

The dimensions of the particles and the mean efficiency of particle trapping were determined from Fig. 2. The results were analyzed by a matrix method. Let us use q_j to denote the activity of the particles in the j-th size range and φ_i to denote the ratio of the activity of the i-th layer in the filter to the total activity of the sample; ε_{ij} denotes the average efficiency of the i-th layer of the filter for the j-th range of size. Then for a three-layer filter we may write the following system of equations

$$\begin{cases} \varphi_1 = \varepsilon_{11}q_1 + \varepsilon_{12}q_2 + \varepsilon_{13}q_3; \\ \varphi_2 = (1-\varepsilon_{11})\,\varepsilon_{21}q_1 + (1-\varepsilon_{12})\,\varepsilon_{22}q_2 + (1-\varepsilon_{13})\,\varepsilon_{23}q_3; \\ \varphi_3 = (1-\varepsilon_{11})\,(1-\varepsilon_{21})\,\varepsilon_{31}q_1 + (1-\varepsilon_{12})\,(1-\varepsilon_{22})\,\varepsilon_{32}q_2 + (1-\varepsilon_{13})\,(1-\varepsilon_{23})\,\varepsilon_{33}q_3. \end{cases}$$

The solution of the system of equations for q_1, q_2, and q_3 for each isotope gives the proportion of the total activity of the isotope concentrated in the particles of the size range selected, as in [2] (Table 1).

It follows from the results that, at the time of sampling the air close to the ground, most of the radioactive isotopes in the global fallout lay in particles with radii of under 0.5 μ. The isotopes Cs^{137}, Ru^{103}, and Rh^{106}, having volatile ancestors, and also the cosmogenic isotope Be^7, were concentrated in far smaller particles than Ce^{144}, Zr^{95}, and Nb^{95}. The agreement between the particle distribution of Zr^{95} and its daughter isotope Nb^{95} indicates that the method of determining the dispersion composition of the radioactive aerosols by filtration in multilayered filters was fairly accurate. The relative means square error for all the isotopes studied, obtained by averaging the results over three or four samples, was 15%, except for the fraction with r > 0.5 μ, for which only rough values were obtained (error ~100%).

The results correspond to existing data regarding the formation of radioactive aerosols in the cloud of a nuclear explosion. According to these views, the isotopes having volatile ancestors should concentrate

Declassified and Approved For Release 2013/03/01 : CIA-RDP10-02196R000300100005-6

Declassified and Approved For Release 2013/03/01 : CIA-RDP10-02196R000300100005-6

in the finer particles. After radioactive aerosols have passed into the atmosphere, the differences in the sizes of the particles (independently of the isotopes concentrated within them) arise mainly from processes of washing out and coagulation with natural aerosols [3, 4].

Residual differences may be explained in two ways: first, the samples were taken at the spring maximum, when intensive exchange with the stratosphere was taking place; secondly, at this period "fresh" fission products from the nuclear explosion of September 29, 1969 were falling out [5].

The authors wish to thank G.V.Sukhov for help in the measurements with the semiconducting spectrometer.

LITERATURE CITED

1. I.V.Petryanov et al., Fibrous Filter Materials FP [in Russian], Znanie, Moscow (1968).
2. L.Lockhart et al., J.Geophys.Res., 70, 6033 (1965).
3. B.Shleen et al., Science, 147, 290 (1965).
4. Ya.I.Gaziev, in: Radioactive Isotopes in the Atmosphere and Their Use in Metrology [in Russian], Atomizdat, Moscow (1965), p.153.
5. R.Weinrecih et al., Z.Naturforsch., 25a, 1156 (1970).

Declassified and Approved For Release 2013/03/01 : CIA-RDP10-02196R000300100005-6

Declassified and Approved For Release 2013/03/01 : CIA-RDP10-02196R000300100005-6

INTERACTION AND WETTABILITY IN URANIUM DIOXIDE AND ZIRCONIUM-BASED MELTS

A. T. Ageenkov, S. E. Bibikov,
G. P. Novoselov, and V. F. Savel'ev

UDC 621.039.54

Thermal breaching of fuel elements using oxide fuel through the melting of their steel jackets was discussed in [1]; it would be desirable to use this method on fuel elements with zirconium jackets as well. However, attempts to melt zirconium jackets directly have not yet brought the desired results because at and above the melting point of zirconium (1860°C) there is intensive interaction between the uranium dioxide and the melt. At the same time, eutectic alloys of zirconium with such metals as Be, Fe, Ni, Cu, Cr, and others have much lower melting points (930-1300°C) [2].

Investigations have therefore been conducted on the conditions of the alloying of zirconium with various metals, as well as on the wetting and interaction taking place in a system consisting of a metal alloy and solid uranium dioxide. The added material must satisfy the following conditions: alloyability with the zirconium jacket at a relatively low temperature; oxygen affinity lower than that of zirconium; low volatility; easy availability; and relatively low price. On the basis of the above criteria, we selected copper, iron, nickel, and stainless steel for our investigation. Iron forms two eutectics with zirconium [at 934°C (16% Fe) and at 1330°C (84% Fe)] and an intermetallic compound Fe_2Zr (1600°C) [2]. Zirconium alloys containing more than 15% copper are in the liquid state at temperatures above 1300°C [3]. Nickel and zirconium form two eutectics [at 960°C (15% Ni) and 1340°C (84% Ni)] and an intermetallic compound Ni_3Zr (1700°C) [4].

TABLE 1. Amount of Uranium Going into the Melt and Contact Angles of Wetting (Exposure time 30 min)

Specimen No.	Additive	Additive in the alloy melt, wt.%	Temperature of experiment, °C	Uranium content in melt, wt.%	Contact angle of wetting, deg
2	Iron	11,1	1250	0,12	68±5
3	The same	19,2	1250	0,18	75±5
7	Nickel	20,2	1300	1,92	44±4
8	"	30,3	1300	2,20	37±5
9	Copper	20,0	1200	0,48	62±5
12	Steel Kh18N10T	4,9	1300	0,92	71±5

In our experiments we investigated zirconium iodide, an alloy of zirconium with 1% niobium, iron (St.3 steel),

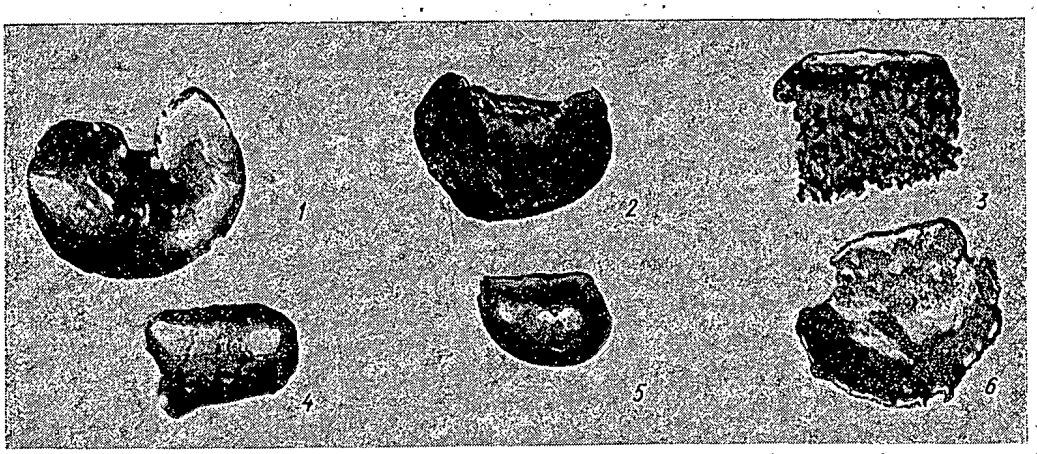

Fig. 1. External appearance of alloys with additives: 1) 10% Si; 2) 20.2% Ni; 3) 30.1% Ni; 4) 49.2% Fe; 5) 29.4% Fe; 6) 46.3% Cu.

Translated from Atomnaya Énergiya, Vol. 32, No. 6, pp. 490-491, June, 1972. Original article submitted August 12, 1971.

© 1972 Consultants Bureau, a division of Plenum Publishing Corporation, 227 West 17th Street, New York, N. Y. 10011. All rights reserved. This article cannot be reproduced for any purpose whatsoever without permission of the publisher. A copy of this article is available from the publisher for $15.00.

Declassified and Approved For Release 2013/03/01 : CIA-RDP10-02196R000300100005-6

Declassified and Approved For Release 2013/03/01 : CIA-RDP10-02196R000300100005-6

M1 copper, N1 nickel, and Kh18N10T stainless steel. We studied the conditions for the alloying of zirconium with these metals in the phase interval bounded by the points of intersection of the liquidus line with the 1300°C isotherm. The alloying of zirconium with the metals and the interaction of the melts with UO_2 were carried out in crucibles of transparent quartz in an induction-type vacuum furnace. The temperature was measured with an optical pyrometer. In studying the wettability of uranium dioxide by the melts, we used the stationary-drop method. The experiments were conducted in a resistance furnace at a vacuum of $5 \cdot 10^{-2}$ mm Hg.

When we heated zirconium specimens with metals, the liquid phase was formed as a result of contact melting in every experiment. The zirconium alloying process is fastest (10-20 sec) with copper, which may be explained by the absence of high-melting compounds in this system. At temperatures below 1300°C, specimens containing 11-30% iron, 12-30% nickel, or 5-28% stainless steel (see Fig. 1) become completely melted.

The resulting zirconium alloys have high fluidity and low surface tension, and therefore they spread out over the bottom of the crucible.

The zirconium alloys wet the uranium dioxide to different degrees. The contact angle of wetting is largest for zirconium–iron alloys [(68-75) ± 5°] (see Table 1). At 1250-1300°C there is a slight interaction of the zirconium in the melt with the solid uranium dioxide: $Zr + UO_2 = ZrO_2 + U$. The reduced uranium is dissolved in the melt. The amount of uranium going into the melt is largest in the case of zirconium alloyed with nickel (2.2%) and stainless steel (0.92%) and smallest in the case of alloys with iron (0.18%) and copper (0.48%).

Thus, we have experimentally established the conditions for the alloying of zirconium with a number of metals at temperatures ranging up to 1300°C. We have shown the absence of any substantial interaction or wettability of the uranium dioxide with the melts containing zirconium and the specified additives. The resulting data make it possible to undertake research on the thermal breaching of fuel elements with zirconium jackets by melting the jackets in the presence of metallic additives.

The authors wish to express their gratitude to N. A. Nilov for his interest and assistance in connection with the work, as well as to E. M. Valuev and É. V. Komarov for their help in carrying out the experiments.

LITERATURE CITED

1. G. P. Novoselov and A. T. Ageenkov, Atomnaya Énergiya, Vol. 16, 230 (1969).
2. E. Hayes et al., Trans. ASM, Vol. 43, 888 (1951).
3. C. Lundin et al., J. Metals, Vol. 5, 273 (1953).
4. B. Lustman and F. Kerze, The Metallurgy of Zirconium [Russian translation], IL, Moscow (1959).

Declassified and Approved For Release 2013/03/01 : CIA-RDP10-02196R000300100005-6

Declassified and Approved For Release 2013/03/01 : CIA-RDP10-02196R000300100005-6

X-RAY FLUORESCENCE ANALYSIS OF HEAVY ELEMENTS BY αX-COINCIDENCE

B. M. Aleksandrov, S. M. Solov'ev,
L. I. Tyvin, and V. P. Éismont

UDC 543.53

One of the important methods of radioisotope analysis of heavy elements is the α-spectrometer. At the present time, about 1000 α-lines of 40 natural and 240 artifical α-emitters are known [1]. However, more than 90% of these lines are concentrated in a narrow energy range (4.5-8.0 MeV). Therefore, it is natural that the α-lines of many elements appear very close to one another and cannot be resolved by semiconductor α-spectrometers applicable to isotope analysis, the better models of which have a 10-15 keV resolution. At the same time, one can only obtain such resolution with very narrow sources.

The α-, γ-coincidence appears to be ineffective in several cases; for example, for even–even nuclei. All are characterized by the rotational nature of the low-lying (the most intensively populated) excitation levels whose energies differ little from nucleus to nucleus. Aside from this, transitions from these levels are highly converted (the internal conversion coefficient ~1000) so that they are relegated to a very small part of the γ-radiation. However, as a result of the internal conversion, there arises an intense x-ray L-radiation with the transition on the order of 0.1 quantum per α-decay. On the energy distribution curve for the fluorescent L-radiation obtained by ionization processes, there are three high spikes L_α, L_β, and $L\gamma$, whose energies increase regularly with an increase in the nuclear charge Z shifting with $\Delta Z = 1$ by roughly 300, 500, and 700 eV, respectively [2]. This shift appears sufficient for definite separation of adjacent elements with respect to Z, if one utilizes up-to-date semiconductor Si(Li)- or Ge(Li)-spectrometers whose energy resolution is several hundred electron volts for measurement of the spectra. The limitation of the x-ray fluorescence technique, associated with the difficulties of its utilization for the analysis of the isotopes

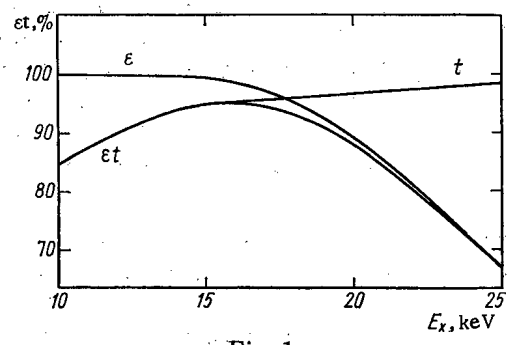

Fig. 1

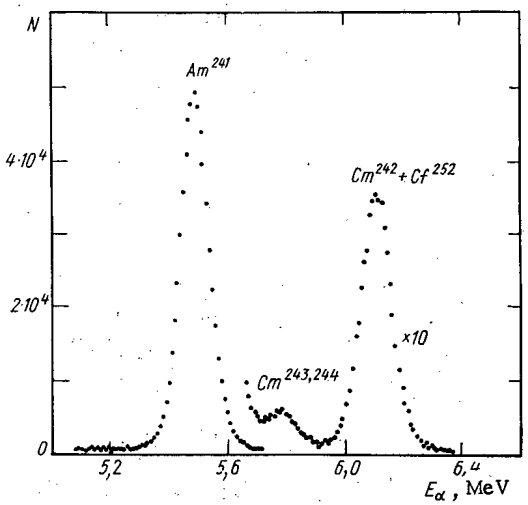

Fig. 2

Fig. 1. Dependence of the response εt of the spectrometer on the radiation energy (ε is the sensitivity; t is the penetration factor).

Fig. 2. The α-particle spectrum for the target being analyzed.

Translated from Atomnaya Énergiya, Vol. 32, No. 6, pp. 491-493, June, 1972. Original article submitted August 17, 1971.

© 1972 Consultants Bureau, a division of Plenum Publishing Corporation, 227 West 17th Street, New York, N. Y. 10011. All rights reserved. This article cannot be reproduced for any purpose whatsoever without permission of the publisher. A copy of this article is available from the publisher for $15.00.

Declassified and Approved For Release 2013/03/01 : CIA-RDP10-02196R000300100005-6

Declassified and Approved For Release 2013/03/01 : CIA-RDP10-02196R000300100005-6

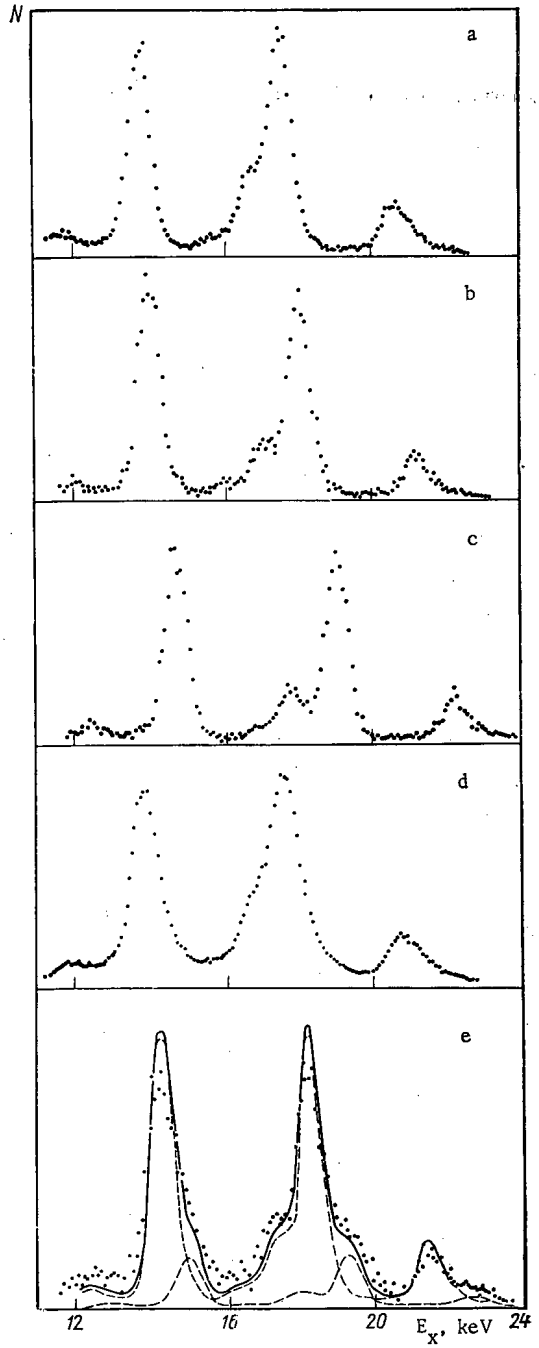

Fig. 3. Spectra of characteristic L-radiation accompanying α-decay: Am^{241} (a); Cm^{242} (b); Cf^{252} (c); $Am^{241} + Cm^{242-244} + Cf^{252}$ isotope mixture (d); and $Cm^{242} + Cf^{252}$ mixture (e). The individual spectra for Cm^{242} and Cf^{252} (in the ratio, found through the number of spontaneous fissions), as well as their sum, are shown in the last figure.

of a single element, appears to be unimportant mostly due to the well-known regularities of the α-decay coinciding with the α-spectra of nuclei differing with respect to A and Z. For example, the lines of Pu^{238} (5499 keV, 71%; 5456 keV, 29%) and Am^{241} (5486 keV, 86%; 5443 keV, 13%); as well as Cm^{242} (6112 keV, 74%; 6068 keV, 26%) and Cf^{252} (6118 keV, 84%; 6075 keV, 16%) are similar.* Apart from this, with absence of energy shifts in the L-radiation (in isotopes of a single element), analysis with respect to the number of quanta of L-radiation per decay event, which can be different for different isotopes, is possible. These considerations also led to development of the αX-coincidence method for the analysis of heavy elements.

Surface-barrier Si(Au)- and diffusion-drift Si(Li)-detectors are utilized for the measurement of α-particle and x-ray quanta energy distributions, respectively. They were enclosed in a single vacuum chamber into which a cold-duct was introduced. In the cold-duct, which is lowered into a Dewar of liquid nitrogen, there were mounted an x-ray detector and a field transistor [3]. Above the detector, a covered, 0.1 mm thick, beryllium disk, there is located, at a distance of several millimeters from gold foil, the target being analyzed, above which, in its turn, there is arranged an α-radiation detector. The energy resolution is about 700 eV for the x-ray channel, and 80 eV for the α-particle channel. The resolving time for the coincidence circuit $2\tau \approx 1$ μsec and cannot be substantially reduced because the lifetime of the low-lying excited levels of several nuclei, for example, the 59.6 keV level of Am^{241}, amounts to several times 10^{-8} sec.

Semiconductor detectors of electromagnetic radiation require sensitivity calibration and determination of its dependence on the energy of the radiation. For this, the widths of the "window" and of the operation area are measured. In the present work, these quantities were determined for the relative intensities of x-ray and soft γ-radiation lines in Co^{57} and Am^{241} spectra, which were shown to be equal to 0.007 and 2.45 mm, respectively. The energy response curve εt for the x-ray channel allowing for absorption in the target backing, the beryllium disk, and the window of the counter is shown in Fig. 1.

In the capacity of a control model, we solved the problem of determining a small amount of californium in a target of $Am^{241} + Cm^{242-244} + Cf^{252}$. As has already been mentioned, the α-lines of Cf^{252} and Cm^{242} are similar to one another, and a direct determination of Cf^{252} through the α-spectrum is difficult. The spectrum of the target being analyzed is shown in Fig. 2. The prominent lines are Am^{241}, $Cm^{243,244}$, and $Cm^{242} + Cf^{252}$; the last also includes several transitions to the lower levels of Cm^{243}: their contributions to this line comprises several percent. With utilization of the αX-coincidence method for the quantitative analysis of the relative contributions of curium and californium to the overall α-line, it is assumed that the relative yields in x-rays per α-decay event are well-known for these elements. For the determination of the relative yields of radiation for Cm^{242} and Cf^{252}, there were prepared two additional

*The relative intensities of the lines are indicated by the percentages.

Declassified and Approved For Release 2013/03/01 : CIA-RDP10-02196R000300100005-6

Declassified and Approved For Release 2013/03/01 : CIA-RDP10-02196R000300100005-6

targets: $Am^{241} + Cm^{242}$ and $Am^{241} + Cf^{252}$. All three targets were prepared by the technique of thermal pulverization in a vacuum of a blended mixture of the respective isotopes that by itself did not only attain a high uniformity, but also identical surface distributions of curium, californium, and americium. This allowed us to utilize the americium as a reference for each of our targets. All of the measurements for each of the targets were also carried out relative to this reference by means of a step-by-step separation of the corresponding α-lines (with the aid of a differential α-channel discriminator). The spectrum of the L-radiation, corresponding to this line, was measured, and the number of αL-coincidences per α-particle $N_{\alpha L}/N_\alpha$ for americium and the respective isotopes (or their mixture) was determined. In this way, the relative yields of L-radiation per α-decay were determined for Cm^{242}, Cf^{252}, and $Cm^{242} + Cf^{252}$:

$$\delta N' = \frac{N'_{\alpha L}/N'_\alpha}{N_{\alpha L}/N_\alpha}; \quad \delta N'' = \frac{N''_{\alpha L}/N''_\alpha}{N_{\alpha L}/N_\alpha}; \text{ and } \delta N''' = \frac{N'''_{\alpha L}/N'''_\alpha}{N_{\alpha L}/N_\alpha}.$$

In each case, more than 10,000 coincidences were registered and it was found that $\delta N' = 0.310$, $\delta N'' = 0.147$, and $\delta N''' = 0.277$. The background level was high only for $Cm^{242} + Cf^{252}$, where it comprised about 50% of the total number of coincidences. However, the background had to be determined with a specified precision, so that the relative error in the value of δN did not exceed 2%. Denoting through p that part of the α-activity of Cf^{252} in common with the α-lines of Cm^{242}, it is not difficult to obtain the ratio $p = (\delta N' - \delta N''')/\delta N' - \delta N''$ and one finds that $p = 0.20 \pm 0.05$. (In addition, the contribution of the californium's activity to the total α-activity of the target equals 0.016 ± 0.002.)

New information on the composition of the isotope and its atomic number (when the composition of the elements is unknown), can be obtained from the L-radiation spectra. The energy distribution of the L-series of the characteristic radiation, obtained by us, during α-decay of Am^{241} (a), Cm^{242} with the admixture of Cm^{243} mentioned previously (b), Cf^{252} (c) as well as L-radiation spectra of the target being analyzed without coincidence with some α-line (d), and under conditions involving coincidence with an α-line of $Cm^{242} + Cf^{252}$ (e) are presented in Fig. 3. It is seen that an overwhelming part of the target's total x-ray spectrum is due to the americium. In the same spectrum, corresponding to the α-line of Cm + Cf, the contribution of the californium is already found to be pronounced.

In the present work, the $Cm^{242} + Cf^{252}$ combination was not selected by chance. The californium isotope has a high rate of spontaneous fission that allows an independent estimate of its content in a target. It was found that the fraction of α-activity p for californium in the Cm + Cf line is 0.26 ± 0.02 which, within the limits of error in the determination, coincides with the value cited above. The value $(\delta N'/\delta N'') = 2.11 \pm 0.06$, therefore, the contribution of californium to the L-radiation of the two isotopes, calculated in this way, equals 0.15 ± 0.02 (with a total L-radiation for the target of 0.0033 ± 0.0004). For comparable cross sections with the ratio $(1-0.15)/0.15$, the distributions for Cm^{242} and Cf^{252} are added. These components and the results of their addition are shown in Fig. 3e. The comparison shows that the measured L-radiation distribution for a mixture of these isotopes agrees with the theoretical distribution. Some broadening in the spectrum of the mixture in comparison with the sum of the spectra for the individual components is associated with the large, in this case, load of the x-ray channel, rather than with measurements of the spectra for the separate isotopes.

In our opinion, the example presented corroborates the possiblity and feasibility for the utilization of a semiconductor αX-coincidence spectrometer for the analysis of a complex mixture of the heavy elements.

The authors thank N.A. Perfilov for interest in the work.

LITERATURE CITED

1. J. Post, Actinides Rev., 1, 55 (1967).
2. E. Storm and H. Israel, Nucl. Data Tables, A7 (1970), p. 565.
3. S.M. Solov'ev et al., Pribory i Tekhnika Éksperimenta, No. 1 (1972).

Declassified and Approved For Release 2013/03/01 : CIA-RDP10-02196R000300100005-6

Declassified and Approved For Release 2013/03/01 : CIA-RDP10-02196R000300100005-6

EFFECTIVE NEUTRON ABSORPTION CROSS SECTIONS FOR Cf^{252} AND Cf^{253} IN THE CENTRAL CHANNEL OF AN SM-2 REACTOR

V. A. Anufriev, V. D. Gavrilov,
Yu. S. Zamyatnin, V. V. Ivanenko,
and G. N. Yakovlev

UDC 539.125.5.173

The effective cross sections for absorption of neutrons by californium isotopes, measured for various reactors, differ from each other by an order of magnitude, which is significantly greater than the experimental error [1, 2].

The variation in the characteristics of reactor neutron spectra, which is one of the causes of the observed spread, limits the possibility of using the cross sections in the calculation of isotope-accumulation processes in inhomogeneous reactors.

To determine the effective neutron-absorption coefficients in the central channel of the SM-2 reactor, we irradiated two targets consisting of Cf^{252} with an impurity of a lighter californium isotope (~20%). The isotope composition of the irradiated targets was investigated on a semiconductor α-spectrometer having an energy resolution ≈25-30 keV. The integrated neutron fluxes measured by cobalt monitors were $1.8 \cdot 10^{21}$ and $1.1 \cdot 10^{21}$ neutrons/cm^2. The Cf^{252} depletion cross section was found to be 72 ± 18 barn. Keeping in mind the theoretical estimates for the Cf^{252} fission cross sections [3], one may attribute the measured value completely to the value of the effective radiation-capture cross section. For Cf^{253}, whose content in the samples after irradiation was determined by the accumulation of daughter Es^{253}, the effective absorption cross section was found to be 6260 ± 1800 barn. Due to the smallness of the integrated fluxes, the quantitative Cf^{254} content in the irradiated samples can be estimated only approximately. Assuming that the depletion cross section of Cf^{254} is ≤100 barn, the Cf^{253} radiation-capture cross section is estimated to be ≈10 barn.

The magnitudes for the cross sections which we have found in this work are significantly larger than the published findings [1, 2, 4]. A possible reason for this is the hardness of the neutron spectrum of the SM-2 reactor. The ratio of the fission and radiation-capture cross sections for Cf^{253} is significantly greater than the analogous ratios for other transuranic nuclei and it limits the possibility of Cf^{254} accumulation. Inasmuch as the Cf^{253} depletion probability is much greater than its β-decay probability, the optimal regime for obtaining einsteinium isotopes appears to be the alternation of cycles of irradiation with extraction which allows transformation of accumulated Cf^{253} into Es^{253}.

LITERATURE CITED

1. E. Hyde et al., Nuclear Properties of the Heavy Elements [Russian translation], Vol. 2, Atomizdat, Moscow (1968), p. 61.
2. I. Halperin, ORNL-4306 (1968).
3. A. Prince, in: Californium-252, Proc. of Symposium, CONF-681032, Sponsored by the New York Metropolian Section of the American Nuclear Society, New York (1968), p. 23.
4. I. Halperin, Nucl. Sci. and Engng., 37, 228 (1969).

Translated from Atomnaya Énergiya, Vol. 32, No. 6, pp. 493-494, June, 1972. Original article submitted August 20, 1971.

© 1972 Consultants Bureau, a division of Plenum Publishing Corporation, 227 West 17th Street, New York, N. Y. 10011. All rights reserved. This article cannot be reproduced for any purpose whatsoever without permission of the publisher. A copy of this article is available from the publisher for $15.00.

Declassified and Approved For Release 2013/03/01 : CIA-RDP10-02196R000300100005-6

Declassified and Approved For Release 2013/03/01 : CIA-RDP10-02196R000300100005-6

UNFOLDING FAST-NEUTRON SPECTRA FROM THRESHOLD DETECTOR ACTIVITIES

A. M. Aglitskii, S. S. Lomakin,
A. G. Morozov, V. I. Petrov,
and S. G. Popov

UDC 621.039.512.45

Integral fast-neutron spectra in the experimental channels of the reactor at the Novo-Voronezh Atomic Power Station were measured by the threshold detector method and the values of the activation integrals were determined for each detector [1].

In this paper, differential fast-neutron spectra are unfolded on the basis of the values of the activation integrals found in [1]. The Dierckx method, the iteration method [2], a rapid method [3], and the spectral indices method [4] were used to unfold the spectra. The essence of all these methods is the following.

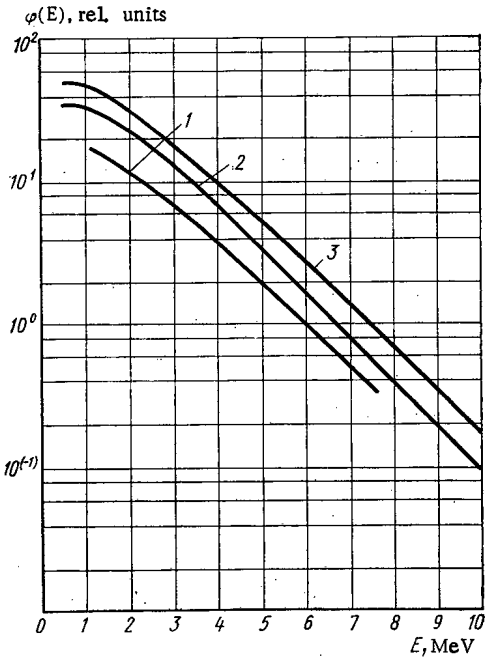

Fig. 1

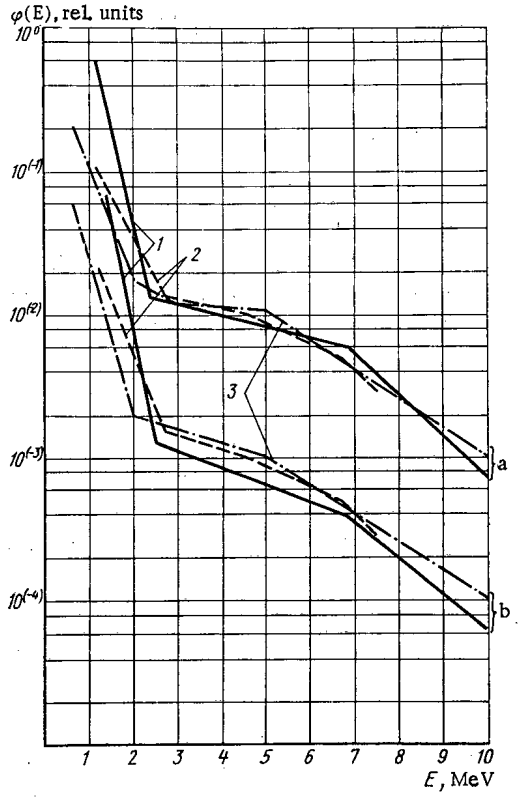

Fig. 2

Fig. 1. Fast-neutron spectra at the center of the reactor core: 1) neutron spectrum unfolded by the rapid method; 2) fission-neutron spectrum; 3) neutron spectrum unfolded by the method of spectral indices.

Fig. 2. Fast-neutron spectra inside (a) and outside (b) the reactor vessel as unfolded: 1) by the iteration method; 2) by the rapid method; 3) by Dierckx method.

Translated from Atomnaya Énergiya, Vol. 32, No. 6, pp. 494–495, June, 1972. Original article submitted September 2, 1971.

© 1972 Consultants Bureau, a division of Plenum Publishing Corporation, 227 West 17th Street, New York, N. Y. 10011. All rights reserved. This article cannot be reproduced for any purpose whatsoever without permission of the publisher. A copy of this article is available from the publisher for $15.00.

Declassified and Approved For Release 2013/03/01 : CIA-RDP10-02196R000300100005-6

Declassified and Approved For Release 2013/03/01 : CIA-RDP10-02196R000300100005-6

The specific activity A of irradiated threshold detectors (activation integral) is related to the threshold reaction cross section $\sigma_i(E)$ and the desired neutron spectrum $\varphi(E)$ by an integral relation of the form

$$A_i = \int_0^\infty \sigma_i(E)\,\varphi(E)\,dE,\ i = 1, 2, 3, \ldots, n, \tag{1}$$

where n is the number of threshold detectors. For a unique solution of this equation system, it is necessary to make some assumption about the mathematical form of the desired spectrum $\varphi(E)$, i.e., it is necessary to represent spectra in the form of expressions with a finite number of unknown parameters.

In the first three methods, the energy range under consideration is broken up into intervals in each of which the desired spectrum is in the form

$$\varphi(E) = C\exp(-\mu E). \tag{2}$$

The boundaries of the intervals are determined by the threshold detector sensitivity functions $\sigma_i(E)\varphi(E)$. The unknown parameters C and μ in each interval are determined from the continuity condition for the spectrum and from the equations obtained when Eq. (2) is substituted into Eq. (1). It is necessary to have two threshold detectors in the last interval. The activation integrals A_i are used as input data in Dierckx' method; in the rapid and iteration methods, the integral fast neutron fluxes determined by the effective threshold cross section method are used. The effective threshold energy E^i_{eff} and the effective threshold cross section σ^i_{eff} are introduced in the following manner:

$$A_i = \int_0^\infty \sigma_i(E)\,\varphi(E)\,dE = \sigma^i_{eff}\int_{E^i_{eff}}^\infty \varphi(E)\,dE = \sigma^i_{eff}\,\Phi(E^i_{eff}), \tag{3}$$

where $\Phi(E^i_{eff})$ is the integral flux of neutrons with energies greater than E^i_{eff}.

In the rapid method, σ^i_{eff} and E^i_{eff} are determined from several known spectra [3]. In the iteration method, these quantities are determined from the fission-neutron spectrum in accordance with Grundl and Usner [5]. Using these values, one unfolds a desired neutron spectrum from which new values of E^i_{eff} are determined (σ^i_{eff} retains its previous value). Then the procedure is repeated.

In all the methods mentioned above, the unfolding process starts with the last interval.

The method of spectral indices is used in the case where the desired spectrum is not much different from the fission-neutron spectrum. Such a spectrum can be represented in the form

$$\varphi(E) = CE^{1/2}\exp(-\beta E) \tag{4}$$

(for a fission spectrum β = 0.775). Values of the activation integrals

$$\tilde{A}_i = \int_0^\infty CE^{1/2}\exp(-\beta E)\,\sigma_i(E)\,dE \tag{5}$$

are calculated for various β.

By comparison of the experimental quantities A_i/A_j and the calculated $\tilde{A}_i/\tilde{A}_j$, that value of β is selected for which the difference between these ratios is a minimum.

Fast-neutron spectra unfolded by these methods are shown in Figs. 1 and 2.

On the basis of these results, one can arrive at the following conclusions: 1) the neutron spectrum at the center of the core is similar to a fission-neutron spectrum; 2) the neutron spectrum inside the reactor vessel has a shape characteristic of spectra from neutrons that have penetrated a layer of water; 3) the neutron spectrum outside the reactor vessel is "softer" than the neutron spectrum inside the vessel; 4) the neutron spectra obtained by the various methods are in satisfactory agreement. The greatest difference is observed in the low-energy region.

LITERATURE CITED

1. S. S. Lomakin et al., At. Energ., 31, 54 (1971).
2. Neutron Dosimetry, IAEA, Vienna (1963), pp. 27, 325.

Declassified and Approved For Release 2013/03/01 : CIA-RDP10-02196R000300100005-6

Declassified and Approved For Release 2013/03/01 : CIA-RDP10-02196R000300100005-6

3. V.S.Troshin and E.A.Kramer-Ageev, At.Énerg., 29, 37 (1970).
4. K.Beckurts and K.Wirtz, Neutron Physics [Russian translation], Atomizdat, Moscow (1967).
5. W.Zijp, Review of Activation Methods for the Determination of Fast Neutron Spectra Pattern (May, 1965), p.45.

Declassified and Approved For Release 2013/03/01 : CIA-RDP10-02196R000300100005-6

Declassified and Approved For Release 2013/03/01 : CIA-RDP10-02196R000300100005-6

ANGULAR DISTRIBUTIONS OF PHOTONEUTRONS FROM Al, Ti, Cu, Mo, W, AND Pb

V. P. Kovalev, V. P. Kharin,
V. V. Gordeev, and V. I. Isaev

UDC 539.125.5.18

Information on the angular distributions of photoneutrons for energies of excitation of the nucleus of 15 to 30 MeV is important for clarifying the mechanism of photonuclear reactions in the region of the giant dipole and quadrupole resonances.

In most studies of the angular distributions of photoneutrons [1-4] targets were irradiated by collimated beams of γ-rays of various energies. Considerably less effort has been devoted to the study of the angular distributions of photoneutrons from various targets bombarded directly with electrons, although in most practical applications just such a method is used to obtain photoneutrons [5].

It is shown in [6] that the cross section for the electron disintegration of a nucleus in the 13-17.5 MeV range is about 400 times smaller than the corresponding cross section for photodisintegration, but the energy thresholds of the reactions are the same. One can conclude from this that for electron energies of ~20 MeV most of the photoneutrons are produced in (γ, n) reactions.

TABLE 1. Angular Distributions of Photoneutrons

Target	Electron energy, MeV	Detector	Angle, deg							B/A
			30	50	70	90	110	130	150	
Al	22,5	$P^{31}(n,p)$	1,05±0,08	1,03±0,08	0,97±0,08	1,0±0,08	0,98±0,08	1,02±0,08	1,04±0,08	Isotropic
	22,5	$Al^{27}(n,p)$	0,90±0,15	0,95±0,15	1,02±0,15	1,00±0,14	0,96±0,13	1,07±0,13	1,01±0,13	"
Ti	22,5	$P^{31}(n,p)$	1,04±0,07	0,96±0,07	1,03±0,07	1,00±0,07	0,98±0,07	1,05±0,07	1,03±0,07	"
	22,5	$Al^{27}(n,p)$	1,06±0,13	0,94±0,13	1,04±0,12	1,00±0,12	0,95±0,11	0,98±0,11	1,02±0,10	"
Cu	12,8	$P^{31}(n,p)$	0,97±0,10	1,04±0,10	1,02±0,10	1,00±0,10	1,01±0,10	0,90±0,10	0,96±0,10	"
	17,0	$P^{31}(n,p)$	1,03±0,07	0,97±0,07	1,00±0,07	1,00±0,07	1,06±0,07	0,95±0,07	0,88±0,07	"
	22,5	$P^{31}(n,p)$	0,87±0,05	0,94±0,05	0,97±0,05	1,00±0,05	0,99±0,05	0,93±0,05	0,91±0,05	0,18±0,04
	22,5	$Al^{27}(n,p)$	0,75±0,09	0,86±0,07	0,98±0,06	1,00±0,05	1,02±0,05	0,94±0,04	0,90±0,04	0,28±0,06
Mo	22,5	$P^{31}(n,p)$	0,90±0,05	0,93±0,05	0,98±0,05	1,00±0,05	0,99±0,05	0,92±0,05	0,84±0,05	0,21±0,04
	22,5	$Al^{27}(n,p)$	0,80±0,08	0,95±0,08	0,95±0,07	1,00±0,06	0,94±0,05	0,83±0,04	0,72±0,04	0,44±0,08
	22,5	$Al^{27}(n,\alpha)$	0,72±0,08	0,84±0,08	0,89±0,08	1,00±0,08	0,95±0,08	0,87±0,08	0,63±0,08	0,78±0,18
W	22,5	$P^{31}(n,p)$	0,85±0,04	0,90±0,04	0,98±0,04	1,00±0,04	0,98±0,04	0,92±0,04	0,087±0,04	0,25±0,04
	22,5	$Al^{27}(n,p)$	0,78±0,06	0,84±0,06	0,89±0,05	1,00±0,05	0,97±0,04	0,86±0,04	0,75±0,04	0,54±0,06
Pb	22,5	$P^{31}(n,p)$	0,79±0,04	0,85±0,04	0,96±0,04	1,00±0,04	0,98±0,04	0,88±0,04	0,84±0,04	0,36±0,05
	22,5	$Al^{27}(n,p)$	0,70±0,09	0,81±0,08	0,94±0,07	1,00±0,06	0,94±0,06	0,80±0,05	0,69±0,05	0,69±0,12

Translated from Atomnaya Énergiya, Vol. 32, No. 6, pp. 496-497, June, 1972. Original article submitted September 6, 1971.

© 1972 Consultants Bureau, a division of Plenum Publishing Corporation, 227 West 17th Street, New York, N. Y. 10011. All rights reserved. This article cannot be reproduced for any purpose whatsoever without permission of the publisher. A copy of this article is available from the publisher for $15.00.

Declassified and Approved For Release 2013/03/01 : CIA-RDP10-02196R000300100005-6

Declassified and Approved For Release 2013/03/01 : CIA-RDP10-02196R000300100005-6

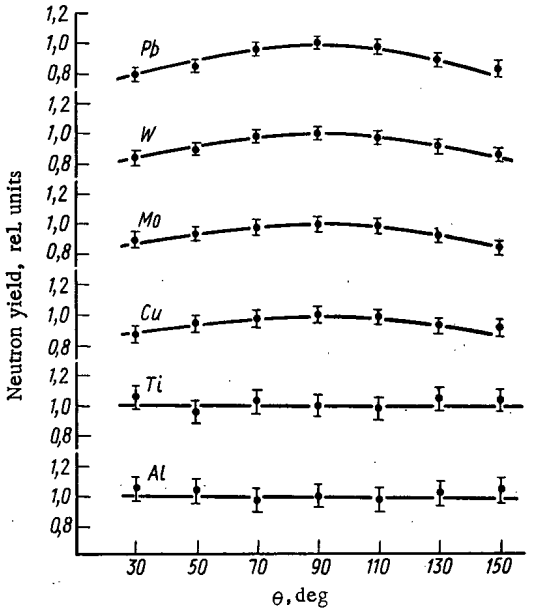

Fig. 1. Angular distributions of fast photoneutrons from Al, Ti, Cu, Mg, W, and Pb bombarded with 22.5 MeV electrons. P^{31} (n, p) Si^{31} detector.

We have studied the angular distributions of photoneutrons from Al, Ti, Cu, Mo, W, and Pb targets bombarded with monoenergetic electrons having energies from 12 to 23 MeV. The targets were cylindrical in form and 15 mm in diameter. The target thicknesses were as follows:

Element	Al	Ti	Cu	Mo	W	Pb
Thickness, g/cm^2	4.05	6.75	13.32	15.54	19.3	17.0

The threshold reactions P^{31} (n, p) Si^{31}, Al^{27} (n, p) Mg^{27}, Al^{27} (n, α) Na^{24} with effective thresholds of 2.7, 4.5, and 8.1 MeV, respectively, were used for detection. The experiments were performed with a linear electron accelerator beam having a maximum energy of 25 MeV [7]. An electron beam ~10 mm in diameter was directed onto the face of a target placed 30 cm from the exit window of the accelerator. The neutron detectors were placed around the target at fixed angles. The angles subtended by the detectors were 4 and 6°, respectively, for phosphorus and aluminum detectors. The activity induced as a result of the P^{31} (n, p) Si^{31} reaction was recorded by a gas counter combined with standard counting equipment. The Al^{27} (n, p) Mg^{27} and Al^{27} (n, α) Na^{24} reactions were detected by their characteristic γ-radiation using a single-crystal γ-spectrometer. The results of the measurements with the P^{31} (n, p) detector and an electron energy of 22.5 MeV are shown in Fig. 1. The a[illegible]ar distributions of the fast photoneutrons are approximated by the relation

$$f(\theta) = A + B\sin^2\theta. \quad (1)$$

Analysis of the experimental data shows that for light elements (Al, Ti) the angular distributions are isotropic within the limits of statistical error. As the atomic number increases the angular distributions tend to become more anisotropic around 90°. The ratio B/A of Eq. (1) is used as an anisotropy index. The anisotropy also increases with increasing threshold for detecting neutrons.

Table 1 shows the results of the measurements of the angular distributions of photoneutrons. They are presented as yields relative to the yield at 90°. The ratio B/A is given as a function of electron energy and the threshold energy for detecting neutrons.

The shape of the angular distributions of photoneutrons for elements of medium and high atomic numbers indicates the dipole character of the absorption of γ-rays in the energy range studied. No appreciable asymmetry in the angular distributions of photoneutrons is observed at these excitation energies.

LITERATURE CITED

1. L. E. Lazareva and A. I. Lepestkin, Yadernaya Fizika, 11, 266 (1970).
2. F. Ferero et al., Nuovo Cimento, 4, 2, 418 (1956).
3. K. McNeill et al., Canad. J. Phys., 46, 1974 (1968).
4. Hiroaki Tsubota et al., J. Phys. Soc. Japan, 26, 1 (1969).
5. D. Gayther and P. Goode, J. Nucl. Energy, 21, 733 (1967).
6. L. Skaggs et al., Phys. Rev., 73, 420 (1948).
7. V. I. Ermakov et al., Atomnaya Énergiya, 29, 206 (1970).

Declassified and Approved For Release 2013/03/01 : CIA-RDP10-02196R000300100005-6

Declassified and Approved For Release 2013/03/01 : CIA-RDP10-02196R000300100005-6

CALCULATION OF THE BOUNDARY EFFECT IN PARTICLE-TRANSPORT PROBLEMS

S. I. Durinov, V. V. Uchaikin, and A. M. Kol'chuzhkin

UDC 539.12.172

The particle flux at a medium–vacuum boundary for a plane-parallel geometry can be expressed in terms of the particle flux in a homogeneous infinite medium (which is an easier calculation to make), and the differential albedo – whose numerical values are given in the literature for a number of cases.

We introduce the following notation: ω and E are the direction and energy of the moving particles, and $j(z, \omega, E)$ is the differential particle flux along the z axis, which is related to the differential flux Φ by

$$j(z, \omega, E) = \cos\theta \Phi(z, \omega, E).$$

For definiteness, we assume that the particle source is to the left of the observation point z. Evidently, the particle flux j_1 that intersects the density z = const for the first time equals the particle flux under the boundary-geometry conditions (when the medium–vacuum boundary passes through the point z).

In an infinite medium, a fraction of these particles are reflected from the right with respect to the point z of the half-space and generate a flux j_2 in the half-space, which is related to j_1 by

$$j_2(z, \omega, E) = \hat{A} j_1(z, \omega, E),$$

where

$$\hat{A} = -\int d\omega' \int dE' a(\omega, E \mid \omega', E')$$

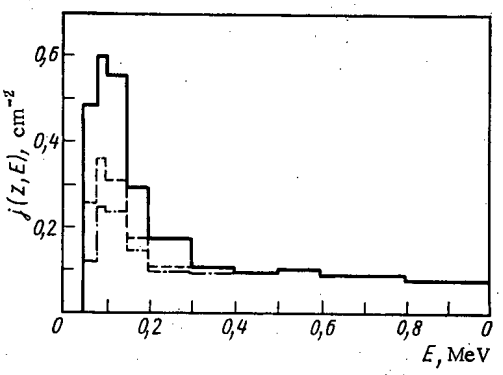

Fig. 1

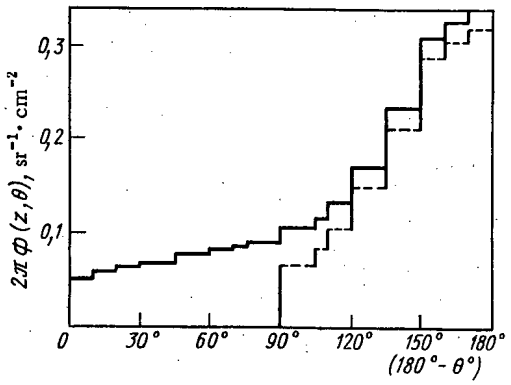

Fig. 2

Fig. 1. Effect of boundary on energy distribution of quanta ($\mu_0 z = 4$): ——) energy distribution of quanta in infinite medium; – – – –) energy distribution of quanta at the medium–vacuum boundary in the $j_1 = j_+$; –·–·–·) energy distribution of quanta at the medium–vacuum boundary, obtained from Eq. (7).

Fig. 2. Effect of boundary on angular distribution of quanta ($\mu_0 z = 4$): ——) angular distribution of quanta in infinite medium; – – – –) angular distribution of quanta at the medium–vacuum boundary, obtained from Eq. (7).

Translated from Atomnaya Énergiya, Vol. 32, No. 6, pp. 497-499, June, 1972. Original article submitted October 7, 1971.

© 1972 Consultants Bureau, a division of Plenum Publishing Corporation, 227 West 17th Street, New York, N. Y. 10011. All rights reserved. This article cannot be reproduced for any purpose whatsoever without permission of the publisher. A copy of this article is available from the publisher for $15.00.

Declassified and Approved For Release 2013/03/01 : CIA-RDP10-02196R000300100005-6

Declassified and Approved For Release 2013/03/01 : CIA-RDP10-02196R000300100005-6

TABLE 1. Dose Buildup Factors B for an Infinite Medium and at the Medium–Vacuum Boundary

$\mu_0 z$	$\cos\theta_0=1$			$\cos\theta_0=0{,}75$			$\cos\theta_0=0{,}5$		
	B	B_+	B_1	B	B_+	B_1	B	B_+	B_1
0,5	1,57	1,45	1,42	1,68	1,51	1,47	1,82	1,62	1,57
1,0	2,03	1,81	1,77	2,24	1,99	1,92	2,61	2,29	2,20
2,0	2,98	2,64	2,57	3,63	3,14	3,09	5,40	4,79	4,69
4,0	5,10	4,48	4,39	8,85	7,87	7,71	27,4	24,1	23,7

Note: B_1 are exact values; B_+ are values from the $j \approx j_+$ approximation.

is the integral operator of the albedo, whose kernel is the differential current albedo $a(\omega, E|\omega', E')$, where

$$a(\omega, E|\omega', E')=0, \quad \cos\theta'\cos\theta>0. \tag{1}$$

As a result of the reflection of the particle flux j_2 from the left half-space, a flux

$$j_3(z, \omega, E)=\hat{A}j_2(z, \omega, E)$$

is generated, etc. For the j_n-th flux, we have the recurrence relation

$$j_{n+1}(z, \omega, E)=\hat{A}j_n(z, \omega, E), \tag{2}$$

and the sum of all these fluxes is equal to the particle flux in the infinite medium:

$$j(z, \omega, E)=\sum_{n=1}^{\infty} j_n(z, \omega, E), \tag{3}$$

which we assume to be known. Note that

$$\left.\begin{aligned} j_{2n}(z, \omega, E)&=0, \quad \text{for} \quad \cos\theta>0;\\ j_{2n+1}(z, \omega, E)&=0, \quad \text{for} \quad \cos\theta<0. \end{aligned}\right\} \tag{4}$$

Substituting Eq. (2) into (3) and summing the operator series, we obtain the relation

$$j_1(z, \omega, E)=j(z, \omega, E)-\hat{A}j(z, \omega, E), \tag{5}$$

which relates the radiation field at the boundary and the field in the infinite medium. This equation is valid for any source with plane symmetry.

We introduce the notation

$$\begin{aligned} j_+(z, \omega, E)&=\begin{cases} j(z, \omega, E), & \cos\theta>0;\\ 0, & \cos\theta<0; \end{cases}\\ j_-(z, \omega, E)&=\begin{cases} 0, & \cos\theta>0;\\ j(z, \omega, E), & \cos\theta<0. \end{cases} \end{aligned} \tag{6}$$

Assuming in Eq. (5) first $\cos\theta > 0$, and then $\cos\theta < 0$, and taking account of (1), (4), and (6), we obtain

$$\left.\begin{aligned} j_1(z, \omega, E)&=j_+(z, \omega, E)-\hat{A}j_-(z, \omega, E);\\ j_-(z, \omega, E)&=\hat{A}j_+(z, \omega, E), \end{aligned}\right\} \tag{7}$$

whence

$$j_1(z, \omega, E)=[1-\hat{A}^2]j_+(z, \omega, E). \tag{8}$$

For $\|\hat{A}^2\| \ll 1$, the second term in Eq. (8) can be neglected, and we can assume

$$j_1(z, \omega, E)\approx j_+(z, \omega, E).$$

This approximation was used by Fano et al. [1] to estimate the boundary effect in the theory of γ-radiation transport.

A numerical example illustrating Eqs. (7) is given in Fig. 1 for a γ-quanta flux in a plane-perpendicular source with $E_0 = 1$ MeV in aluminum. From Fig. 1 we can see that the boundary effect is most important in the low-energy part of the spectrum, where the correction due to the second term in (7) can be considerable.

Figure 2 shows the angular distribution of the photon flux obtained from (7). The figure shows that the difference between the fluxes in the infinite medium and at the boundary depends weakly on θ for $\theta = \pi/2$. This result is related to the fact that the boundary affects primarily the low-energy part of the spectrum, which has an angular distribution that is nearly isotropic.

If the detector recording the radiation flux has a sensitivity function $p(\omega, E)$, then for the functional

$$J(z)=\int d\omega \int dE\, p(\omega, E)\sec\theta\, j(z, \omega, E)$$

Declassified and Approved For Release 2013/03/01 : CIA-RDP10-02196R000300100005-6

Declassified and Approved For Release 2013/03/01 : CIA-RDP10-02196R000300100005-6

from Eqs. (7) we obtain

$$J_1(z) = J_+(z) - \int d\omega' \int dE' j_-(z, \omega', E') \sec\theta' \, p(\omega', E') \, A(\omega', E'), \tag{9}$$

where

$$A(\omega', E') = \int d\omega \int dE \, a(\omega, E \mid \omega', E') \left| \frac{\cos\theta'}{\cos\theta} \right| \frac{p(\omega, E)}{p(\omega', E')}$$

is the integrated albedo [2].

Table 1 shows the results of a calculation based on Eq. (9) for the dose buildup factor for concrete layers for various incident angles of primary γ-quanta with $E_0 = 1$ MeV. In the present study the differential particle flux in the infinite medium was calculated by the Monte-Carlo method, and the data on the albedo was taken from [3]. The calculated values of the buildup factors are in good agreement with the results from a direct calculation by the Monte-Carlo method [3].

Equations (7) and (9) can be used in problems with neutrons, γ-quanta, electrons, and other particles, if their differential fluxes in an infinite medium and integrated albedo are known.

LITERATURE CITED

1. U. Fano, L. Spencer, and M. Berger, γ-Radiation Transport [Russian translation], Atomizdat, Moscow (1963).
2. B. P. Bulatov et al., γ-Radiation Albedo [in Russian], Atomizdat, Moscow (1968).
3. D. J. Raso, Nucl. Sci. and Engng., 17, 411 (1963).

Declassified and Approved For Release 2013/03/01 : CIA-RDP10-02196R000300100005-6

Declassified and Approved For Release 2013/03/01 : CIA-RDP10-02196R000300100005-6

METHODS FOR CALCULATING NONSTATIONARY PROCESSES INVOLVING SEPARATION OF MULTICOMPONENT ISOTOPIC MIXTURES IN PACKED COLUMNS

I. A. Vereninov and Yu. V. Rakitskii

UDC 621.039.31

The use of a digital computer for investigating separation processes requires the development of a mathematical model whose form is capable of being realized in the computer.

Consider a rectangular-multistage system used in two-phase separation of an m-component mixture without isotope exchange. A mathematical model which has been discussed previously [1, 2] may be described by a set of partial differential equations in the joint domain satisfying the following conditions at the section boundaries:

$$\left.\begin{aligned}
&\frac{\partial x_i^s}{\partial \zeta^s}+\frac{\Omega^s H^s}{L^s}\cdot\frac{\partial x_i^s}{\partial t}=\frac{N^s G^s}{L^s}(y_i^s-W_i^s)=\frac{G^s}{L^s}\cdot\frac{\partial y_i^s}{\partial \zeta^s};\\
&W_i^s=x_i^s(1-\varepsilon_{iq})-V_i^s;\ V_i^s=x_i^s\sum_{r=1}^{m}\varepsilon_{qr}x_r^s;\\
&G^2y_i^2(0,\ t)+Fy_{iF}=G^1y_i^1(1,\ t);\\
&E_K^s\frac{dx_i^s(1,\ t)}{dt}=(L^s-L^{s+1})[x_i^s(1,\ t)-y_{ik}^s(t)];\\
&G^sy_i^s(1,\ t)=G^{s+1}y_i^{s+1}(0,\ t)+(L^s-L^{s+1})\,y_{ik}^s(t);\\
&E_K^0\frac{dx_i^1(0,\ t)}{dt}=G^1[y_i^1(0,\ t)-x_i^1(0,\ t)].
\end{aligned}\right\}\qquad(1)$$

Here the superscript s denotes the section number (s = 1, 2, 3, . . . , b); the subscript i denotes the component number; ζ is a dimensionless coordinate which varies from 0 to 1 along the direction of motion of the fluid; x_i and y_i are the concentrations of the i-th component in the liquid and gas currents; L, G, and F are the liquid, gas, and supply currents; Ω is the liquid holdup; H is the height of a section; N is the number of stages; E_K is the quantity of liquid in the phase return systems; and ε_{iq} is the enrichment factor for the i–q isotope pair.

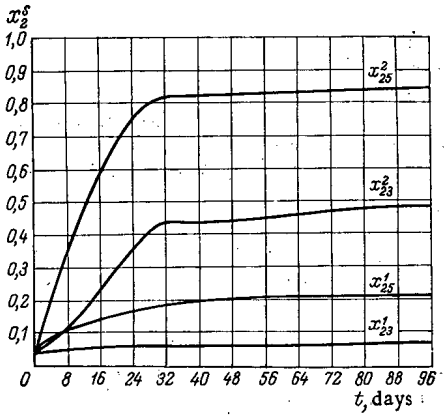

Fig. 1. Curves for attainment of the steady state by a two-section stage for an average component x_2^S (set p_1, is used for t = 0 and set p_2 is used for t = 30 days, where $M^1 = M^2 = 5$).

In order to solve (1) it is necessary to convert it to a set of difference equations, but in this case we do not get satisfactory speed and accuracy of solution by straightforward mesh and collocation methods on account of the details of the processes considered, which are reflected in (1) and represent a two-dimensional boundary layer with the parameters N, Ω, E_K, G, and L. To construct the physical and mathematical basis of a different model, the following are therefore necessary:

to use an integral form for (1);

to carry out asymptotic transformations with respect to t and the functions $y_i^S(\zeta^S, t)$ of the variable ζ^S for the boundary conditions in the phase transformation systems [3];

to make the most accurate approximation the asymptotic form for $y_i^S(\zeta^S, t)$.

Translated from Atomnaya Énergiya, Vol. 32, No. 6, pp. 499-501, June, 1972. Original article submitted October 7, 1971.

© 1972 Consultants Bureau, a division of Plenum Publishing Corporation, 227 West 17th Street, New York, N. Y. 10011. All rights reserved. This article cannot be reproduced for any purpose whatsoever without permission of the publisher. A copy of this article is available from the publisher for $15.00.

Declassified and Approved For Release 2013/03/01 : CIA-RDP10-02196R000300100005-6

Declassified and Approved For Release 2013/03/01 : CIA-RDP10-02196R000300100005-6

We can use the values and derivatives of the variables at the approximation points, so it is best to use Hermite polynomials for the $x_i^S(\zeta^S, t)$ [4].

The differential-difference model was constructed by taking for each section M^S points with steps of $h^S = \zeta_{n+1}^S - \zeta_n^S$, where n is the number of the point.

We get from asymptotic transformation at selected points the following forms for (1), the integral forms of these and the functions $y_i^S(\zeta^S, t)$

$$\left.\begin{aligned}
&\frac{\partial x_i^s}{\partial \zeta^s}\Big|_{\zeta^s=\zeta_n^s}+\frac{\Omega^s H^s}{L^s}\frac{\partial\ {}^s_i}{\partial t}\Big|_{\zeta^s=\zeta_n^s}=\frac{N^s G^s}{L^s}(y_i^s-W_i^s)\Big|_{\zeta^s=\zeta_n^s}=\frac{G^s}{L^s}\frac{\partial y_i^s}{\partial \zeta^s}\Big|_{\zeta^s=\zeta_n^s};\\
&y_i^s(\zeta_n^s+h^s,\ t)-y_i^s(\zeta_n^s,\ t)-\frac{\Omega^s H^s}{G^s}\int_{\zeta_n^s}^{\zeta_n^s+h^s}\frac{\partial x_i^s}{\partial t}\,d\zeta^s+\frac{L^s}{G^s}[x_i^s(\zeta_n^s,\ t)-x_i^s(\zeta_n^s+h^s,\ t)]=0;\\
&y_i^s(\zeta_n^s,\ t)=\sum_{j=0}^{R}\left(\frac{1}{N^s}\right)^j\frac{\partial^j W_i^s}{\partial(\zeta^s)^j}\Big|_{\zeta^s=\zeta_n^s}+0\left[\left(\frac{1}{N^s}\right)^{R+1}\right]\\
&\qquad(\text{where } n=1,\ 2,\ \ldots,\ M^s-1);\\
&y_i^1(0,\ t)=\frac{E_K^0}{G^1}\cdot\frac{dx_i^1(0,\ t)}{dt}+x_i^1(0,\ t);\\
&y_i^b(1,\ t)=-\frac{E_K^b}{L^b}\cdot\frac{dx_i^b(1,\ t)}{dt}+x_i^b(1,\ t);\\
&y_i^1(1,\ t)=\frac{G^2}{G^1}y_i^2(0,\ t)+\frac{F}{G^1}y_{iF};\\
&y_i^s(1,\ t)=\frac{G^{s+1}}{G^s}\sum_{j=0}^{R}\left(\frac{1}{N^{s+1}}\right)^j\frac{\partial^j W_i^{s+1}}{\partial(\zeta^{s+1})^j}\Big|_{\zeta^{s+1}=0}+\frac{1}{G^s}\left[(L^s-|L^{s+1})x_i^s(1,\ t)\right.\\
&\qquad\left.-E_K^s\frac{dx_i^s(1,\ t)}{dt}\right]+0\left[\left(\frac{1}{N^{s+1}}\right)^{R+1}\right]\\
&\qquad(\text{for } s=2,\ 3,\ \ldots,\ b-1).
\end{aligned}\right\}\qquad(2)$$

The integrals are approximated by quadrature formulas to obtain the final system of ordinary differential equations for the approximate values of the concentrations $x_{in}^S(t)$ in (2), while the multiplicative forms V_i^S are approximated by Lagrange interpolation formulas, and the functions $x_i^S(\zeta^S, t)$ are approximated by Hermite formulas with two repeated points [4], followed by solution for the time derivatives.

The final form for the system of ordinary differential equations is

$$\left.\begin{aligned}
&\frac{dx_{in}^s(t)}{dt}=\sum_{s=1}^{b}\sum_{n=1}^{M^s-1}[A_{in}^s x_{in}^s(t)+B_{in}^s V_{in}^s(t)],\\
&\text{where } i=1,\ 2,\ \ldots,\ m;\ x_{in}^s(0)=x_{in}^{s0}.
\end{aligned}\right\}\qquad(3)$$

The constants A_{in}^S and B_{in}^S in (3) depend on the step length, the type of quadrature and interpolation formulas, and all of the stage parameters.

The above method gives well-defined matrices for the coefficients A_{in}^S and B_{in}^S, and so it is permissible to use the simplest methods of numerical integration in solving (3). It has been found that production of solutions correct to two significant figures requires the points to be taken on the average at intervals of 100 separation stages, with never less than three approximation points per section. The length of the time integration step is about 0.1 day for Euler piecewise methods. The Adams and Runge–Kutta methods are not appropriate in this case.

As an example of this method, Fig. 1 shows the results obtained for the separation of a four-component mixture of sulfur isotopes in a two-section stage with the two sets p_1 and p_2 with an infinite pool at the intake; the following parameters were used:

$$x_{1F}=0.0076;\ x_{2F}=0.0422;\ x_{3F}=0.00014;$$
$$N^1=N^2=400;\ \Omega^1=0.0027\ \text{mole}\cdot\text{cm}^{-1};$$
$$\Omega^2=0.0004\ \text{mole}\cdot\text{cm}^{-1};$$
$$H^1=20\ \text{m};\ H^2=12\ \text{m};\ p_1=0.028\ \text{mole/day};$$
$$p_2=0.01335\ \text{mole/day};\ E_k^1=E_k^2=0.01\ \text{mole};$$
$$L^1=38.88\ \text{mole/day};\quad L^2=7.776\ \text{mole/day};\quad \varepsilon_{14}=0.006;\ \varepsilon_{24}=0.011;\ \varepsilon_{34}=0.022.$$

Declassified and Approved For Release 2013/03/01 : CIA-RDP10-02196R000300100005-6

Declassified and Approved For Release 2013/03/01 : CIA-RDP10-02196R000300100005-6

The order of (3) is in this case 24; for a process lasting 100 days, the solution requires 3 min on an M-220 computer, with a maximum error of 0.2%.

LITERATURE CITED

1. A.M.Rozen, Theory of Isotope Separation in Columns [in Russian], Atomizdat, Moscow (1960).
2. R.Ya.Kucherov and V.P.Minenko, At. Énerg., 19, 360 (1965).
3. I.A.Vereninov et al., Kernenergie, 14, 190 (1971).
4. I.S.Berezin and N.P.Zhidkov, Computational Methods [in Russian], Vol.1, Fizmatgiz, Moscow (1959).

Declassified and Approved For Release 2013/03/01 : CIA-RDP10-02196R000300100005-6

Declassified and Approved For Release 2013/03/01 : CIA-RDP10-02196R000300100005-6

ASYMPTOTIC STABILITY OF A REACTOR WITH THERMIONIC CONVERTER

V. P. Gorbunov, N. V. Isaev,
O. V. Komarov, A. V. Kryanev,
N. N. Petrov, A. F. Piskunkov,
and S. B. Shikhov

UDC 621.039.514

The problems of dynamics and stability of a reactor, in whose active zone thermionic converters connected with the fuel elements are placed, still remain open in the general nonlinear form, although articles have appeared which consider either the linearized model [1] or a model taking account of the effect of delayed neutrons and the construction of the converter in a simplified way, where it is possible to use Belton criterion for such simplified cases [2].

We consider a reactor in which the active zone consists of electrogenerating elements described in [3]. Keeping in mind the results of investigations discussed in [4], a reactor with thermionic converter can be regarded as an object with lumped parameters:

$$\frac{dW(t)}{dt}=\frac{\delta k-\beta}{l}W(t)+\sum_{i=1}^{\sigma}\frac{1}{\tau_i}R_i(t); \tag{1}$$

$$\frac{dR(t)}{dt}=\frac{\beta_i}{l}W(t)-\frac{1}{\tau_i}R_i(t),\quad i=1,\ \ldots,\ 6. \tag{2}$$

The reactivity δk is a function of the temperatures of the separate parts of the active zone:

$$\delta k=\sum_{j=1}^{4}-\alpha_j[T_j(t)-T_j(0)], \tag{3}$$

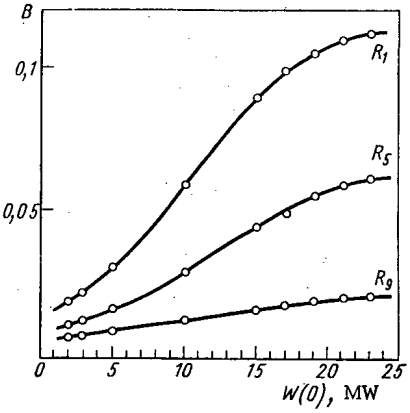

Fig. 1. Variation of the coefficient B as a function of the reactor power W in idling regime for different load resistances ($R_1 = 6.72 \cdot 10^{-3}$ Ω; $R_5 = 1.34 \cdot 10^{-3}$ Ω; $R_9 = 0.11 \cdot 10^{-3}$ Ω).

where α_j is the reactivity coefficient for temperature T_j. The heat balance equations for the fuel, the cathode, the anode stack, and the heat-transfer agent can be written in the form:

$$M_f C_f \frac{dT_f}{dt}=-a_1(T_f-T_c)+bW; \tag{4}$$

$$M_c C_c \frac{dT_c}{dt}=a_1(T_f-T_c)-a_2(T_c-T_a)-\sigma\varepsilon F_c(T_c^4-T_a^4)$$
$$+j^2(T_c,\ T_a)F_c^2R_{el}-j(T_c,\ T_a)F_c\left(X_a+\frac{2kT_a^e}{e}+V_1\right); \tag{5}$$

$$M_a C_a \frac{dT_a}{dt}=a_2(T_c-T_a)-a_3(T_a-T_h)$$
$$+\sigma\varepsilon F_c(T_c^4-T_a^4)+j^2(T_c,\ T_a)F_c^2R_{el}$$
$$+j(T_c\ \ T_a)\left(X_a+\frac{2kT_a^e}{e}\right)F_c; \tag{6}$$

$$M_h C_h \frac{dT_T}{dt}=a_3(T_a-T_h)-a_4(T_h-T_{h.u}), \tag{7}$$

where W(t) is the power of the reactor; T_j is the mean temperature; M_j, C_j are respectively the mass and the specific heat of the j-th

Translated from Atomnaya Énergiya, Vol. 32, No. 6, pp. 501-503, June, 1972. Original article submitted October 7, 1971; revision submitted January 10, 1972.

© 1972 Consultants Bureau, a division of Plenum Publishing Corporation, 227 West 17th Street, New York, N. Y. 10011. All rights reserved. This article cannot be reproduced for any purpose whatsoever without permission of the publisher. A copy of this article is available from the publisher for $15.00.

Declassified and Approved For Release 2013/03/01 : CIA-RDP10-02196R000300100005-6

Declassified and Approved For Release 2013/03/01 : CIA-RDP10-02196R000300100005-6

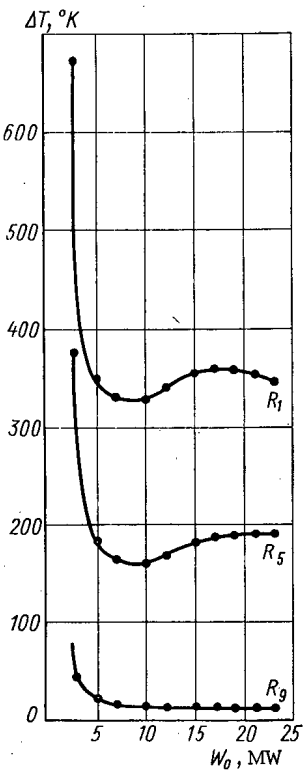

Fig. 2. Admissible deviations of cathode and anode temperatures from their stationary values for different load resistances ($R_1 = 6.72 \cdot 10^{-3}$ Ω; $R_5 = 1.34 \cdot 10^{-3}$ Ω; $R_9 = 0.11 \cdot 10^{-3}$ Ω).

layer, X_a is the work function of the anode surface; T_a^e is the temperature of the electrons at the anode; k is Boltzman constant; e is electron charge; b is the fraction of energy-release in the fuel; j is the density of current from the surface of the cathode; R_{el} is the effective resistance of the electrode; V_l is the voltage drop in the load; a_j are positive constants proportional to heat-transfer coefficients or to thermal resistance of the layer; σ is Stephen–Boltzmann constant; ε is the effective degree of blackness; and F_c is the emitting surface of the cathode.

Experimental volt–ampere characteristics of the thermionic converters, obtained in isothermal regime [5], were used in the solution of the above equations of dynamics. The temperature dependence of the current density was described by an empirically chosen law:

$$j(T_c, T_a) = j_0(T_a T_c - \xi T_a^2), \tag{8}$$

where ξ is a positive nondimensional quantity which can be assumed constant for a certain neighborhood near the stationary value of the anode temperature; j_0 is a constant characterizing the slope of the experimental curves. It is convenient to use the dependence (8) in the analysis of the stability of the stationary regime:

$$W = W(0); \quad R_i = R_i(0); \quad T_j = T_j(0) \geqslant T_u. \tag{9}$$

In Eqs. (1)–(7) we make a change of variables:

$$w(t) = \frac{W(t) - W(0)}{W(0)}, \quad w(t) > -1; \tag{10}$$

$$r_i(t) = \frac{R_i(t) - R_i(0)}{R_i(0)}, \quad r_i(t) > -1; \tag{11}$$

$$x_i(t) = T_j(t) - T_j(0), \quad x_j(t) > -T_j(0), \tag{12}$$

after which they become

$$l\dot{w} = (w+1)\Big(-\sum_{j=1}^{4}\alpha_j x_j - \sum_{i=1}^{6}\beta_i\Big) + \sum_{i=1}^{6}\beta_i (r_i + 1); \tag{13}$$

$$\tau_i \dot{r}_i = (w+1) - (r_i + 1); \quad i = 1, \ldots, 6. \tag{14}$$

$$\dot{x}_f = -\frac{a_1}{M_f C_f}(x_f - x_c) + \frac{bW(0)}{M_f C_f} w; \tag{15}$$

$$\dot{x}_c = \frac{a_1}{M_c C_c}(x_f - x_c) - \frac{a_2}{M_c C_c}(x_c - x_a) - \frac{h}{M_c C_c}\{j[T_c(0) + x_c, T_a(0) + x_a] - j[T_c(0), T_a(0)]\}$$
$$- \frac{c}{M_c C_c}\{[T_c(0) + x_c]^4 - [T_a(0) + x_a]^4 - T_c^4(0) + T_a^4(0)\} + \frac{d_2}{M_a C_a}\{j^2[T_c(0) + x_c, T_a(0) + x_a] - j^2[T_c(0), T_a(0)]\}; \tag{16}$$

$$\dot{x}_a = \frac{a_2}{M_a C_a}(x_c - x_a) - \frac{a_3}{M_a C_a}(x_a - x_h) + \frac{h}{M_a C_a}\{j[T_c(0) + x_c, T_a(0) + x_a] - j[T_c(0), T_a(0)]\}$$
$$+ \frac{c}{M_a C_a}\{[T_c(0) + x_c]^4 - [T_a(0) + x_a]^4 - T_c^4(0) + T_a^4(0)\} + \frac{d_3}{M_a C_a}\{j^2[T_c(0) + x_c, T_a(0) + x_a] - j^2[T_c(0), T_a(0)]\}; \tag{17}$$

$$\dot{x}_h = \frac{a_3}{M_h C_h}(x_a - x_h) - \frac{a_4}{M_l C_l} x_h, \tag{18}$$

where $c = \varepsilon\sigma F_c$, $h = F_c(X_a + 2kT_e^a)$, $d_2 = F_c^2(R_{el} + R_l)$, $d_3 = F_c^2 R_{el}$, $T_u = \text{const}$.

The nonlinearities in Eqs. (16) and (17) are such that it is possible to separate out the nonlinear parts in them. We write Eqs. (15)–(18) in vector form

$$\dot{\mathbf{X}} = \hat{C}\mathbf{X} + \mathbf{b}W(0)\, w + \mathbf{Z}(x_c, x_a), \tag{19}$$

where $\hat{C}$ is a nonsingular matrix composed of the constants of the linear part of Eqs. (15)–(18); the vector $\vec{Z}$ is composed of the nonlinear terms of these equations, while the vector $\vec{b}$ has the form

$$\mathbf{b} = \begin{pmatrix} b/M_f C_f \\ 0 \\ \vdots \\ 0 \end{pmatrix}.$$

Declassified and Approved For Release 2013/03/01 : CIA-RDP10-02196R000300100005-6

Declassified and Approved For Release 2013/03/01 : CIA-RDP10-02196R000300100005-6

Let us assume that W(0), the steady-state power, belongs to a range of powers, where the matrix $\hat{C}$ has different negative eigenvalues. We shall reduce matrix $\hat{C}$ to the diagonal form by the substitution $\vec{X} = \hat{P}\vec{Y}$:

$$\dot{Y}_j = -\lambda_j Y_j + \frac{bW(0)(\hat{P}^{-1})_{j1}}{M_f C_f} w + (\hat{P}^{-1})_{j2} Z_2 + (\hat{P}^{-1})_{j3} Z_3, \tag{20}$$

where λ_j are the eigenvalues of matrix $\hat{C}$.

We write Lyapunov function of such a system of equations in the form

$$L = l[w - \ln(w+1)] + \sum_{i=1}^{6} \beta_i \tau_i [r_i - \ln(r_i+1)] + \frac{1}{2} \sum_{j=1}^{4} A_j Y_j^2. \tag{21}$$

It is obvious that the function L is positive definite in the variables Y_j, r_i, w, if all $A_j > 0$. The total time derivative of L, computed in accordance with Eqs. (13), (14), (20) has the form

$$\frac{dL}{dt} = -\sum_{i=1}^{6} \frac{\beta_i (w - r_i)^2}{(w+1)(r_i+1)} - \sum^{4} A_j \lambda_j Y_j^2 + Z_2 \sum_{j=1}^{4} A_j (\hat{P}^{-1})_{j2} Y_j + Z_3 \sum_{j=1}^{4} A_j (\hat{P}^{-1})_{j3} Y_j. \tag{22}$$

The quantity A_j is chosen in such a way that the condition

$$A_j = \frac{M_f C_f \sum_{l=1}^{4} \alpha_l (\hat{P})_{lj}}{b W(0) (\hat{P}^{-1})_{j1}} > 0 \tag{23}$$

is satisfied.

The condition for asymptotic stability is the requirement that the derivative dL/dt be negative definite. The first term in (22) is negative in view of the nonnegative nature of the variables $w + 1$, $r_i + 1$; therefore in the case of asymptotic stability the following inequality must be satisfied:

$$Z_2 \sum_{j=1}^{4} A_j (\hat{P}^{-1})_{j2} Y_j + Z_3 \sum_{j=1}^{4} A_j (\hat{P}^{-1})_{j3} Y_j - \sum_{j=1}^{4} A_j \lambda_j Y_j^2 < 0. \tag{24}$$

In the case of a linear feedback (Z = 0) Eqs. (21) and (22) coincide with the corresponding equations of [6].

Thus it is possible to formulate a criterion for the sufficient conditions of the stability of the point model of the reactor with thermionic converter. In order to ensure the asymptotic stability of the reactor it is sufficient that all the eigenvalues of matrix $\hat{C}$ be negative, all the temperature coefficients of reactivity satisfy the inequalities $(1/(\hat{P}^{-1})_{j1}) \sum_{l=1}^{4} \alpha_l (\hat{P})_{lj} > 0$, while all the variables occurring in the nonlinear terms of the feedback equations satisfy inequalities (24). Since the second method of Lyapunov gives only the sufficient conditions of asymptotic stability, the actual region of stability may be much larger than that determined by the method indicated above. The dimensions of the region of stability are determined by the operating regime of the reactor. In the idling regime the current flowing through is equal to zero and the heat transfer from the cathode to the anode is accomplished only by radiation.

The range of stability is defined by the inequalities

$$\left.\begin{aligned} |c[x_c^4 + f(x_c)]| &\leqslant B|x_c|; \\ |c[x_a^4 + f(x_a)]| &\leqslant B|x_a|. \end{aligned}\right\} \tag{25}$$

Figure 1 shows how the coefficient B changes depending on the steady-state level of the power of the reactor whose stability is being investigated. In the operating regime the limits, in which inequalities (24) are fulfilled, change depending on the load resistance R. The slope of the curves of the volt–ampere characteristic determine the value of the constants in inequalities (24). Computations show that there is a limiting value of the steady-state power depending on the load resistance of the external circuit; on reaching this value the conditions of asymptotic stability are not fulfilled or the admissible deviations of the temperatures from the stationary value are very small (10-30°K). The admissible deviations of the temperatures of the cathode and the anode from their stationary values are shown in Fig. 2 as functions of the reactor power for different

Declassified and Approved For Release 2013/03/01 : CIA-RDP10-02196R000300100005-6

Declassified and Approved For Release 2013/03/01 : CIA-RDP10-02196R000300100005-6

load resistances. The results obtained here can be used advantageously in the development of power installations of a given class; in each specific case it is necessary to carry out special investigations to determine the safest regimes of operation of the reactor.

LITERATURE CITED

1. Von E. Wolf and V. Speidel, Atomkernenergie (ATKE), Bd16 (4), 19 (1970).
2. R. Brehm, D. Hetrick, and F. Schmidt, Direct Conversion of Thermal Energy into Electrical Energy and Fuel Elements, No. 1 (102), 129 (1971).
3. Yu. A. Broval'skii et al., in: Thermionic Conversion of Energy [in Russian], VNIIT, Moscow (1969), p. 281.
4. G. A. Baryshinkov et al., ibid, p. 391.
5. V. Wilson and J. Lawrence, Advanced Energy Conversion, 4, 195 (1964).
6. V. D. Goryachenko and Yu. F. Trugin, Atomnaya Énergiya, 23, 499 (1967).

Declassified and Approved For Release 2013/03/01 : CIA-RDP10-02196R000300100005-6

Declassified and Approved For Release 2013/03/01 : CIA-RDP10-02196R000300100005-6

CALCULATION OF BUILDUP FACTORS AT DEEP PENETRATIONS

Sh. S. Nikolaishvili, A. I. Gabrashvili,
N. N. Dzhgarkava, and É. A. Iordanishvili

UDC 539.12.122:539.12.172

We discuss the generalization of the moments method as applied to the calculation of γ-ray and neutron distributions at arbitrarily large distances from sources. The generalization is concerned with that part of the method which reconstructs the required solution from a finite number of its moments. Since many papers have been published on the moments method and its applications [1-3] we confine our discussion to the problem of reconstructing a function from its moments.

Let $\psi(t)$ be a continuous function at t defined on the interval $(0, \infty)$ and proportional to $t^s e^{-t}$ as $t \to \infty$, where s is a real number greater than -1. We assume that the first $3m + 1$ even moments of $\psi(t)$ are known:

$$\mu_n = \frac{1}{(2n)!} \int_0^\infty \psi(t)\, t^{2n}\, dt, \quad n = 0, 1, \ldots, 3m. \tag{1}$$

It is required to construct an approximate representation of $\psi(t)$ which can be used to compute its value at arbitrarily large t.

Following Spencer and Fano [4] we introduce two sets of polynomials forming together a biorthogonal system on the interval $(0, \infty)$ with a weight function $t^s e^{-t}$. Let $U_k(t)$ be a polynomial of degree k, and $V_l(t)$ an even polynomial of degree $2l$ in t. We require

$$\int_0^\infty t^s e^{-t} U_k(t)\, V_l(t)\, dt = \begin{cases} 1, & k = l, \\ 0, & k \neq l. \end{cases} \tag{2}$$

Polynomials $V_k(t)$ satisfying this condition have the form

$$V_k(t) = \sum_{p=0}^{k} \frac{(-1)^p}{\Gamma(2p+s+1)} \binom{k}{p} t^{2p}, \tag{3}$$

where $\Gamma(x) = \int_0^\infty e^{-t} t^{x-1} dt$ is the γ-function, and the polynomials $U_k(t)$ satisfy the recurrence relations

$$U_k(t) = \frac{1}{2k}\left[(2k+s-1-t)\, U_{k-1}(t) + t\frac{dU_{k-1}(t)}{dt}\right], \quad k \geqslant 1. \tag{4}$$

If the supplementary condition $U_0(t) = 1$ is added, Eqs. (3) and (4) uniquely determine the polynomials $U_k(t)$ and $V_k(t)$. Thus we have constructed the biorthogonal system of interest to us.

We now return to the problem posed and assume

$$\psi(t) \approx \frac{t^s e^{-t}}{1 + t^{2m}} \sum_{k=0}^{2m} b_k U_k(t), \tag{5}$$

where the b_k are constants to be determined. To find them we multiply both sides of (5) by $(1 + t^{2m})V_k(t)$ and integrate with respect to t from 0 to ∞. By using the orthogonality relations (2) we obtain

$$b_k = \int_0^\infty (1 + t^{2m})\, V_k(t)\, \psi(t)\, dt, \quad k = 0, 1, \ldots, 2m. \tag{6}$$

Translated from Atomnaya Énergiya, Vol. 32, No. 6, pp. 504-505, June, 1972. Original article submitted November 22, 1971.

© 1972 Consultants Bureau, a division of Plenum Publishing Corporation, 227 West 17th Street, New York, N. Y. 10011. All rights reserved. This article cannot be reproduced for any purpose whatsoever without permission of the publisher. A copy of this article is available from the publisher for $15.00.

Declassified and Approved For Release 2013/03/01 : CIA-RDP10-02196R000300100005-6

Declassified and Approved For Release 2013/03/01 : CIA-RDP10-02196R000300100005-6

TABLE 1. Values of $B_E(t)$ in Iron at Various Distances from a 3 MeV Source

Value of t	Plane source	Point source	Value of t	Plane source	Point source
1	−4,283 (1,830)	0,120 (1,474)	40 60	39,65 66,58	38,44 65,20
2	2,307 (2,427)	1,476 (1,991)	80 100	96,89 130,0	95,39 128,4
4	3,694 (3,683)	3,160 (3,142)	200 250	327,7 442,3	236,0 440,7
7	5,768 (5,769)	5,117 (5,119)	300 350	565,5 696,3	563,9 694,8
10	8,079 (8,078)	7,344 (7,343)	400 450	833,9 977,9	832,6 976,8
20	17,10 17,09	16,15 (16,15)	500	1128	1127

TABLE 2. Values of $B_E(t)$ Calculated by Eq. (5) for Various Values of m

m	t = 1	2	4	10	20	40	100	500
1	1,924	2,479	3,644	8,185	17,96	42,75	142,5	1247
	1,473	2,015	3,141	7,357	16,41	39,42	132,2	1161
2	1,917	2,426	3,682	8,078	17,09	39,57	129,3	1119
	1,498	1,987	3,142	7,343	16,15	38,34	127,5	1113
3	−4,283	2,307	3,693	8,079	17,10	39,65	130,0	1128
	+0,119	1,476	3,160	7,344	16,15	38,44	128,4	1127
4	−2,354	6,206	3,711	8,079	17,09	39,71	131,3	1152
	−1,542	−31,43	3,419	7,345	16,15	38,48	129,7	1153

Substituting the value of $V_k(t)$ from (3) into (6) and using definition (1) we find

$$b_k = \sum_{p=0}^{k} (-1)^p \frac{(2p)!}{\Gamma(2p+s+1)} \binom{k}{p} \left[\mu_p + \frac{(2m+2p)!}{(2p)!}\mu_{p+m}\right]. \qquad (7)$$

The formula obtained shows that the evaluation of all the coefficients b_k on the right hand side of Eq. (5) requires the first 3m + 1 even moments of $\psi(t)$, which is just the number we assumed known.

The main feature of (5) is the fact that as $t \to \infty$ for any value of m its right hand side approaches $b_{2m}t^s e^{-t}/\Gamma$ (2m + s + 1), which for large t is proportional to the function $\psi(t)$ being approximated. For sufficiently large m Eq. (5) determines the asymptotic values of $\psi(t)$ to any given accuracy.

Thus the main idea of our approach to reconstructing a function from its moments is the fact that the representation sought is given in the form of a function with the required asymptotic behavior which we suppose is known beforehand to within a constant. It is obvious that the algorithm described can be generalized to problems in which the behavior of the solution at infinity is different from $t^s e^{-t}$. However, the method may turn out to be much more complicated numerically since the calculation of the coefficients of the polynomials of the biorthogonal system may not be so simple with another weight function.

As an illustration of the method we present the results of calculating the energy buildup factor $B_E(t)$ in iron for 3 MeV γ-rays from plane isotropic and point isotropic sources. Table 1 lists the values of $B_E(t)$ calculated by using Eq. (5) with m = 3 and s = 1.36 for a point source, and s = 0.36 for a plane source. For distances t up to 30 mfp at the source energy the values of $B_E(t)$ were calculated by the method of polynomial expansions also. The results of these calculations are given in parentheses under the corresponding values of $B_E(t)$ found by Eq. (5).

In order to judge the convergence of the algorithm presented Table 2 lists the values of $B_E(t)$ found for m = 1, 2, 3, and 4. For each m the upper row of numbers corresponds to a plane isotropic source and the lower to a point isotropic source. As one should expect Eq. (5) shows a divergence for small values of t. Table 2 confirms the asymptotic convergence of Eq. (5). It is clear from the table that as t increases the ratio of $B_E(t)$ for plane isotropic and point isotropic sources approaches unity in accord with the familiar fact that $B_E(t)$ is independent of the source geometry.

The calculations were made on the M-220M and the BÉSM-6 computers of the Institute of Applied Mathematics of Tbilisi State University with the cooperation and support of R. K. Peradze, K. H. Samsonie, and E. N. Kipianya to whom the authors are deeply grateful.

LITERATURE CITED

1. H. Goldstein, Fundamental Aspects of Reactor Shielding, Addison–Wesley, Reading (1959).
2. U. Fano, L. Spencer, and M. Berger, Transport of γ-Radiation [Russian translation], Gosatomizdat, Moscow (1963).
3. O. I. Leipunskii, B. V. Novozhilov, and V. N. Sakharov, The Propagation of γ-Rays in Matter [in Russian], Fizmatgiz, Moscow (1960).
4. L. V. Spencer and U. Fano, J. Res. Nat. Bur. Stds., 46, 446 (1951).

Declassified and Approved For Release 2013/03/01 : CIA-RDP10-02196R000300100005-6

Declassified and Approved For Release 2013/03/01 : CIA-RDP10-02196R000300100005-6

PRODUCTION AND ACCELERATION OF MULTIPLY-CHARGED PHOSPHORUS AND ZINC IONS

A. S. Pasyuk, Yu. P. Tret'yakov, and B. A. Zager

UDC 621.3.038.612:621.3.038.628

In order to carry out experiments on the synthesis of far transuranic elements, and also in order to solve other current physical problems, ion sources allowing the working substance to be used in the solid phase have been developed. In the Nuclear-Reactions Laboratory of the Joint Institute for Nuclear Research, several means of feeding solid working substances into plasma ion sources have been tried: the evaporation of the substance from a crucible with an external heater [1], cathodic sputtering [2], and the evaporation of the substance by an electron beam [3]. The largest currents of tenfold charged zinc and fivefold charged phosphorus ions, required for the synthesis of elements 107 and 125, were obtained from a source using a reflex arc discharge, the substance being fed in by evaporation from a crucible [1]. Several improvements have now been introduced into the construction and supply system of the source.

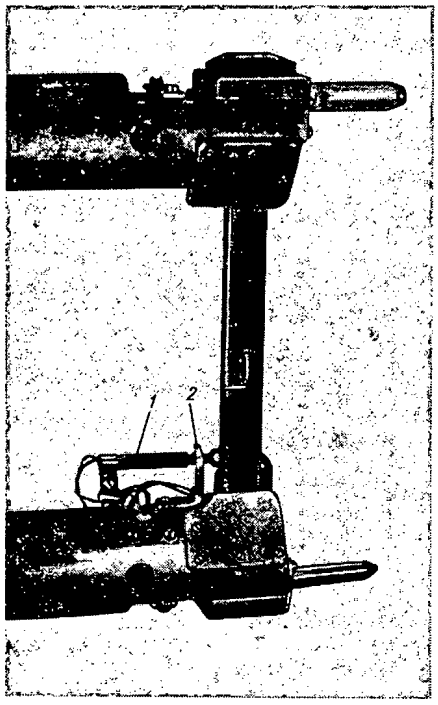

Fig. 1

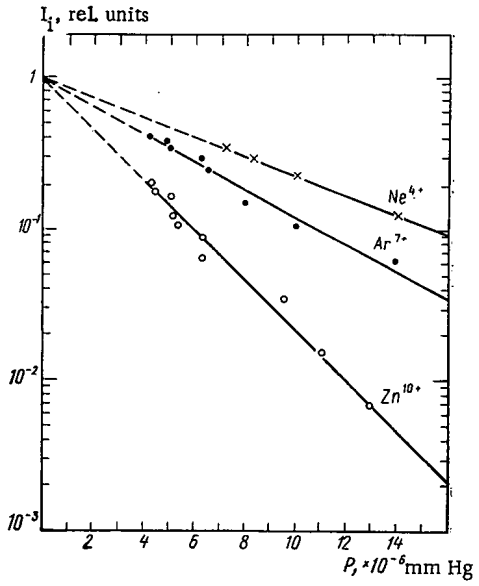

Fig. 2

Fig. 1. External view of the source: 1) crucible containing working substance; 2) thermal screen.

Fig. 2. Dependence of the ion currents extracted from the U-300 cyclotron on the vacuum in the accelerator chamber.

Translated from Atomnaya Énergiya, Vol. 32, No. 6, pp. 505-508, June, 1972. Original article submitted December 24, 1971.

© 1972 Consultants Bureau, a division of Plenum Publishing Corporation, 227 West 17th Street, New York, N. Y. 10011. All rights reserved. This article cannot be reproduced for any purpose whatsoever without permission of the publisher. A copy of this article is available from the publisher for $15.00.

Declassified and Approved For Release 2013/03/01 : CIA-RDP10-02196R000300100005-6

Declassified and Approved For Release 2013/03/01 : CIA-RDP10-02196R000300100005-6

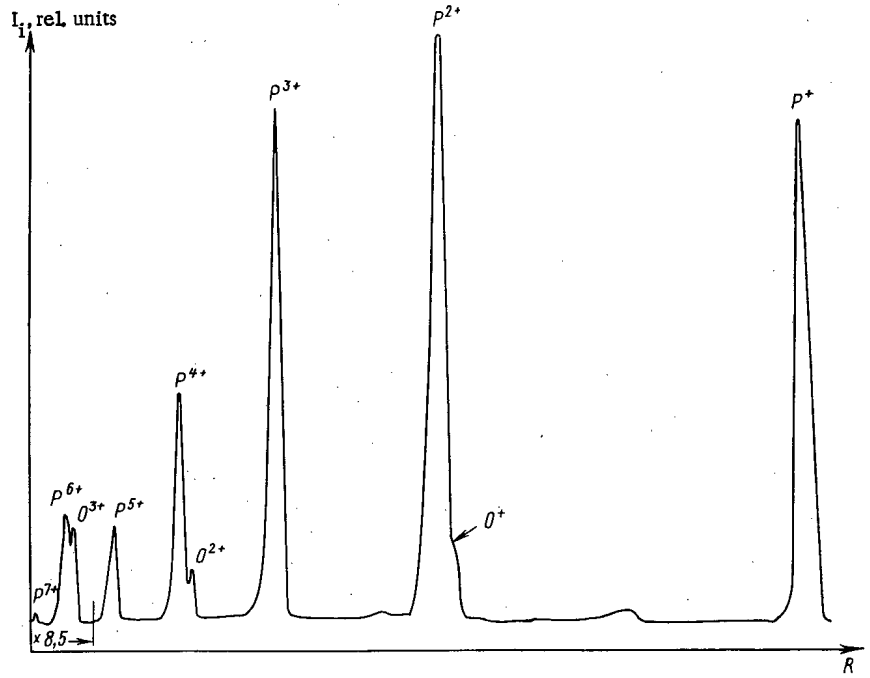

Fig. 3. Charge spectrum of phosphorus ions obtained in the test system [R – position of ion collector].

Analysis of the results of [4] shows that the intensity of the flows of various multiply-charged ions may be described as a function of the concentration of neutral particles in the discharge chamber n (under our own conditions n is proportional to the amount of gas passing into the discharge Q) by the expression

$$I = ae^{-bn},$$

where a and b are constants depending on the ionizing substances and the charge of the ion. The flow of vapor into the gas-discharge chamber Q is in turn proportional to the vapor pressure in the crucible p, which is related to the temperature T of the working substance by

$$\log p = A - \frac{B}{T},$$

where A and B are constants depending on the substance being evaporated. We see that the dependence of the yield of multiply-charged ions on the crucible temperature is very strong. This leads to two requirements: a) stabilization of the crucible-heating current; b) a low thermal inertia of the crucible.

The construction of the source is shown in Fig. 1. The main constructional difference from the source described in [1] lies in the unit for feeding the working substance. Instead of an external coaxial furnace we use direct heating of the crucible by a current passing directly through its walls. Between the crucible and the gas-discharge chamber is a Duralumin screen polished to specular luster. In this type of heating, the thermal time constant of the system for feeding the vapor of the working substance is more than an order of magnitude lower than in the previous construction.

The crucible is supplied from a variable stabilized rectifier. The stabilization coefficient (not less than 0.2%) was chosen on the basis of the relationship between the vapor tension of zinc and temperature [5] and also that between the crucible temperature and the heating current, which we measured experimentally.

The use of a crucible with direct heating and current stabilization greatly improved the quality of the feed regulation of the working substance; together with other improvements this increased the current of accelerated ions. The supply of a small quantity of argon (~0.1 cm^3/min) to the cathode region helped stabilize the operation of the source.

Acceleration of Zinc. In this case the working substance fed into the thin-walled stainless steel crucible (side walls 0.1 mm thick) was commercial zinc. The mean consumption of zinc during work in the U-300 cyclotron was 0.035 g/h.

Declassified and Approved For Release 2013/03/01 : CIA-RDP10-02196R000300100005-6

Declassified and Approved For Release 2013/03/01 : CIA-RDP10-02196R000300100005-6

The current of the inner beam of Zn^{10+} ions was not measured owing to the much larger current of Zn^{2+} ions accelerated in the fifth harmonic, and also the current of other ions, which exceeded that of the Zn^{10+} ions by more than an order of magnitude in advance of the commutating magnet. In order to measure the current of the extracted beam we made an uncooled ion collector with an insulation resistance of over 10^{10} Ω. The signal was taken from a resistance of 10^9 Ω and measured with a V2-5 electrometer [6]. Measurement of the ion energy by means of a silicon detector showed [7] that the beam contained a considerable number of five-times charged sulfur ions; the current of S_{32}^{5+} often exceeded that of the Zn_{64}^{10+}. In the physical experiments a beam of Zn_{66}^{10+} ions was used, in which the proportion of S_{32}^{5+} was comparatively small. The composition of the beam was constantly monitored with a silicon detector. The greatest current of Zn_{66}^{10+} ions was 0.02 μA (10^9 particles/sec) with the following source operating conditions: arc current in the pulse I_g = 7 A, voltage in pulse U_g = 700 V, pulse length τ = 1 msec, frequency f = 180 cps, crucible temperature T = 400°C.

Since the charge exchange of Zn^{10+} ions at the onset of acceleration may be considerable, we measured the dependence of the current of Zn_{66}^{10+} ions on the pressure in the accelerator chamber, and also the same relationship for Ar^{7+} and Ne^{4+} ions. The pressure in the vacuum chamber was regulated by varying the pumping speed. The resultant curves are shown in Fig. 2, from which we see that the fall in the beam intensity with rising pressures in the chamber occurs more rapidly for the ions with the greater charge. An estimate of the average cross section of the processes leading to a change of charge based on the formula [8]

$$I/I_0 = \exp\left[-10^{27} p \int_0^t \sigma(\beta)\,\beta\,dt\right]$$

(β = v/c, where v is the velocity of the ion; t is the acceleration time in sec; p is the pressure in the accelerator chamber in mm Hg) gives a value of $\sigma \approx 0.8 \cdot 10^{-16}$ cm² for zinc. For Ar^{7+} and Ne^{4+} the value is respectively two and three times smaller.

Acceleration of Phosphorus. Phosphorus ions were obtained with red phosphorus as source material. The mean consumption of phosphorus during work on the cyclotron was 0.13 g/h.

The screen (Fig. 1) shielding the crucible from heating by the radiation of the hot gas-discharge chamber was very necessary when working with phosphorus. If the screen were absent or inadequately polished, the crucible overheated, and this increased the feeding of phosphorus into the discharge, the yield of five-times charged phosphorus diminishing. Figure 3 shows the charge spectrum of the phosphorus ions obtained in an ion-source test-bed (the method of recording such spectra was given in [4, 9]). In recording the P^{6+}, P^{7+}, and O^{3+} peaks the amplification was increased 8.5 times. In the optimum discharge mode we obtained the following pulsed phosphorus ion currents: P^+ – 3.4 mA; P^{2+} – 9.4 mA; P^{3+} – 7.6 mA; P^{4+} – 5.8 mA; P^{5+} – 2.9 mA; P^{6+} – 0.54 mA; P^{7+} – 0.03 mA. In the cyclotron the extracted beam of P^{5+} ions measured with a weak-current integrator [10] was 20 μA. A typical working mode was I_d = 12 A, U_g = 550 V, τ = 1.5 msec, f = 180 cps, T = 270-320°C. During the operating period, the crucible temperature had to be raised owing to the diminishing amount of material in the crucible, and also owing to the fact that the phosphorus employed constituted a mixture of different forms, differing in their rate of evaporation at a particular temperature.

The ion source described in this paper has been used for several months in the U-300 cyclotron of the Joint Institute for Nuclear Research. The authors consider that in a source of this construction multiply-charged ions of simple substances and compounds requiring the heating of the crucible and chamber to temperatures of 1000°C or under for their evaporation may readily be obtained. It must of course be remembered that the use of new working substances, particularly chemical compounds, introduces its own special features, and considerable technological difficulties may arise.

In conclusion, the authors wish to thank G. N. Flerov for constant interest in the work and discussion of the results, A. A. Pleve for help in the cyclotron measurements, and also V. M. Plotko, S. G. Chebonenko, and A. A. Eropkin for assembling the ion sources and I. P. Kuznetsova for help in the test-bed source tests.

LITERATURE CITED

1. A. S. Pasyuk et al., At. Énerg., 28, 75 (1970).
2. Yu. P. Tre'yakov et al., At. Énerg., 28, 423 (1970).
3. A. I. Vladimirov, V. A. Saenko, and Yu. P. Tret'yakov, Preprint JINR, R13-5559, Dubna (1971).

Declassified and Approved For Release 2013/03/01 : CIA-RDP10-02196R000300100005-6

Declassified and Approved For Release 2013/03/01 : CIA-RDP10-02196R000300100005-6

4. A.S.Pasyuk, Yu.P.Tret'yakov, and S.K.Gorbachev, At.Énerg., 24, 21 (1969).
5. M.von Ardenne, Tables of Electron Physics, Ion Physics, and Electron Microscopy, Vol.II, VEB Deutscher Verlag der Wissenschaft, Berlin (1956), p.654.
6. Radiation-Measuring Instruments, Catalog-Handbook [in Russian], NII TRIR, Moscow (1964), p.10.
7. Kh.Kekk et al., Pribory i Tekh.Éksperim., No.4, 27 (1963).
8. A.Ghiorso et al., IEEE Trans.Nucl.Sci., 13, No.4, 280 (1966).
9. A.S.Pasyuk, Go Tsi-Tsyan', and Yu.P.Tret'yakov, Preprint JINR, 1523, Dubna (1964).
10. A.A.Kurashov and A.F.Linev, Pribory i Tekh.Éksperim., No.2, 70 (1957).

Declassified and Approved For Release 2013/03/01 : CIA-RDP10-02196R000300100005-6

Declassified and Approved For Release 2013/03/01 : CIA-RDP10-02196R000300100005-6

CHRONICLES

MEETING OF PROGNOSIS OF DEVELOPMENT OF NUCLEAR ENERGETICS

Yu. I. Koryakin

A meeting of the specialists from the member countries of SÉV (Council for Mutual Economic Aid) was held in Warsaw from March 21 to March 24, 1972 to discuss the mathematical models used in the prognosis of the development of nuclear energetics, the composition of the basic information used in them, and also technical–economic estimates of the development of power reactors that are most promising for the member countries of the SÉV and the reprocessing of irradiated fuel. Thirty six specialists from Bulgaria, Hungary, GDR, Poland, Rumania, USSR, and Chzecoslovakia participated in the meeting. Seventeen papers were presented and discussed so that to a certain extent the meeting acquired the character of a symposium.

The meeting was conducted within the framework of operation of SÉV on joint prognosis of the development of nuclear energetics in accordance with the complex program of further intensification, improvement of collaboration, and the development of socialistic economic integration of the member countries of the SÉV. This was the first meeting of its kind.

The materials presented were arbitrarily divided into two groups. The first group covered the discussion of types of power reactors, their existing and expected technical–economical indices, and also the indices of reprocessing of irradiated nuclear fuel and the external fuel cycle of nuclear energetics, which are important for the prognosis of its development and are used as parameters in mathematical models.

Such problems as the requirement of uranium in the period of prognosis, expected tendencies of change in the graph of the loads of APP with different types of reactors in perspective, requirements on the operational characteristics of APP and so forth, i.e., either emanating from the problems of prognosis or appearing as prognosis problems, were also touched upon.

The second group consisted of papers on mathematical models used in the prognosis of the development of nuclear energetics and on preliminary results obtained in the member countries of the SÉV. At the present stage of prognosis these problems are most important. Here papers pertaining to the procedures of development and principles of construction of mathematical models, ways of their further improvement, and also programming on computers were discussed. Optimization and immitation (also called simulation) types of mathematical models and their role in the solution of prognosis problems were discussed. The discussion showed that it is necessary to use both types of models; wherever possible the optimization models should be given preference and the immitation model must serve as an instrument for the analysis of the optimum variants.

A majority of the papers of the second group contained the results of mathematical modeling of the development of national nuclear power systems which are the starting point and form a component part of the complex joint prognosis of the development of nuclear energetics within the framework of the SÉV, optimized according to some object function.

From the Secretariat section of the SÉV, I. Shkrabal addressed the meeting. His report was concerned with the connections of work on joint prognosis of the development of nuclear energetics in the member countries of the SÉV with the work and problems of the units of the SÉV in the field of planning and study of fuel-power branches and machine construction.

The Soviet delegation presented three papers. The first was concerned with the investigation of tendencies in the development of different types of reactors and the structure of nuclear energetics on the basis of analysis of patent information using regression analysis of the patent foundation. The second paper

Translated from Atomnaya Énergiya, Vol. 32, No. 6, pp. 509-510, June, 1972.

© 1972 Consultants Bureau, a division of Plenum Publishing Corporation, 227 West 17th Street, New York, N. Y. 10011. All rights reserved. This article cannot be reproduced for any purpose whatsoever without permission of the publisher. A copy of this article is available from the publisher for $15.00.

Declassified and Approved For Release 2013/03/01 : CIA-RDP10-02196R000300100005-6

Declassified and Approved For Release 2013/03/01 : CIA-RDP10-02196R000300100005-6

described the mathematical models (developed in the USSR) of optimization of the structure of nuclear energetics within the framework of SÉV by minimizing the requirement for nuclear fuel. The third described the mathematical model for a long-range prognosis of the development of the national nuclear energetics based on economic criterion.

One of the main tasks of the meeting was to discuss and match the principles of construction of mathematical models in the prognosis of the development of nuclear energetics within the SÉV. The refined methodological bases of prognosis and mathematical models presented by the Soviet delegation were approved.

The discussion of the papers and the exchange of opinions showed a significant progress in mathematical modeling of the development of nuclear energetics in the member countries of the SÉV and a high scientific level of the discussed works. It was noted that the nuclear energetics in the member countries of the SÉV represented in the meeting is becoming, or will become in the near future, an important branch of power industry. Therefore it was stressed that the prognosis, which is closely connected with the planning activity (prognosis is the scientific-research basis for a plan), is a continuous process in which mathematical models (as the basic tool of prognosis) are improved, and the initial data and obtained results are refined. The work done so far is the first step of joint investigations on the prognosis of the development of nuclear energetics in the member countries of the SÉV.

As a rule, mathematical models are used for a period of prognosis of 30-50 yr. Within national framework it is considered advisable to carry out prognosis of nuclear energetics according to an economic criterion in its financial expression. The indeterminacy in the initial data leads in the prognosis to a zone of indeterminacy of the accepted solutions; an important step in the study of this indeterminacy is a multifactor analysis of the system with the purpose of determining the degree of importance of the initial information.

The discussion showed that the work on mathematical modeling in the member countries of the SÉV is at different stages of development and different approaches are being used. Thus, in Poland both optimization and immitation models are being developed with success. Great attention is given to the analysis of the system of enterprises of external fuel cycle. In Czechoslovakia the work is proceeding on a very wide front, which is indicated by the number of papers from the ChSSR presented at the meeting. However, the main attention is concentrated on immitation models. The immitation models developed in GDR are distinguished by a careful and intensive study of the problem.

A resolution was passed with recommendations for the delegation of the organizing country (USSR) as well as for the operating units of the PKIAÉ. These recommendations pertain to the conditions and problems (composition of the initial information, multivariant nature of the dynamic consideration of the system, determination of the regime of operation of different types of reactors in the period of prognosis, life and economic indices of the enterprises of external fuel cycle, and so forth) arising as a result of the use of mathematical models in the member countries of the SÉV. The fulfilment of these recommendations will facilitate a more qualitative prognosis of the development of nuclear energetics within SÉV and also the refinement of its indices.

Considering that a meeting of this kind was held for the first time and that the problems of economics and prognosis are highly important for the search of the most effective ways and strategies of further use of nuclear energetics in power industry, it was decided to publish the material of the meeting. The contacts, discussion, and the exchange of opinions were very useful for the participants of the meeting.

Declassified and Approved For Release 2013/03/01 : CIA-RDP10-02196R000300100005-6

Declassified and Approved For Release 2013/03/01 : CIA-RDP10-02196R000300100005-6

EXCHANGE OF EXPERIENCE IN THE FIELD OF DEVELOPMENT AND UTILIZATION OF EQUIPMENT OF A WATER-COOLED WATER-MODERATED REACTOR

A. P. Barchenkov

A seminar on the exchange of accumulated experience in the utilization and operation of atomic power plants in Reinsberg and Novo-Voronezh was held in Noilobsov (GDR) from February 29 to March 3, 1972 in accordance with the decision of the XXI meeting of PKIAÉ. The aim of the seminar was to fulfill the measures stipulated in the complex program of further intensification and improvement of the collaboration and the development of socialistic integration of the member countries of the SÉV in creating necessary organizational, scientific, and industrial prerequisites for the introduction of atomic energy into the national economy of the member countries on industrial scales.

Seventy-nine specialists from the member countries of the SÉV participated in the seminar. Twenty-eight papers on scientific–technical problems related to the installation, start, and operation of atomic power plants with reactor installations of type VVÉR (water-cooled water-moderated) were presented. The papers by scientists and specialists of GDR on six years experience in the operation of an industrial–experimental APP with VVÉR type reactor in Reinsberg were especially interesting. Designed for 70 MW the APP is at present in stable operation at 80 MW power. During the total period of its operation ~2 bill. kWh of electrical power has been generated. The use of the installed power of the APP comprises about 5500-6000 eff.h/yr. All this results from an increase in the level of the scientific–technical knowledge of the personnel of the APP, which makes it possible to ensure a reliable, accident-free and safe operation, and also from extensive scientific-research work helping to increase further the technical–economic indices of the APP and to improve individual units in the instrumentation of the reactor installations of this type.

Results of a more intensive burning of nuclear fuel have been obtained; large scale experimental investigations have been successfully carried out on the appropriation of a reliable and efficient liquid method of controlling the reactor (with the use of boric acid).

The results from the experience gained are passed on to the member countries without any cost for use at APP with reactors of this type.

The accumulated experience in the installation and operation of the APP and the scientific–technical knowledge in the field of reactor science and technology and nuclear energetics have enabled GDR to start, with the aid of the Soviet Union, the construction of more powerful APP, whose installation is the beginning of the fulfilment of a large program intended for the development of nuclear energetics in GDR.

The papers from Soviet scientists and specialists on the experience gained in the start-adjustment work on the second and third blocks of Novo-Voronezh APP were equally interesting. The third block of the APP with a VVÉR type reactor installation having 440 MW (el) power and with two turbogenerators of 220 MW each is typical of the APP being constructed in Bulgaria, GDR and USSR, and planned to be constructed in Rumania, Czechoslovakia, Hungary, and Poland. Therefore, the large interest in the starting operation on the first reactor of this type is completely explainable.

It was mentioned that the physical and power-producing lunch of the first APP with a VVÉR-440 type reactor and the start-adjustment operations went on successfully. A significant reduction of the time between the physical and power-producing launch of the reactor to five days was achieved, whereas usually this operation took several months.

Translated from Atomnaya Énergiya, Vol. 32, No. 6, pp. 510-511, June, 1972.

© 1972 Consultants Bureau, a division of Plenum Publishing Corporation, 227 West 17th Street, New York, N. Y. 10011. All rights reserved. This article cannot be reproduced for any purpose whatsoever without permission of the publisher. A copy of this article is available from the publisher for $15.00.

Declassified and Approved For Release 2013/03/01 : CIA-RDP10-02196R000300100005-6

Declassified and Approved For Release 2013/03/01 : CIA-RDP10-02196R000300100005-6

DIARY OF COLLABORATION

The First Meeting of the Soviet of the International Economic Union on Nuclear Instrument Manufacture "Interatominstrument." This meeting established in accordance with the agreement signed by the governments of Bulgaria, Hungary, GDR, Poland, USSR, and Czechoslovakia, was held in Warsaw on February 23-24, 1972. The representatives of all economic organizations and enterprises, that are members of "Interatominstrument," took part in the meeting. Representatives of Rumania and the secretariat of the SÉV were also present in the meeting as observers.

I. Traikov, permanent representative of the State Economic Union "Respor" (Bulgaria), was elected as the chairman of the Soviet of "Interatominstrument."

Having examined the proposals and material presented at the meeting, the Soviet nominated Z. Tvardon (Poland) the director of the Union, accepted the project of rules of procedure, worked out by the preparatory committee of "Interatominstrument," as the basis in the initial work of the Soviet, commissioned the director of the Union to conduct this project entirely in accordance with the Agreement and Rules of "Interatominstrument" and to present it at the second meeting. The Soviet also confirmed the Statute about the personnel of the Union; it agreed to the proposal of manning the Union by specialists; approved the tentative financial plan for 1972, commissioning the director of the Union to refine it and present it to the Soviet for confirmation; took decision on other problems related to the start of the activity of the day for the second meeting of the Soviet, which was marked for May 10-11 of the current year.

At the second meeting it is intended to examine and confirm the rules of procedure of the Soviet, the Statute on the activity of revision commission, nomenclature of the products coming within the sphere of activity of the Union, the plan of work of the Soviet and refined financial plan of the Union for 1972, to discuss the problems of economic efficiency of the activity of the Union and the feasibility of arranging an exhibition of nuclear apparatus in 1973, and so forth.

The meeting of the Soviet of "Interatominstrument" went on in a friendly and business-like atmosphere.

Coordinated Meeting of Specialists from Member Countries of the SÉV on the Theme: "Development of Instruments and Apparatus of General, Dosimetric, and Radiometric Control for Nuclear Reactors." This was held in Prague on March 21-23, 1972 in accordance with the plan of work of PKIAÉ SÉV. Specialists from Bulgaria, Poland, Rumania, Soviet Union, and Czechoslovakia participated in the meeting. The theme includes 11 tasks stipulating the development of general concept and structure of the system of control of radiation characteristics of the reactor, mechanical constructions of the system, instrumentation of the subsystem of control of the hermeticity of the casings of fuel elements, systems of information, control and program signals, electronic instrumentation of the SUZ (control and safety rods), dosimeters, ionization chambers, instruments for recording radioactive substances in air and liquid media, and so forth. The USSR is the organizing country for the theme as a whole.

The plan of the report on the fulfilment of this theme in 1971, prepared by the Soviet delegation, was discussed and approved; within the framework of the general working plan on the theme, worked out by the working group on nuclear instrument manufacture and approved by PKIAÉ SÉV, stepped plans of work on individual tasks for 1972-1975 were approved. In conclusion there was a unanimous opinion that at the first stage work should be carried out as applicable to water–water power reactors of APP, installed at present in the member countries of SÉV.

Translated from Atomnaya Énergiya, Vol. 32, No. 6, p. 511, June, 1972.

© 1972 Consultants Bureau, a division of Plenum Publishing Corporation, 227 West 17th Street, New York, N. Y. 10011. All rights reserved. This article cannot be reproduced for any purpose whatsoever without permission of the publisher. A copy of this article is available from the publisher for $15.00.

Declassified and Approved For Release 2013/03/01 : CIA-RDP10-02196R000300100005-6

Declassified and Approved For Release 2013/03/01 : CIA-RDP10-02196R000300100005-6

During the start-adjustment operations the operating regime of the turbogenerators of the reactor block was determined at minimum power for transition from forced to natural water circulation in the first contour, which improves the conditions of reactor cooling in accident situations. The possibility of replacing the control rods by boric acid was checked during the operation at 50% of the designed power.

Other improvements in the operation of the reactor installation of VVÉR-440 type were also noted, which were obtained as a result of systematic work of scientists and construction personnel on further refinement of the installation.

The exchange of scientific–technical experience in the field of reactor technology and nuclear energetics acquires ever increasing significance in view of the development of this field in the member countries of the SÉV and will help in further refinement of the reactor power installations. This exchange will also promote the imparting of the necessary minimum knowledge to the specialists of individual countries, which is required for the installation of first APP.

Declassified and Approved For Release 2013/03/01 : CIA-RDP10-02196R000300100005-6

Declassified and Approved For Release 2013/03/01 : CIA-RDP10-02196R000300100005-6

INFORMATION

THE THIRTY-FIRST SESSION OF THE SCIENTIFIC COUNCIL OF THE JOINT INSTITUTE FOR NUCLEAR RESEARCH (USSR)

V. A. Biryukov

During January 4-7 in Dubna, there occurred the Thirty-First Session of the Academic Council of the JINR (USSR). The Country's scientists who are members of the JINR heard reports concerning the activity of the laboratory, the science advisory units, and management of the Institute for 1971. Opening the session, N.N.Bogolyubov, the Director of the JINR, reported on the course of achievements of the Academic Council.

D.I.Blokhintsev, the Director of the Laboratory of Theoretical Physics, told about the most important results of research conducted by the Institute's theorists in the areas of elementary particle physics and the atomic nucleus. The program of work on the nonlocal scalar field has been completed. A nonlocal quantum theory of electromagnetic and weak interactions has been constructed with a unitary, causal, and gradient-invariant S-matrix. All asymptotic forms of meson dynamics for highly inelastic photon–nucleon and photon–photon processes are considered on the basis of summation methods. The predicted equality of the cross sections for the scattering of longitudinal γ-quanta by protons and neutrons can be confirmed experimentally. Similarity principles have been formulated, determining the asymptotic behavior of cross sections for strong, electromagnetic and weak interactions of nonleptons.

A quantitative method for the study of small nucleon systems developed by the Laboratory was that of associated channels for nuclear reactions. Interesting results have been obtained by the theory for deformed nuclei. Significant progress is being attained in the semimicroscopic description of highly excited nuclear states; such an approach can serve as a basis for the study of neutron resonance structure.

In connection with experiments, carried out at the JINR in a pulse reactor, at the Laboratory there was completed important work on the theory of the solid and condensed state.

The results of scientific studies obtained at the High Energy Laboratory were presented in a paper by A.M.Baldin. Several experiments were performed in the 76 GeV accelerator of the High Energy Physics Institute at Serpukhov. The processing of data obtained during the course of experiments on the investigation of elastic pp- and pd-scattering at small angles has been completed. The energy dependence of the obliquity parameter for the diffraction cone in elastic pp- and pd-scattering and the ratio of the real to the imaginary parts of their amplitudes have been thoroughly studied in the 8-70 GeV energy region. For the first time it has been established that the pp-scattering range grows logarithmically with an energy increase in the 10-70 GeV interval. The experimental data is consistent with calculations based on dispersion relations.

The asymptotic behavior of the neutral K-meson scattering amplitude in experiments on meson regeneration is being studied. Groups of physicists and engineers from the High Energy Physics Institute (Serpukhov), the Central Institute of Physical Research of the Hungarian Academy of Sciences, the Physical Institute of the Czechoslovakian Academy of Sciences, the Physical Institute of the Bulgarian Academy of Sciences, and the High Energy Physics Institute of the Academy of Sciences of the German Democratic Repulic are participating with scientists from the JINR in conducting experiments and processing data. It has been found that the phase difference of the elastic forward scattering amplitudes for K^0_p and $\tilde{K}^0_p$ is approximately constant over the 14-42 GeV/c momentum interval investigated and its modulus decreases with an increase in the energy of the incident K-mesons as $\sim 1/E^{1/2}$.

Translated from Atomnaya Énergiya, Vol. 32, No. 6, pp. 513-515, June, 1972.

© 1972 Consultants Bureau, a division of Plenum Publishing Corporation, 227 West 17th Street, New York, N. Y. 10011. All rights reserved. This article cannot be reproduced for any purpose whatsoever without permission of the publisher. A copy of this article is available from the publisher for $15.00.

Declassified and Approved For Release 2013/03/01 : CIA-RDP10-02196R000300100005-6

Declassified and Approved For Release 2013/03/01 : CIA-RDP10-02196R000300100005-6

More than 100,000 photographs have been obtained with a two-meter propane chamber exposed to a beam of 40 GeV π^--mesons. The successful triggering of the apparatus occurred with a two-meter liquid-hydrogen chamber, "Lyudmila" Ten photoemulsion cameras were exposed to 50-70 GeV protons; their processing is being supervised in the laboratories of many countries who are collaborators of the JINR.

In experiments with relativistic deuterons (6-10 GeV/c) in an LVÉ synchrophasotron, there was discovered a cumulative effect – a many-baryon collision with the concentration of energy in one pion. The cross section for the cumulative production of pions by deuterons in copper nuclei comprises ~5% of the production cross section of their nucleons. The pions created are recorded by a system of differential Cerenkov counters. By using photoemulsions which have been exposed to deuterons, it was found that the fraction of nuclear proton stripping of a deuteron compared with all the inelastic interactions comprises 14 ± 2%.

In the Laboratory of Nuclear Problems there has been completed a series of experiments related to the verification of conservation laws and the study of particle structure. V.P. Dzhelepov reported on this. In the examination of rare meson decays there was obtained a low estimate for the upper limits of the relative probabilities for the processes: $R \leq 3.5 \cdot 10^{-9}$ for $\mu^+ \to e^+e^+e^-$ and $R \leq 5 \cdot 10^{-9}$ for $\pi^+ \to e^+e^+e^-\nu_e$. Study of the inverse process for the electroproduction of pions $\pi^-p \to e^+e^-n$ at an energy of 275 MeV in the region of timelike transmitted momenta up to $q^2 = 2\ F^{-2}$ provided a value for the pion and nucleon form-factors $F_\pi = F_1^V = 1.07^{+0.14}_{-0.17}$ (on the assumption that $F_1^V = F_\pi$). There have been completed on the Yerevan synchrotron, measurements of the differential elastic ep-scattering cross section at an energy of 4.13 GeV in a region of small transmitted momenta. A determination of the proton's electromagnetic radius provided a value of 0.79 ± 0.04 F.

In experiments with a meter propane bubble chamber on a π^--meson beam with 5 GeV/c momentum from a synchrophasotron there was obtained new data concerning the coherent production of a complex of three pions by a nucleus of pure carbon. The cross section for the process is $(264 \pm 37) \cdot 10^{-30}$ cm^2 and falls sharply with a decrease in the energy of the primary particles. In the study of pion interactions with carbon there has been detected the occurrence of double Λ^0-hyperon creation. This explained the possibility for the formation of a long-lived meson with M = 1.9-2.0 GeV and S = 2 upon interaction of a π^--meson with a quasideuteron in a carbon nucleus.

By using a spectrometer with a helium streamer chamber at high pressure, the scattering of charged pions by helium is being studied. As a result of processing 120,000 stereophotographs obtained in a pion beam from a synchrocyclotron at an energy of 96 ± 6.0 MeV, the angular distributions of elastically scattered π^+- and π^--mesons have been measured over the 25-165° angular interval. The total elastic scattering cross sections equal $\sigma^- = 50.7 \pm 1.8$ mb and $\sigma^+ \pm 3.3$ mb.

In extensive studies of the cluster structure of the nucleus by electronic methods there have been measured high energy spectra of deuterons and He^3 near an angle of 5.5° (l.s.k.) corresponding to processes involving quasielastic scattering of accelerated protons and meson formations by nucleons and double nucleon combinations in Li, Be, and C nuclei.

Studies of the energy spectra and the relative probabilities for the emission of protons, deuterons, and tritons with the capture of negative pions by Be, Al, C, Ca, Cu, De, and Pb nuclei have been completed. The measurements were carried out by means of a system of silicon surface-barrier detectors. The data obtained permitted one to propose that the mechanism of pion capture is determined by the structural properties of the nucleus and, probably, does not depend on the nature of the original, fundamental interaction process.

The formation of B^8 by the capture of stopped π^--mesons by nitrogen nuclei has been investigated using the photoemulsion method.

The Laboratory's scientists subjected to the effects of the beam from the 76 GeV accelerator IFVÉ (Serpukhov) an apparatus constructed by them to search for Dirac monopoles. The preliminary data provided an upper bound for the production cross section of monopoles with large magnetic charges (30-68.5 e): $\sigma < 5 \cdot 10^{-38}$ cm^2.

V.P. Sarantsev told about the work related to the study of the collective method of acceleration. The problem of the joining of the magnetic fields pulses for the blocking and transmitting (to the accelerating unit) section was solved by the collective accelerator model.

Declassified and Approved For Release 2013/03/01 : CIA-RDP10-02196R000300100005-6

Declassified and Approved For Release 2013/03/01 : CIA-RDP10-02196R000300100005-6

The formation of the field at the junction is accomplished by a special correcting coil. A field of a given form at the transmission section is established by means of coils. In the electron duct of the injector (LIU-3000) there has been installed new focusing lenses and additional coils that allowed one to increase the current of the accelerator beam by a factor of one and one half. A stable operating region is attained by the thermal resonator established here. In the resonator there is achieved an electric field intensity of 90 kV/cm along with a magnetic field on the order of 10^4 G.

In the experimental unit of the SILUND accelerator, there was completed a series of accelerations of a gas-focused beam. The electron beam with a 2000 A current has been accelerated up to an energy of 500 keV. The installation and completion of the electrical alignment of only the SILUND accelerator, designed for an energy of 3 MeV, has been accomplished. A reinforced version of the vacuum chamber of the Adgezator-2 has been manufactured and tested; the walls of the chamber are made of stainless steel.

The apparatus has been constructed with an accuracy of measurement of the pulse magnetic fields having a relative error of 0.1%, an absolute error of 1%.

M.G.Meshchernyakov spoke on the activity of the Laboratory of Computational Engineering and Automation (LCEA). Mathematically rigorous algorithms for multimachine systems have been developed and servicing programs within the limits of the "Dubna" monitoring system for the BÉSM-6 have been written. Operating experience has yielded the communication line "Minsk-2" with the BÉSM-6; with this, the processing time for experimental γ-spectra with the utilization of a FORTRAN program is approximately 100 times shorter. Together with the Central Institute of Physical Research of the Hungarian Academy of Sciences there has been continued work on the development of the apparatus and the mathematical aspects of Fortran systems based on the TRA type Hungarian electronic computer. Connections between the basic BÉSM-6 machine and other electronic computers at eight locations in all have been established.

The effectiveness of the mathematical aspects of the system for the BESM-6 have been significantly improved thanks to the introduction into the operation of a new kind of program-dispatcher and expansion of the program library. The conversion of machines completely into a multiprogram operation raised the effectiveness of the utilization of the central processor by a factor of one and a half to three. A new version of the system has been furnished by the national organizations of countries which are members of the JINR. External control programs have been constructed by devices for small TRA machines.

Groups in the German Democratic Republic and the USSR have extended the manufacture of the "Spiral Meter" scanning equipment. The first sample of the device has been installed in the LVTA and is being adjusted. Mathematically rigorous programs are being developed for the meter. The Laboratory of Nuclear Problems has modernized automation of the electron-beam tube for the processing of spark chamber photographs.

The arrangement of the devices and the storage and processing of the spectrometric information (POFI-2) produced by the equipment at the measuring center of the Laboratory of Neutron Physics (BÉSM-4) has been exploited.

Applied calculations in connection with the leading research at the JINR have prominent place in the Laboratory's operations. The average work is involved in analytic and numerical studies of nonlinear equations in plasma theory and relativistic electron and electron–ion rings carried out in connection with the study of the collective acceleration method. A method for calculating the quantum mechanical three-body problem was developed and the work was extended to the enlargement of the groups of programs for model calculations of the properties of complex nuclei and many others.

I.M.Frank reported on the creation at the Laboratory of Neutron Physics of an installation for work with ultracold neutrons (UCN) in the IBR-30 reactor. Studies of the influence of the temperature, converter materials, and the moderator's geometry on the output of UCN have been conducted. In conjunction with the I.V.Kurchatov Institute of Atomic Energy, work on the reactor maintained by this institute reconstructed the channel of UCN and installed a circulating water converter. The output was raised to 100 neutrons/sec.

The scanning of nuclei for which nα-reactions by resonance neutrons are possible has led to the discovery of nα-decays of Zn^{64}, Zn^{67}, and Hf^{177} resonances. Previously, detailed measurements of the observed α-decay of Sm^{147} resonances enabled one, for the first time, to verify the prediction of the statistical theory concerning the distribution of the partial α-widths. The experimental and theoretical results are found to be in satisfactory agreement. There were also measurements of the spectra of α-particle triple fission of 11 U^{235} resonances.

Declassified and Approved For Release 2013/03/01 : CIA-RDP10-02196R000300100005-6

Declassified and Approved For Release 2013/03/01 : CIA-RDP10-02196R000300100005-6

Within the limits of the method developed at the Laboratory, investigations of the ne-interaction were carried out by measuring the neutron diffraction at a fixed angle with respect to the time-of-flight simultaneously for two noncrystals of Tungsten containing different amounts of the W^{186} isotope. The interaction amplitude $a_{ne} = (-1.32 \pm 0.11) \cdot 10^{-16}$ cm.

Experiments on the determination of the neutron–neutron scattering length a_{nn} from the kinematics of the whole experiment on the $H^3(t, n He^4)$ n reaction have been accomplished by means of an electrostatic generator. It has been found that $a_{nn} = -15.0 \pm 1.0$ F.

Great success is being achieved in a Mossbauer spectroscope on Zn^{67} whose nucleus has the narrowest line width on record $\sim 10^{-15}$. The quadrupole splitting of zinc oxide lines has been measured by a new method. The thermal shift of the lines has also been measured; the sign of the electric field gradient in zinc oxide has been measured directly.

New spectrometers have been constructed for the study of condensed media by means of neutrons: the Cracow–Dubna spectrometer with a reverse geometry and the Warsaw phonon spectrometer. They have been developed for prospective utilization in the new IBR-2 pulse reactor whose planning and construction is being successfully managed.

G.N. Flerov reported on the work completed by scientists of the Nuclear Reactions Laboratory. Xenon ions have been accelerated by using a tandem system of the U-300 and U-200 cyclotrons at the Laboratory. Beams of $Xe^{+27}_{132(136)}$ ions with an intensity of $\sim 3 \cdot 10^9$ particles/sec at an energy of ~700 MeV and of Xe^{+30}_{136} ions with an intensity of $\sim 3 \cdot 10^8$ particles/sec at an energy of 850 MeV have been obtained. Preliminary results of studies on the interaction of xenon ions with Ta, Tb, Bi, and U nuclei were obtained.

An isotope of Ku^{259} has been synthesized in work on the synthesis and study of the properties of the transfermium elements. The measured period of its half-life $T_{1/2} = 4.5$ sec and the period of spontaneous decay $T_{sf} \geq 25$ sec.

Ku^{259} has been isolated in chemical experiments by the method of frontal thermochromatography of chlorides. After acceleration in a U-300 cyclotron, phosphorus ions undertake a trial-and-error search for the spontaneous fission of the 107^{262} isotope among the reaction products for the complete fusion of the $U^{235} + P^{31}$ nuclei. A spontaneously decaying emitter with $T_{1/2} \sim 1$ sec, which can be attributed to the 107-th element has been observed.

The search for naturally occurring superheavy elements has been carried out. The average number of neutrons per spontaneous fission event was measured for samples of galena, lead glass, concretions, and 150 specimens of processed, semimetallic ores in a salt mine at a water equivalent depth of 1100 m. A search program was carried out for possible specimens having concentrations of superheavy elements, in particular natural, subterranean water, containing chemical analogues of the superheavy elements – lead, mercury, thallium, et al.

Experiments have been extended to search for nuclei undergoing ground state proton decay. Using a mass-separator installed in the beam of the U-300, there has been discovered among the products of the $Ru^{96} + S^{32}$ reaction a weak proton radiation with a half-life of ~1 sec and a decay energy of 0.7-0.8 MeV. It is assumed that it had been caused by the decay of one of the light isotopes of lanthanum or praseodymium.

Several spontaneously decaying isomers of Pu, Cm, and Bk were obtained in the U-200 cyclotron at the Laboratory of Nuclear Reactions of JINR and the U-120 cyclotron of the Atomic Physics Institute at Bucharest upon irradiation of targets of Th, Pu, and Am by α-particles with energies of 21-36 MeV. Their production cross sections have been measured.

An additional experimental indication of the nuclear instability of He^{10} was obtained in studies of the neutron-rich isotopes of the light elements. In experiments with heavier ions, there was found with the irradiation of Th^{232} by Ar^{40} ions 17 new neutron-rich isotopes with Z in the 12-17 range and their production cross sections were measured.

A. Mikhul, Assistant Director of the JINR, gave a talk on a paper concerned with international cooperation. He emphasized the joint leadership by the Institute's scientists and groups of specialists at the regional national laboratories – membership of the JINR physical research and methods development as an important aspect of the cooperation. In 1971 there were 270 such projects conducted. Cooperative experiments both at the primary installations of the JINR and at accelerators and reactors in Moscow, Serpukhov,

Declassified and Approved For Release 2013/03/01 : CIA-RDP10-02196R000300100005-6

Declassified and Approved For Release 2013/03/01 : CIA-RDP10-02196R000300100005-6

Yerevan, Sofia, Bucharest, Budapest, and Leipsig are reported to them. From Dubna's regional laboratory –collaborators of the JINR are supplied materials for processing in the form of photographs with a bubble chamber, nuclear photoemulsions, and magnetic tapes; radioactive isotopes are regularly supplied. The Institute cooperates with 18 laboratories in eight regions in the processing of photographs with a two-meter propane chamber; 80% of the experimental material is transmitted to these laboratories where approximately 100 people are engaged in its processing. The magnetic spark spectrometer, the spiral meter, and spectrometers for neutron experiments were mentioned among the most prominent of the joint methodological developments. The regional laboratories which are members of the JINR are actively participating in the development of apparatus for experiments in the new IBR-2 reactor under construction at Dubna.

Many foreign scientists arrive at Dubna annually. Approximately 550 specialists from countries which are members of the JINR (not counting the conference participants), 225 people from other countries visited the Institute in 1971. About 400 collaborators of the JINR left for other countries.

In 1971, the JINR arranged 11 science and 16 science-organization conferences at which about 2000 specialists from the JINR and various countries participated. Among the conferences there were the International Symposium on High Energy Physics at Dresden (together with the Academy of Sciences of the German Democratic Republic), the International School of High Energy Physics at Varna (together with the European Organization for Nuclear Studies), the International Conference on Heavy Ion Physics at Dubna, et al.

The plan for 1972 provides for conducting a series of international conferences, among which there are the Second Symposium on High Energy Physics in Czechoslovakia, the International School of Nuclear Structure at Alushta, the Symposium on Collective Method Accelerators at Dubna et al.

N.N.Bogolyubov awarded Honorary Diplomas from the Science Council to the authors of the best papers honored with an award by the JINR. The first prizes were awarded for the papers "α-Decay of nuclear neutron resonances" and "Experiments on the acceleration of α-particles by the collective method."

Declassified and Approved For Release 2013/03/01 : CIA-RDP10-02196R000300100005-6

Declassified and Approved For Release 2013/03/01 : CIA-RDP10-02196R000300100005-6

THIRD ALL-UNION CONFERENCE ON DISSOCIATING GASES

V. B. Nesterenko

The Third All-Union Conference on dissociating gases as heat-transfer agents and operating substances in APP was held in January, 1972 at the Institute of Nuclear Energetics of the Academy of Sciences, Belorussian SSR (IYaÉ AN BSSR). The Conference was conducted in accordance with the plan of the Academy of Sciences of the USSR with the participation of the State Committee of the Soviet of Ministers of the USSR on science and technology, the State Committee of the USSR on the utilization of atomic energy, and the division of physicotechical problems of energetics of the Academy of Sciences of the USSR.

Three hundred and seventeen persons from 89 scientific-research institutes, industries, organizations, and a number of ministries and departments of the country participated in the Conference.

In the plenary session four review papers were presented on some of the main directions of work in the field of dissociating heat-transfer agents ("Gas-cooled fast reactors operating on dissociating gases" by A. K. Krasin, "Analysis and optimization of parameters of atomic power plants with gas-cooled fast reactor operating on dissociating heat-transfer agent with 1000 MW (el) block" by V.B. Nesterenko, "Corrosion of materials in nitrogen tetroxide" by A.M. Sukhotin). One hundred and twenty five papers and communications were presented in the sectional meetings.

The Conference was conducted in six sections:

1. Schemes and cycles of power installations operating on dissociating gases.
2. Thermophysical properties of chemically reacting gases.
3. Heat exchange of dissociating heat-transfer agent.
4. Gasdynamics of dissociating heat-transfer agent.
5. Technology of dissociating heat-transfer agents and corrosion stability of materials in dissociating systems.
6. Problems of physics of fast reactors with dissociating gaseous heat-transfer agents.

It was noted by the participants that during the three years that had elapsed after the Second All-Union Conference, significant progress had been made in the study of the properties of dissociating gases and their potential as heat-transfer agents and operating substances in APP. A large number of investigations have been carried out at IYaÉ AN BSSR, which is the leading organization in this direction, and also in a number of other organizations.

The following studies have been completed:

1) computational-theoretic investigations of the thermodynamic and transfer properties of the dissociating system N_2O_4 have been carried out in a wide range of temperatures and pressures; the corresponding constants have been calculated taking into account the nonideal character of the gas; the effect of the kinetics of chemical reactions on the thermodynamic and transfer properties of chemically reacting gaseous systems has been investigated;

2) the thermodynamic and transfer properties of N_2O_4 have been investigated experimentally in the subcritical range of the parameters and experimental values of the corresponding constants have been obtained;

Translated from Atomnaya Énergiya, Vol. 32, No. 6, p. 516, June, 1972.

© 1972 Consultants Bureau, a division of Plenum Publishing Corporation, 227 West 17th Street, New York, N. Y. 10011. All rights reserved. This article cannot be reproduced for any purpose whatsoever without permission of the publisher. A copy of this article is available from the publisher for $15.00.

Declassified and Approved For Release 2013/03/01 : CIA-RDP10-02196R000300100005-6

Declassified and Approved For Release 2013/03/01 : CIA-RDP10-02196R000300100005-6

3) experimental data have been obtained on the heat conductivity and the specific heat at constant pressure for N_2O_4 in the range of supercritical parameters (pressures up to 160 atm and temperatures up to 500°C);

4) the procedure for the computation of the thermodynamic cycle using N_2O_4 has been developed taking into account of the kinetics of the chemical reactions and a program for the computation has been compiled;

5) the heat exchange in the chemically reacting N_2O_4 system has been extensively investigated and data on convective heat exchange in the subcritical and supercritical ranges of the parameters and on heat exchange at boiling and condensation have been obtained;

6) mathematical models have been developed and computer programs have been written for the thermal computation of gas-cooled nuclear reactor, heat exchangers, and gas turbines operating on chemically reacting heat exchangers for the case of chemical equilibrium and for the case of finite rates of chemical reactions;

7) the composition of the chemically reacting heat exchanger N_2O_4 has been investigated in static conditions and in flow conditions at pressures up to 10 atm and temperatures up to 600°C;

8) the thermal radiation stability of N_2O_4 has been investigated in static conditions at pressures up to 50 atm and temperatures of 200-550°C;

9) the corrosion stability of constructional materials in N_2O_4 medium has been investigated in static conditions at 150 atm and 700°C and in dynamic conditions at velocities of 30-50 m/sec, pressures up to 150 atm, and temperatures up to 550°C;

10) a large gasdynamic test station "Vikhr-1" has been built at the IYaÉ AN BSSR having 1000 kW thermal power with a turbine operating on dissociating gas; investigations carried out on this station (at 500°C and 5 atm) confirm the thermal reversibility of closed gas–liquid cycles with dissociating N_2O_4 and the feasibility of prolonged stable operation of power installations operating on this heat-transfer agent;

11) a loop equipment PGZh-1 has been built on the reactor IRT of the IYaÉ AN BSSR for the first time in the USSR, on which the thermal radiation stability of N_2O_4 has been investigated in the conditions of n, γ-radiation of the reactor and also the first results on the corrosion stability of constructional materials have been obtained; some elements of the technology of the use of N_2O_4 as the heat-transfer agent in nuclear reactors have been mastered;

12) the thermophysical and physical characteristics of high-power fast reactors operating on N_2O_4 have been investigated and a technical–economical comparison of fast reactors with different heat-transfer agents (N_2O_4, He, and CO_2) has been made; the advantages of fast reactors with dissociating gas heat-transfer agents and the prospects of their use in large power installations are shown.

Thus, under the leading role of the IYaÉ AN BSSR the scientific–technical bases for the use of dissociating gases as heat-transfer agents and operating substances in APP have been worked out; the obtained results offer the hope of the construction of powerful fast reactors operating on dissociating gases with a duplication time of 5-7 years.

The resolution of the Conference noted a large prospect of continuing the scientific-research and test-construction work on the development of APP with gas-cooled fast reactors having 1000 MW (el) power and operating on N_2O_4 at gas parameters 150-170 atm and 450-500°C. It was pointed out that along with the design developments directed toward the construction of the test-industrial APP BRG-30 and industrial APP with a power of the order of 1000 MW (el) and with gas-cooled fast reactors operating on dissociating N_2O_4, further fundmental investigations of the properties and the perfection of the technology of the use of N_2O_4 in nuclear energetics are necessary. The main directions of the investigations were defined and the next conference was fixed for 1975.

The abstracts of the papers presented at the Conference have been published.

Declassified and Approved For Release 2013/03/01 : CIA-RDP10-02196R000300100005-6

Declassified and Approved For Release 2013/03/01 : CIA-RDP10-02196R000300100005-6

FOURTH INTERNATIONAL CONFERENCE ON HIGH ENERGY PHYSICS AND STRUCTURE OF THE NUCLEUS

R. A. Éramzhyan

The Fourth International conference on high-energy physics and structure of the nucleus was held in Dubna from September 7 to 11, 1971. Conferences on this large and important topic are held according to the recommendations of IUPAP (International Union of Pure and Applied Physics) regularly once every two years. The preceding conference was held in New York (USA) in 1969.

Two hundred and forty-five delegates from 25 countries participated in the conference which was conducted by an organizing committee headed by V. P. Dzhelepov. The following problems were discussed in 20 review papers and 19 reported papers: 1) diffraction phenomena in the presence of interaction of elementary particles and nuclei with nuclei; 2) production of particles and resonances in nuclei; 3) baryon resonances and hypernuclei; 4) interaction of adrons with nuclei; 5) investigation of nuclear structure at high energies; 6) interaction of π- and K-mesons with nuclei in the energy range below 1 GeV; 7) new atoms and nuclei; 8) μ-mesoatoms and mesochemistry; 9) weak interactions and nuclear structure; 10) electromagnetic interactions and nuclear structure; 11) new accelerators and the prospects of the investigation of nuclear structure with the use of high-energy particles.

The first section of the conference was devoted to Glauber approximation in the theory of scattering of high-energy particles by nuclei. From the results presented in the papers by R. Glauber (USA) and V. Chizh (Poland) it follows that the contemporary theoretical ideas about the mechanism of scattering of high-energy particles (up to 20 GeV) by nuclei for small imparted momentums (of the order of or smaller than a few hundred MeV/c) are largely substantiated by experimental results. The divergence from the theory begins at large imparted momentums. It was clearly observed for the first time in the scattering of pions and protons (with energies of 9 and 12 GeV respectively) by duterons for imparted momentums of 1.0-1.5 GeV/c.

In a number of studies an attempt has been made to refine Glauber approximation. In a paper by R. Glauber a correction was discussed which is due to the motion of nuclei. The yield of nucleons and the departure from the geometrical optics may noticeably affect the amplitude of scattering (V. M. Kolybasov, USSR). V. N. Gribov (USSR) considered the effect of inelastic screening in scattering of particles with energies above a few GeV at nuclei.

The theory of coherent generation is entirely analogous to the Glauber approach to elastic scattering. In the paper by V. Beish (CERN) new results were communicated on the coherent generation of ρ-mesons, A_1-mesons (CERN), and three-ion systems (OIYaI, MIFI).

Experimental results indicating the possible existence of two- and three-baryon resonances were analyzed in the papers by B. A. Shakhbazyan (OIYaI) and S. Tova (CERN).

The paper by E. Pnevskii (Poland) contained a summary of the results on hypernuclei noting that in experiments conducted recently the excited states H^4_Λ, He^4_Λ, and C^{12}_Λ have apparently been observed for the first time (CERN).

The paper by V. I. Komarov (OIYaI) dealing with the results of experiments on direct nuclear reactions under the action of protons generated large interest. The study of such reactions with the formation of fast neutrons, deuterons, tritium nuclei, and more complex products in the final state offers the possibility of a deeper understanding of the cluster structure of nuclei. Experiments on elastic backscattering of protons by light nuclei (OIYaI) related to this problem were discussed. The results obtained at present indicate the

Translated from Atomnaya Énergiya, Vol. 32, No. 6, pp. 517-518, June, 1972.

© 1972 Consultants Bureau, a division of Plenum Publishing Corporation, 227 West 17th Street, New York, N. Y. 10011. All rights reserved. This article cannot be reproduced for any purpose whatsoever without permission of the publisher. A copy of this article is available from the publisher for $15.00.

Declassified and Approved For Release 2013/03/01 : CIA-RDP10-02196R000300100005-6

Declassified and Approved For Release 2013/03/01 : CIA-RDP10-02196R000300100005-6

development of baryon resonances in elastic scattering of protons by deuterons for large imparted momentums. Some theoretical problems of cluster structure of nuclei were discussed in the paper by V.G.Neudachin (USSR). G.A.Leksin (USSR) analyzed the characteristics of knock-out reactions (π, πx). The contribution of the polar mechanism is inferred from the experimental results.

B.S. Barashenkov (OIYaI) presented the data from the investigation of high-energy interactions of particles and nuclei with nuclei. The results of the computation of inelastic collisions of nuclei with nuclei are of special interest in connection with the production of beams of relativistic nuclei.

The problems related to the properties of highly excited states of nuclei were discussed in the paper by V.V.Balashov (USSR). An analysis of experimental data on photoabsorption, inelastic scattering of electrons, radiation capture of ions, and capture of muons made it possible to establish a universal property of the nucleus: the excitation of a gigantic resonance in all these processes. The model of resonance absorption of muons by nuclei, proposed by Soviet theoreticians several years ago, found its conclusive experimental confirmation. The linear structure of the spectra of neutrons from nuclear μ-capture, which conforms to the predictions of this model, was established for the first time in experiments conducted in the Laboratory of Nuclear Problems of the OIYaI. Later, similar results were obtained at CERN. Experimental results on μ-capture were elucidated in the paper by V.S.Evseev (OIYaI). The author of the present article (OIYaI) discussed different theoretical aspects of this problem. It was shown that, in particular, the new results from the measurement of the asymmetry of escape of neutrons of low energies agree with the theoretical results.

The papers of D.Coltan (USA) and J.Stroot (CERN) were devoted to the interaction of pions with nuclei. The role of different mechanisms in the absorption of pions was discussed also in the paper by T.I. Kopaleishvili (USSR).

Atomic systems, in which Coulomb interaction binds negative pions, K-mesons, Σ-hyperons, or antiprotons, have recently become accessible for experimental investigations. The state of the theory of such atoms was elucidated in the paper by T.Erickson (CERN). Here the main theoretical problem is to take account of the effect of strong interaction on the position and the width of the adron atom level. The estimate of the effect of the electrical polarization of heavy adrons by the static field of the nucleus, presented in the paper, is interesting.

Experimental data on adron atoms were discussed in the paper by G.Bakenshtoss (CERN). The obtained results confirm the earlier detected regularity in the sign of the interaction of pions with nuclei in different orbital states. The results on the spectra of K-mesoatoms, Σ-atoms, and atoms containing antiprotons are essentially new.

The paper by I.S.Shapiro (USSR) was devoted to quasinuclear mesons. According to the studies of I.S. Shapiro nuclear-similar coupled states and resonances in a nucleon–antinucleon system can appear as short-lived mesons. The fact that the first experimental results apparently confirm the theoretical predictions (experiments carried out in the USA with the use of a deuteron and hydrogen chamber), is significant for this field of research.

In the paper by Z.Wu (USA) special attention was given to the dynamic aspects of the physics of μ-mesoatoms and to the correction for vacuum polarization.

This conference was the first in which a new direction of research, namely mesochemistry, was discussed in the plenary session. This field of research emerged and is being successfully developed in Dubna, where basic experiments in this new area have been conducted during the past few years on meson beams from the synchrocyclotron of the Laboratory of Nuclear Problems.

The goal of mesochemistry is to investigate the electronic structure of matter and the kinetics of chemical reactions with the use of pions, muons, and mesoatoms. Problems related to experimental investigation of the chemical structure of matter, the types of chemical bond, and other problems with the use of charge-exchange reactions of residual pions and meso x-ray radiation of mesoatoms were discussed in the paper by V.I.Petrukhin (OIYaI). The paper by L.I.Ponomarev (OIYaI) presented a theory developed by him jointly with S.S.Gershtein, which is based on the so-called model of large mesomolecules proposed by them. The paper by I.I.Gurevich (USSR) presented the results of various physicochemical and chemical investigations of polarization effects in muonium and mesoatoms.

Declassified and Approved For Release 2013/03/01 : CIA-RDP10-02196R000300100005-6

Declassified and Approved For Release 2013/03/01 : CIA-RDP10-02196R000300100005-6

The present state of the problem of weak interaction of nucleons was discussed in the paper by V.M. Lobamev (USSR). The maximum violation of the spatial symmetry (~1.5%) in strong interactions was measured for the highly forbidden γ-transition (E = 0.501 MeV) in Hf^{180} (FRG).

New possibilities for research in the field of neutron physics have appeared after the startup of the large bubble chamber "Gargamel'" at CERN (A. Russe, CERN). The chamber is filled with freon and will be used for the investigation of interaction of neutrinos with nuclei. The large rate of recording of interaction events of neutrinos (one case in 20 photographs) and antineutrinos (one case in 200 photographs) permits the evolution of neutrino experiments from the volume of obtained information at the level of a majority of other experiments in the field of high-energy physics.

In the investigations of electromagnetic interactions (D. Walechka, USA) the most interesting achievements during the recent past have been the following: 1) processing and analysis of experimental data (of the type of phase analysis), which do not depend on the model of the nucleus, enabling one to obtain "absolute" information on the shape and size of nucleus; 2) direct observation of the excited sate of nucleons in experiments on scattering of electrons by nuclei (E. V. Inopin, USSR).

A number of interesting results on photoproduction in nuclei were communicated by K. Shule (France). In particular, the parameters of ρ-ω-electromagnetic blending are in good agreement with the corresponding results obtained in experiments on counter beams.

The paper by L. Rosen (USA) on the meson plant, being constructed in Los Alamos (energy of protons 800 MeV, current up to 1 mA) generated large interest. General information on the plane was given and the parameters of different particle channels were presented; the program of physical and medicobiological investigations of particle beams was also presented. In a joint paper G. Palevskii (USA) presented the program of experiments on the proton beam of this high-power accelerator. The study of scattering of nucleons on nucleons and low-nucleon systems, and of different reaction products offers the possibility of investigating new details of the structure of the nucleus. For this purpose a proton spectrometer with exceptionally high resolution at this energy is being constructed at Los Alamos. The characteristics of partial transitions in nuclei will be obtained for the energy of the incident protons in the range 300-800 MeV, which would give unique information to the physicists.

The acceleration of nuclei to energies of several GeV per nucleon opens up new possibilities in the study of the atomic nucleus. This was reflected in the paper by A.M. Valdin (OIYal) communicating that deuterons were accelerated to 5 GeV/nucleon for the first time in the synchrophasotron of the Laboratory of High Energies of OIYal. It was also communicated (G. Shteiner, USA) that such investigations have been started at Berkley where deuterons, α-particles, and nitrogen ions have been accelerated to 2.6 GeV/nucleon in the bevatron.

Declassified and Approved For Release 2013/03/01 : CIA-RDP10-02196R000300100005-6

Declassified and Approved For Release 2013/03/01 : CIA-RDP10-02196R000300100005-6

INTERNATIONAL CONFERENCE ON THE STATISTICAL PROPERTIES OF NUCLEI

Yu. G. Abov and S. I. Drozdov

In August, 1971, at the State University of New York at Albany, the International Conference on the Statistical Properties of Nuclei took place, organized by the International Union of Pure and Applied Physics and a number of American organizations. The Conference brought together about 150 participants, mainly from the American Continent. Among the foreign delegations, there was a comparatively large one from France, as well as a Soviet delegation of six physicists. L. Benezet, President of the University of Albany, welcomed the Conference participants.

Forty-five papers were presented during the course of nine sessions. The papers contained the results of measurements of scattering cross sections for neutrons and protons at high resolution, new data for their interaction potentials, classification of nuclear resonances, including fission proton, neutron, and radiation widths along with their mutual correlations, data concerning nuclear level densities, work on statistical nuclear theory, as well as calculations of nuclear resonances conforming to a pattern of incoming states. Thus, the Conference was devoted to the problem of nuclear reactions and the properties of a nucleus at a sufficiently high excitation. Analysis of experimental data and theoretical papers had a twofold character: the statistical description of the nucleus was considered in only a part of the papers, while the well-known nuclear models for the quantum-mechanical description of the stationary states of a compound nucleus were investigated in the remaining ones. Various approaches in the description of nuclear resonances, level densities, widths, and the nuclear reactions associated with them, considered in papers by E. Wigner and H. Feshbach (USA), opened the Conference.

E. Wigner gave a review of the present state of statistical nuclear theory and introduced the conference papers on this subject. He stressed that in comparison with statistical mechanics, statistical nuclear physics had less substantiation. Thus, for example, one can also explain purely statistically the fluctuations in the probabilities for transitions from highly excited nuclear states and describe individually, by means of a model, the incoming states. He gave a review of well-known papers in the area of statistical nuclear theory. Pointing out the considerable difficulty of the theory and its obvious disagreement with the experimental data, Wigner concluded that, at the present time, there did not exist a formulation of statistical nuclear theory. He stressed the possibilities for the development of a theory, suggested by analysis of experiments; for example, the appearance of correlation widths between levels with different spins.

H. Feshbach reviewed the current theories for resonance reactions. Nuclear resonances occupied a central place in the papers, and the problem in his words, consists first in the extraction of the resonance parameters (energies, widths) from the experimental data and, second, in the interpretation of this data on the basis of theories of interacting nuclear systems by means of the wave functions or the statistical parameters associated with them. Regardless of the considerable age of this problem, it remains the subject of keen discussions. The debate produced, for example, a choice of a possible formulation on the basis of Bethe's theory, Wigner's R-matrix theory, the Kapur–Peierls formulism, or Feshbach's projection formulism. The speaker thought that, because of satisfying the unitarity requirement, all of these treatments had characteristics in common, and their results were definitive for the observed values extremely near each other. The physical interpretation of the resonance parameters also produced debate. The poles of the scattering matrix give direct information concerning the nuclear interaction only for isolated, narrow resonances. In the case of overlapping resonances, a similar interpretation is difficult, since the separation of the scattering amplitude into potential and resonance parts is ambiguous.

Translated from Atomnaya Énergiya, Vol. 32, No. 6, pp. 518-520, June, 1972.

© 1972 Consultants Bureau, a division of Plenum Publishing Corporation, 227 West 17th Street, New York, N. Y. 10011. All rights reserved. This article cannot be reproduced for any purpose whatsoever without permission of the publisher. A copy of this article is available from the publisher for $15.00.

Declassified and Approved For Release 2013/03/01 : CIA-RDP10-02196R000300100005-6

Declassified and Approved For Release 2013/03/01 : CIA-RDP10-02196R000300100005-6

A. Lane (England) discussed the appearance of correlations between the partial widths for different nuclear reaction channels. He pointed out this phenomenon as one of the high points in the development of nuclear physics in seventy years, comparing it with the discovery of analogous resonances sixty years ago. The occurrence of correlations between the decay widths of a compound nucleus in different channels, in his opinion, is connected with the existence of mutual incoming states for these channels.

The paper by P. Moldauer (USA) showed the possibility for a statistical treatment of the theory of nuclear resonance reactions and, in particular, in the estimations of the energy dependence of the neutron cross sections. The author calculates the fluctuations in the neutron cross sections on the basis of a resonance, for example, the R-matrix, formulism and the optical model.

C. Bloch (France) presented a review of theories of energy level densities and showed that the success of theories in this area are connected primarily with consideration of the simplest models, mainly the independent particle model.

The paper by John French and F. Chang (Canada) was also devoted to the possibility for a description of the nuclear level densities based on the independent particle model, for which a trial was made to take into account the interaction between the particles.

A large amount of experimental data relating to the study of nucleon cross sections, α-particle scattering cross sections, and ions with high energy resolution was presented. In the region where the resonances are well separated, information is obtained concerning the level densities, widths, and interaction potentials. For the theoretical analysis of the cross sections, the R-matrix theory is utilized extensively. The accumulated data permitted one to treat it statistically. Departures from a statistical distribution and the occurrence of correlations due to the presence of incoming states were investigated (papers by M. Moore, John Garg (USA) et al.).

H. Newson (USA) presented new data regarding the measurement of neutron cross sections with good resolution $\Delta E = 200$ keV in the energy interval 1.5-2.0 MeV for closed-shell nuclei. This data indicated the existence of incoming states as well, in neutron scattering processes. Thus, an incoming resonance is established with neutron scattering from Pb^{206} and Pb^{208} nuclei; the Pb^{206} resonance having a fine structure whose widths satisfy a certain sum rule for the incoming states. The absence of fine structure for the resonance in scattering from Pb^{208} is explained by the weak relaxation of the incoming state by the more complex states of the compound nucleus. It was mentioned that the rapid increase in the relaxation widths conforming to the degree of departure from closed shells must lead to a disappearance of intermediate structure in the energy dependence of the cross section. The incoming states appear also in the form of discontinuities in the interaction potentials. The author concludes that the incoming states and the intermediate structure play a role in nearly every neutron cross section, but the relaxation width is usually so large that the incoming states overlap and therefore, with the exception of near magic nuclei, it is difficult to separate these effects from those which are described by the optical model.

E. Bilpuch (USA) presented excitation functions of the reactions (p, p'), (p, n), (p, γ) for nuclei $40 \leq A \leq 64$ with a 200 eV resolution at proton energies near the Coulomb barrier. Due to direct observation of resonances, they gauged the interaction potential and through its discontinuities explained the incoming resonances. Statistical analysis of levels and widths were carried out. For example, in the reaction p + Ti^{48}, 70 levels for the $1/2^+$ nucleus of V^{49} were observed in a one MeV interval; their density satisfied an exponential law, and the widths were well described by the Thomas–Porter distribution. Until recently, similar data was obtained by investigating neutron resonances. New proton data have an advantage in that they give statistical information over a large range of energies, spins, and parities for one and the same isotope.

The last session of the Conference ended in a round table discussion of selected topics under the chairmanship of E. Wigner who stressed that the investigation of the occurrence of correlations between widths by means of the level configurations was new at this Conference. H. Feshbach stressed the role of the incoming states in reactions, operating through many channels, with overlapping resonances. L. Bollinger (USA) pointed out the significance of experiments on radiative neutron capture for a statistical description of a nucleus and stressed the importance of the study of radiative and neutron width correlations in connection with a model of the incoming states. G. Bartholomew (USA) stressed the important value for nuclear physics of the development of new experimental methods being used by electrostatic accelerators and in neutron measurements. Finally, John Garg, a member of the conference's Organization Committee from the University of Albany, reported that the conference proceedings must be published.

The Conference was well organized and took place in an atmosphere of efficient cooperation.

Declassified and Approved For Release 2013/03/01 : CIA-RDP10-02196R000300100005-6

Declassified and Approved For Release 2013/03/01 : CIA-RDP10-02196R000300100005-6

PORTABLE PULSED X-RAY EQUIPMENT "KVANT," IRA-3, RINA-1D

N. I. Komyak and E. A. Peliks

Pulse x-ray radiography, which appeared at the beginning of the forties as a method of investigating rapidly occurring processes in a nontransparent medium, is being extensively used at present for nondestructive control of materials in nonstationary conditions, in medical diagnostics, luminescent analysis of minerals, calibration of radiation detectors, and in many other physical investigations.

The development of a series of manosecond x-ray instruments was completed in 1970 at the SKB (Special Design Office) of x-ray equipment. In these instruments a compact transformer in combination with a discharger–accentuator is used as the high-voltage source. The duration of the leading edge of the high voltage pulse of such a generator is determined by the commutation time of the discharger–accentuator and is constant depending on the parasitic parameters of the circuit. On account of the high gas pressure in the

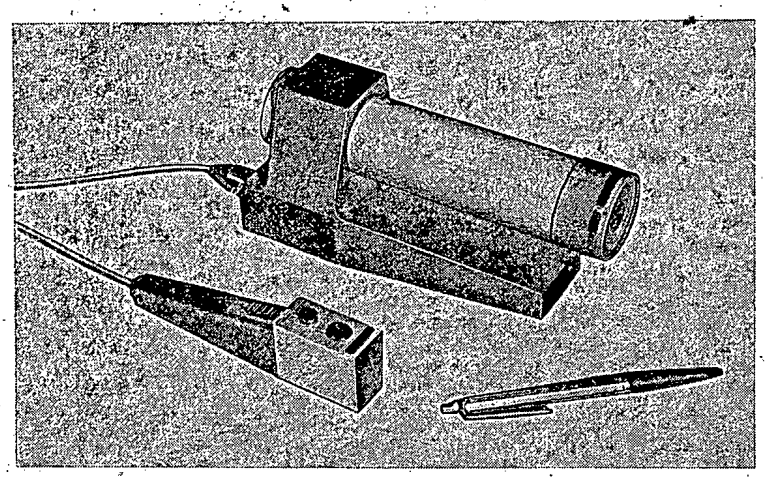

Fig. 1. General view of apparatus "Kvant."

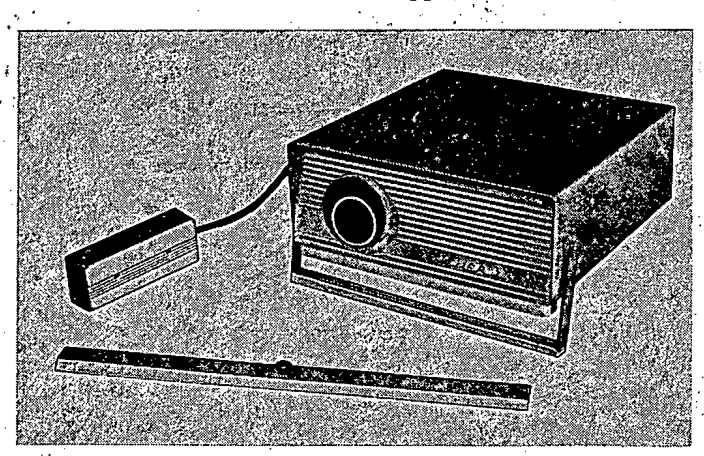

Fig. 2. General view of apparatus IRA-3.

Translated from Atomnaya Énergiya, Vol. 32, No. 6, pp. 520-522, June, 1972.

© 1972 Consultants Bureau, a division of Plenum Publishing Corporation, 227 West 17th Street, New York, N. Y. 10011. All rights reserved. This article cannot be reproduced for any purpose whatsoever without permission of the publisher. A copy of this article is available from the publisher for $15.00.

Declassified and Approved For Release 2013/03/01 : CIA-RDP10-02196R000300100005-6

Declassified and Approved For Release 2013/03/01 : CIA-RDP10-02196R000300100005-6

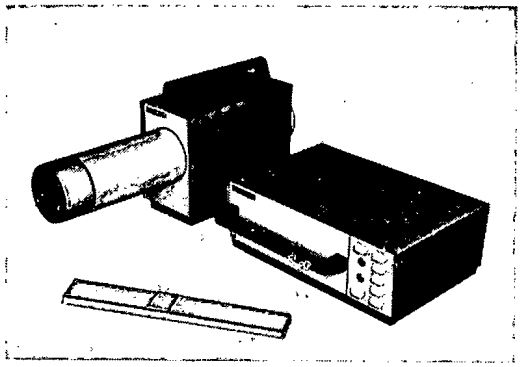

Fig.4. Photograph of five-millimeter welded plate of steel.

TABLE 1. Parameters of RINA-1D and of the Instrument of the Firm Bendix

Characteristics	RINA-1D	"Bendix"
Operating voltage at the x-ray tube, kV	200	110
Thickness of x-rayed steel, mm	20	4
Repetition frequency of x-ray bursts, Hz	15	5
Diameter of focusing spot, mm	3	1,5
Service life of the x-ray tube, pulses	200 000	20 000
Weight of the instrument, kg	5	10

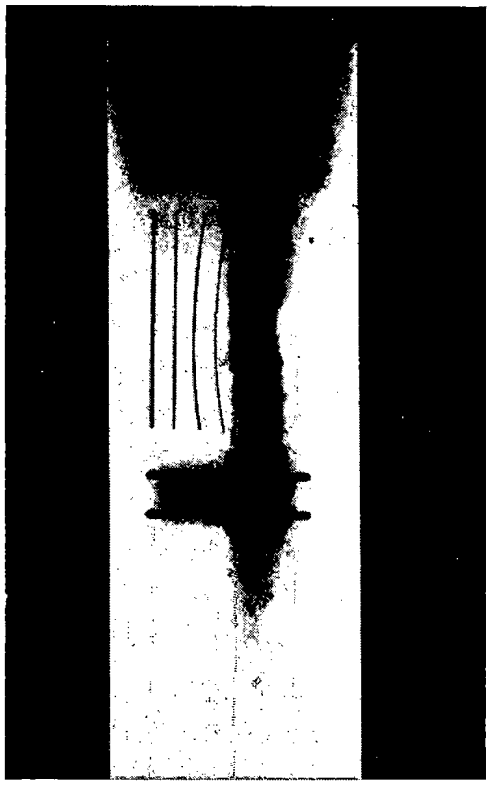

Fig. 3. General view of the apparatus RINA-ID.

operating volume of the discharger, which reaches 30-40 atm, and also due to the coaxial arrangement of all the elements of the generator in a metallic frame the growth time of the voltage pulse at the x-ray tube in these instruments is 10-20 nsec.

Miniature X-Ray Apparatus "Kvant." This is intended for the calibration of detectors of x-ray radiation, luminescent analysis of minerals, and some other x-ray radiographic problems. It generates single x-ray bursts of duration of the order of 10 nsec at a voltage of ~100 kV at the x-ray tube. In size and weight "Kvant" is the smallest x-ray instrument in the world, operating in the voltage range of 100-200 kV. Its weight does not exceed 1.2 kg. The general view of the apparatus is shown in Fig.1.

Desk X-Ray Apparatus IRA-3. This is intended for x-raying of thin-walled products in laboratory conditions, calibration of radiation detectors, and luminiscent analysis of minerals.

Its technical characteristics are:

Operating voltage at the tube.	120-150 kV
Duration of the radiated pulse	10-15 nsec
Thickness of aluminum accessible for x-ray radiography	25-30 mm
Repetition frequency of x-ray bursts.	0.2 Hz
Diameter of the focusing spot . . .	3 mm
Weight of the instrument	not more than 3 kg

The apparatus is controlled with the use of a remote panel at a distance up to 3 m (Fig.2) and does not require special protection measures.

Portable X-Ray Apparatus RINA-1D. Unlike the first two this instrument operates at a higher tube voltage and a high repetition rate of the x-ray bursts. It is mainly used for nondestructive control of materials, in particular, for the control of welded and soldered joints in nonstationary conditions. It consists of

Declassified and Approved For Release 2013/03/01 : CIA-RDP10-02196R000300100005-6

Declassified and Approved For Release 2013/03/01 : CIA-RDP10-02196R000300100005-6

an x-ray block (Fig. 3) and a desk panel for control, which is kept at a distance of 10 m. The exposure time in the apparatus is regulated by a set of number of pulses in the control panel from 60 to 1000. The apparatus does not require special protection measures and can be operated in field and building-assembly conditions at ambient temperature of −20 to +50°C.

The basic parameters of RINA-1D and of a similar instrument of the American firm Bendix are given in Table 1.

The photograph of a welded steel plate of 5 mm thickness, taken with the use of RINA-1D and a wire defectometer of type DIN No. 62 Fe, is shown in Fig. 4. All the seven wires are clearly visible, which corresponds to x-ray radiographic sensitivity of 5%.

All the instruments mentioned above can be used also for obtaining pulsed electron streams. In this case the x-ray tube is replaced by an electron tube, in which a thin beryllium plate is used instead of an anode of heavy metal.

Declassified and Approved For Release 2013/03/01 : CIA-RDP10-02196R000300100005-6

Declassified and Approved For Release 2013/03/01 : CIA-RDP10-02196R000300100005-6

ON THE PLAN OF COLLABORATION WITH THE ATOMIC ENERGY COMMISSION OF THE IRAQIAN REPUBLIC

B. Yu. Golovanov

The project of scientific–technical collaboration in the field of peaceful use of atomic energy between the State Committee on the use of atomic energy in the USSR and the Atomic Energy Commission of the Iraqian Republic during 1972-1973 was signed in Baghdad on December 19, 1971.

In particular, the plan provides for technical assistance to Iraq in modernizing the IRT type nuclear research reactor with a view to increasing its power from 2000 to 8000 kW; this reactor was constructed earlier with the help of the Soviet Union. For this purpose the necessary instrumentation, materials, and fuel elements will be made in the USSR. Soviet specialists will be deputed to Iraq (on the basis of the external trade contract) for participation in the work. Complete modernization is planned for 1973.

Furthermore the plan provides for conducting a number of joint scientific-research works along the following lines:

study of n, γ-reactions;
neutron-activation analysis;
solid state physics;
chemistry of fission products and transuranium elements;
investigation of isotope exchange with the purpose of producing radioactive organic preparations used in medicine;
methods of sterilization of preparations and products used in medicine;
effect of ionizing radiation on man;
use of radioactive isotopes and radiation in medicine;
distribution of aerosols in the respiratory tracts of man;
effect of fast neutrons on induction of dominant mutation.

The collaboration will be accomplished with the participation of Soviet scientific-research institutes such as I.V.Kurchatov Institute of Atomic Energy; the Institute of Biophysics of the Ministry of Health, USSR; Moscow Scientific-Research Institute of X-Ray Radiology of the Ministry of Health, RSFSR; Institute of Nuclear Physics of the Academy of Sciences of the Uzbek SSR; Central Order of Lenin Institute for Advancement of Doctors etc.; and also the Institute of Nuclear Research of the Iraqian Republic and the Moscow Medical Center built in Iraq with the help of the Soviet Union.

The deputation of the Soviet scientists to Iraq and the visit of Iraqian scientists to the USSR for conducting the joint work will be executed on the basis of no-cost equivalent exchange.

Translated from Atomnaya Énergiya, Vol. 32, No. 6, p. 521, June, 1972.

© 1972 Consultants Bureau, a division of Plenum Publishing Corporation, 227 West 17th Street, New York, N. Y. 10011. All rights reserved. This article cannot be reproduced for any purpose whatsoever without permission of the publisher. A copy of this article is available from the publisher for $15.00.

Declassified and Approved For Release 2013/03/01 : CIA-RDP10-02196R000300100005-6

Declassified and Approved For Release 2013/03/01 : CIA-RDP10-02196R000300100005-6

BOOK REVIEWS

N. M. Beskorovainyi, Yu. S. Belomyttsev, M. D. Abramovich, and V. K. Ivanov

NUCLEAR AND THERMOPHYSICAL PROPERTIES, FUNDAMENTALS OF CORROSION AND FIRE RESISTANCE

[VOL. 1. CONSTRUCTION MATERIALS OF NUCLEAR REACTORS]*

Reviewed by I. S. Lupakov

The book is recommended as a textbook for students in the appropriate faculties of technical universities. The first chapter describes the conditions for the utilization of materials used for the preparation of casings of fuel elements, frames, and also materials used in the preparation of elements and units located outside the reactor frame. Conduits of the first contour, steam generators and materials of the pumps pumping the heat-transfer agent are among such units.

Based on the analysis of the conditions of operation, requirements are given that must be satisfied by such materials. Conditions for the selection of steels and alloys for the casing of fuel elements, frames, and the conduits of the installation depending on the heat-transfer agent used are also tentatively indicated in this chapter.

In the second chapter a brief information is given on the nuclear and thermophysical properties of certain metals that form the base for a large number of alloys (iron, aluminum, zirconium, magnesium, nickel) and also of metals used as alloy components in melts (chromium, manganese, vanadium, silicon, tin, etc.). Data on nuclear and thermophysical properties of heat-transfer agents (sodium, potassium, lead, bismuth) are also presented. This chapter also gives an idea about the sources of thermal stresses appearing due to temperature drops in separate parts of the nuclear power installation and the difference in the linear expansion coefficients depending on temperature, and also about the temperature conductivity, heat conductivity, specific heat, thermal expansion coefficients, which influence the level of the thermal stresses.

In the next chapter data on the nuclear–physical properties of heat-transfer agents (mainly of the first contour) are given; it is pointed out that heat-transfer agents must not have a negative influence on the construction materials. A general idea of corrosion of constructional materials in different heat-transfer agents is given.

The problems of corrosion of construction materials in gaseous, water vapor, organic, and liquid-metal heat-transfer agents, and also of the absorption of gases by metals are discussed in the fourth, fifth, and sixth chapters. The mechanism of oxidation of metals, the nature and dynamics of formation of oxide films are elucidated, ways of increasing the fire resistance are indicated. An idea of the electrode processes and factors that affect their rate in aqueous media, is given. Problems of corrosion in organic heat-transfer agents are discussed. Physicochemical interactions of construction materials with liquid-metal heat-transfer agents are elucidated quite thoroughly. Dynamics of dissolution of solid metals in liquids, mass transport, redistribution of impurities among liquid and solid metals are discussed.

The imperfection of crystal structure in metals is discussed in the seventh chapter. The concept of point defects, i.e., vacancies and injected atoms, and of dislocations and their interaction among themselves and with impurity atoms is given. The mechanism of formation of fissures during the interaction of dislocations with barriers is briefly explained.

*Atomizdat, Moscow, 1972.

Translated from Atomnaya Énergiya, Vol. 32, No. 6, pp. 523-524, June, 1972.

© 1972 Consultants Bureau, a division of Plenum Publishing Corporation, 227 West 17th Street, New York, N. Y. 10011. All rights reserved. This article cannot be reproduced for any purpose whatsoever without permission of the publisher. A copy of this article is available from the publisher for $15.00.

Declassified and Approved For Release 2013/03/01 : CIA-RDP10-02196R000300100005-6

Declassified and Approved For Release 2013/03/01 : CIA-RDP10-02196R000300100005-6

The eighth and ninth chapters are devoted to the problems of fire resistance. An idea about the mechanism of creep of materials in prolonged action of stresses and temperatures and about the effect of different factors, including radiation, on fire resistance is given.

The technological properties of materials, which determine the possibility of obtaining intermediate products and also finished parts and units, are discussed in the tenth chapter. Different technological schemes of obtaining metals by the metal–ceramic method and by the method of fusion are analyzed. The casting properties, plasticity in pressing and cutting, and also weldability are estimated.

On the whole a number of remarks can be made on the book.

Thus, in the first chapter extensive use of iron, copper, zinc, lead, and other metals is attributed to the relative ease of obtaining them. In the case of iron one cannot completely agree with this, since the extensive use of iron in technology is explained also by the fact that a large number of different construction and instrumental stainless and magnetic steels are made on its base. In this sense none of the known technical materials possess such universality.

In the section where the requirements on materials of the casing of fuel elements are discussed, one would expect a brief discussion of their compatibility with nuclear fuel.

In enumerating the requirements imposed on frame steels it should have been indicated that carbonite and alloy steels of the perlite class do not have sufficiently high corrosion stability; for this reason the inner surface is plated with a thin layer of stainless austenite steel.

The second chapter is called "Nuclear and thermophysical properties of metals and alloys." The data presented there pertain only to pure elements and nothing is given on alloys.

In the evaluation of lithium as a heat-transfer agent mention should have been made of its very high activity (permeability) with regard to welded joints, which also prevents its extensive use as a heat-transfer agent.

In the section where the interaction of metals with hydrogen is described, it is pointed out that hydrogen facilitates the formation of floccules in steel. The statement should have been made more precise by mentioning that floccules form only in intermediate products of large cross sections and in finished products of some alloy steels; in particular, chrome–nickel steels are highly sensitive to floccule formation.

The reasons for corrosion cracking of austenite steels have been determined with inadequate accuracy and completeness. It should have been mentioned that it appears only in the presence of an oxidant (in particular, oxygen), chlorides, and stretching stresses in the medium. In this case a softening and drying must occur and as a result chlorides get settled on the metallic surface or on the slits and gaps in the constructions, where they get concentrated and lead to corrosion cracking.

The advisability of including the chapter "Technological properties" is questionable, since these problems are presented sufficiently completely in courses on technology of metals.

In conclusion it can be said that despite the indicated drawbacks the book is a useful aid for students of the appropriate universities and also for engineer-technicians of scientific-research institutes, design offices, and factories.

Declassified and Approved For Release 2013/03/01 : CIA-RDP10-02196R000300100005-6

Declassified and Approved For Release 2013/03/01 : CIA-RDP10-02196R000300100005-6

N. I. Chesnokov and A. A. Petrosov

SYSTEMS OF EXPLOITATION OF URANIUM ORE DEPOSITS*

Reviewed by I. F. Medvedev, N. S. Zontov, and L. Ch. Pukhal'skii

During the past 25 years a large amount of experience on the exploitation of radioactive ores all over the world has been accumulated; however, this is not adequately reflected in the scientific-technical literature. Publications abroad are mainly in the form of isolated short articles in mining journals. These problems have been elucidated most completely in the book "Special features of exploitation of deposits of radioactive ores" by G.N. Popov et al., published in the Soviet Union (Atomizdat, Moscow, 1964). However, without disparagement of the obvious merits of this work it must be mentioned that this book was written mainly as a textbook; the small volume of the book did not permit the authors to discuss in sufficient detail all the extensive material on the diverse systems and variants of exploitation of numerous morphological types of uranium deposits.

This omission has been made up to a considerable extent by the book "Systems of exploitation of uranium ore deposits" by N.I. Chesnokov and A.A. Petrosov.

The discussion of the actual materials of the book is prefaced by a chapter dealing with the experience in the exploitation of veins of valuable ores at great depths. Examples of opening up such deposits are discussed and the main systems of exploitation are described. In particular, very interesting data on systems of exploitation used in the classical deposit of polymetallic ores in Prshibram (Czechoslovakia) are presented. In conclusion technical–economic indices of exploitation of veins at large depths are presented and preliminary considerations on the choice of the most rational systems of exploitation for deep horizontal uranium veins in analogous conditions are given.

The authors describe in a maximum compressed form the special features of geological structure of veins of uranium ores, which dictate the choice of the systems of exploitation. Without the information on the morphology of ore veins, conditions of localization of uranium mineralization in veins, the structure of different ore blocks and ore lenses it would be difficult for the readers to understand the subsequent description of the systems of exploitation and the methods of ore extraction. The data on the strength characteristics of interfering rocks and vein filling, and also the information on fissure tectonics and the nature of disintegration of samples of ores and mining rocks are highly interesting.

A detailed analysis of the special features of opening up veins is presented in the book illustrating the systems for opening, ventilation, and detailed reconnaissance in conditions of intensive exploitation of the deposits using simultaneously a large number of levels, blocks, and end faces.

On the basis of the data published in the world literature the authors propose a classification of the systems of exploitation used in uranium deposits of hydrothermal and sedimentary genesis. This classification includes the following systems of exploitation: with open excavated space; with storage of the ore; with packing of the excavated space; with propping; with demolition; combined systems; with boring and logging of blast holes and leaving pillars inside the blocks; underground leaching.

Maximum attention is given to systems of exploitation of veins of uranium ores. Here schemes of preparing the blocks are discussed first. The systems of exploitation with packing of the excavated space are described in detail, in particular, the variant most extensively used in uranium deposits is exploitation

*Atomizdat, Moscow, 1972.

Translated from Atomnaya Énergiya, Vol. 32, No. 6, pp. 524-525, June, 1972.

© 1972 Consultants Bureau, a division of Plenum Publishing Corporation, 227 West 17th Street, New York, N. Y. 10011. All rights reserved. This article cannot be reproduced for any purpose whatsoever without permission of the publisher. A copy of this article is available from the publisher for $15.00.

Declassified and Approved For Release 2013/03/01 : CIA-RDP10-02196R000300100005-6

Declassified and Approved For Release 2013/03/01 : CIA-RDP10-02196R000300100005-6

in horizontal layers with separate extraction of ore and packing of the excavated space by blasted side (interfering) rocks. The systems of exploitation of veins in horizontal layers with propping and packing and the variants of the systems of exploitation of flat-dipping veins are also described fully. The description is accompanied by apt illustrations and basic computation of the main technical–economic indices.

The problems related to the development of mine pressure during the exploitation of veins at great depths and the methods of coping with it, in particular, with the intense mine pressure at upper and deep levels, are discussed in detail. This has enabled the authors to correctly estimate and select the types of propping of horizontal excavation. In this section the results of macroscopic investigations of the nature of the loads on the timbering and displacements of the side rocks in vein drifts are of undoubted interest.

The use of hardening packing is justified for controlling the mine pressure during cleaning operations at great depths, especially in the exploitation of segments of complex vein intersections, and also two- or three-stage extraction of intense vein zones in horizontal layers.

For the readers the methods of sample mining of ore veins, used only in uranium deposits, is particularly interesting. The variants of exploitation with the cancellation of non-ore pillars on the basis of their blast hole radiometric probing have not been so far used in world mining practice. The authors of this book have discussed variants of such systems and the results of investigations of their technical–economic indices for different mining–geological conditions.

The technology of cleaning extraction in the exploitation of veins of uranium ores is reduced by the authors to a strict classification which permits establishing criteria for the choice of the method of extraction: separate extraction of ore lenses with the progressive end face along the rock; slot extraction of ore; single-stage extraction of ore; and finally gross extraction.

From the point of view of improving the technical–economic indices of cleaning extraction of ore the effect of a number of geological and technological factors on the reduction of the width of the cleaning space is considered.

The procedure of estimating the depletion and losses of ore in cleaning operations are described very thoroughly and numerous recommendations on their reduction are given. The problems of economic stimulation of reduction of losses and depletion are discussed for the first time. The operational estimate of losses and depletion in uranium deposits with the use of a wide arsenal of technical means of radiometric service are of undoubted interest.

On the whole the book by N. I. Chesnokov and A. A. Petrosov can be considered highly successful. The large factual material and the scientific inferences contained in it make it interesting for a wide range of readers connected not only with uranium industry but also with other fields of mining industry and mining science.

The book is useful both for experimental mining engineers and students and young specialists.

Declassified and Approved For Release 2013/03/01 : CIA-RDP10-02196R000300100005-6

Declassified and Approved For Release 2013/03/01 : CIA-RDP10-02196R000300100005-6

breaking the language barrier

WITH COVER-TO-COVER ENGLISH TRANSLATIONS OF SOVIET JOURNALS

in mathematics and information science

Title	# of Issues	Subscription Price
Algebra and Logic *Algebra i logika*	6	$110.00
Automation and Remote Control *Avtomatika i telemekhanika*	24	$185.00
Cybernetics *Kibernetika*	6	$125.00
Differential Equations *Differentsial'nye uravneniya*	12	$150.00
Functional Analysis and Its Applications *Funktsional'nyi analiz i ego prilozheniya*	4	$ 95.00
Journal of Soviet Mathematics	6	$135.00
Mathematical Notes *Matematicheskie zametki*	12 (2 vols./yr. 6 issues ea.)	$175.00
Problems of Information Transmission *Problemy peredachi informatsii*	4	$100.00
Siberian Mathematical Journal of the Academy of Sciences of the USSR Novosibirski *Sibirskii matematicheskii zhurnal*	6	$185.00
Theoretical and Mathematical Physics *Teoreticheskaya i matematicheskaya fizika*	12 (4 vols./yr. 3 issues ea.)	$125.00
Ukrainian Mathematical Journal *Ukrainskii matematicheskii zhurnal*	6	$135.00

Back volumes are available.
For further information, please contact the Publishers.

SEND FOR YOUR FREE EXAMINATION COPIES

PLENUM PUBLISHING CORPORATION
Plenum Press • Consultants Bureau
• IFI/Plenum Data Corporation
227 WEST 17th STREET
NEW YORK, N. Y. 10011

In United Kingdom
Plenum Publishing Co. Ltd., Davis House (4th Floor)
8 Scrubs Lane, Harlesden, NW10 6SE, England

Declassified and Approved For Release 2013/03/01 : CIA-RDP10-02196R000300100005-6

Declassified and Approved For Release 2013/03/01 : CIA-RDP10-02196R000300100005-6

breaking the language barrier

WITH COVER-TO-COVER ENGLISH TRANSLATIONS OF SOVIET JOURNALS

in physics

Title	# of Issues	Subscription Price
Astrophysics *Astrofizika*	4	$100.00
Fluid Dynamics *Izvestiya Akademii Nauk SSSR mekhanika zhidkosti i gaza*	6	$160.00
High-Energy Chemistry *Khimiya vysokikh énergii*	6	$135.00
High Temperature *Teplofizika vysokikh temperatur*	6	$125.00
Journal of Applied Mechanics and Technical Physics *Zhurnal prikladnoi mekhaniki i tekhnicheskoi fiziki*	6	$150.00
Journal of Engineering Physics *Inzhenerno-fizicheskii zhurnal*	12 (2 vols./yr. 6 issues ea.)	$150.00
Magnetohydrodynamics *Magnitnaya gidrodinamika*	4	$100.00
Mathematical Notes *Matematicheskie zametki*	12 (2 vols./yr. 6 issues ea.)	$175.00
Polymer Mechanics *Mekhanika polimerov*	6	$120.00
Radiophysics and Quantum Electronics (Formerly Soviet Radiophysics) *Izvestiya VUZ. radiofizika*	12	$160.00
Solar System Research *Astronomicheskii vestnik*	4	$ 75.00
Soviet Applied Mechanics *Prikladnaya mekhanika*	12	$160.00
Soviet Atomic Energy *Atomnaya énergiya*	12 (2 vols./yr. 6 issues ea.)	$150.00
Soviet Physics Journal *Izvestiya VUZ. fizika*	12	$160.00
Soviet Radiochemistry *Radiokhimiya*	6	$145.00
Theoretical and Mathematical Physics *Teoreticheskaya i matematicheskaya fizika*	12 (4 vols./yr. 3 issues ea.)	$125.00

Back volumes are available. For further information, please contact the Publishers.

SEND FOR YOUR FREE EXAMINATION COPIES

PLENUM PUBLISHING CORPORATION
227 WEST 17th STREET
NEW YORK, N. Y. 10011
Plenum Press • Consultants Bureau
• IFI/Plenum Data Corporation

In United Kingdom,
Plenum Publishing Co. Ltd., Davis House (4th Floor)
8 Scrubs Lane, Harlesden, NW10 6SE, England

Declassified and Approved For Release 2013/03/01 : CIA-RDP10-02196R000300100005-6